THE EFFECT OF PHYSICO-CHEMICAL FACTORS ON THE STABILITY AND TRANSPORT OF CLAY PARTICLES

A Thesis

by

DARYA ALEXANDROVNA MUSHAROVA

Submitted to the Office of Graduate Studies of
Texas A&M University
in partial fulfillment of the requirements for the degree of

MASTER OF SCIENCE

May 2012

Major Subject: Petroleum Engineering

The Effect of Physico-Chemical Factors on the Stability and Transport

of Clay Particles

THE EFFECT OF PHYSICO-CHEMICAL FACTORS ON THE STABILITY AND TRANSPORT OF CLAY PARTICLES

A Thesis

by

DARYA ALEXANDROVNA MUSHAROVA

Submitted to the Office of Graduate Studies of
Texas A&M University
in partial fulfillment of the requirements for the degree of

MASTER OF SCIENCE

Approved by:

Chair of Committee,	Hisham Nasr-El-Din
Committee Members,	Walter B. Ayers
	Youjun Deng
Head of Department,	A. D. Hill

May 2012

Major Subject: Petroleum Engineering

ABSTRACT

The Effect of Physico-Chemical Factors on the Stability and Transport of Clay Particles. (May 2012)

Darya Alexandrovna Musharova, B.S., Texas A&M University

Chair of Advisory Committee: Dr. Hisham Nasr-El-Din

Clays which exist in formations in the vicinity of injection and disposal wells is a worldwide problem in the petroleum industry.

Clays can be categorized as two major groups: swelling clays, which include smectite group clays, and dispersing clays, which include the kaolinite groups of clays. Therefore, two basic damage mechanisms of clay minerals are swelling and dispersion. Both mechanisms cause pore plugging, and thus aggravate hydrocarbon ease of flow.

In this thesis, the effect of temperature, injected water chemical composition, pH, and flowrate of the injected fluid were tested experimentally. Clay mineralogy, chemistry, and composition of the exchangeable cations were also examined. The existing theoretical models of evaluation of forces between clay particles and the rock matrix were used to quantify the interactions.

Coreflood experiments were conducted to determine the effect of parameters such as variation of temperature, flowrate, pH, presence of various salts in working solution and their concentration.

The results obtained from experimental and theoretical work show that clay minerals in sandstone formation are subject to fines migration and can cause a detrimental impact on the reservoir permeability. Every aforementioned factor has its influence on clays behavior and therefore, a degree of fines migration. The work accomplished summarizes and concludes what parameters sensitize clays migration. Moreover, recommendations for formation damage due to fines migration are given. The scope of work presented can be useful for petroleum engineers as well as geologists and clay mineralogists.

DEDICATION

Giving praise and glory to God for every thing in my life

ACKNOWLEDGEMENTS

I would like to thank my committee chair, Dr. Nasr-El-Din, and my committee members, Dr. Ayers, Dr. Deng, for their guidance and support throughout the course of this research.

Thanks to my mother for her encouragement and support throughout all time.

Also to my friends and colleagues and the department faculty and staff for making my time at Texas A&M University a great experience.

NOMENCLATURE

CsX	Cs-saturated, 2:1 clay
J^+ (aq)	Hydrated alkali concentration in dilute solution
JX	Alkali-saturated clay
$\Delta G°ex$	Free energy of exchange
$\Delta G°Cs^+(aq)$	Free energy of interlayer surface fization for Cs^+
$\Delta G°J^+(aq)$	Free energy of interlayer surface fization for J^+
$\Delta G°CsX$	Free energy of interlayer surface fization for CsX
$\Delta G°JX$	Free energy of interlayer surface fization for JX
r_a	Anionic radius , $\overset{0}{A}$
A	Area, $\overset{0}{A}^2$
C	Layer charge, equivalent per half unit cell
$\Delta H°JX$	Enthalpy of fixation, kcal/mole
q_1,q_2	Charge of the cation (+1) and the equivalent anion (-1)
r_c	Radius of J^+, the fixed alkali cation
PE	Potential energy
Φ	Osmotic coefficient, V
$m\pm$	Mean ionic molality, mol/kg
$\gamma\pm$	Mean ionic activity coefficient
R	Universal gas constant, J/(mol-K)
T	Temperature, K

$V_t(h)$	Total potential, J/m^2
$V_{LVA}(h)$	London Van Der Waals attraction force, J/m^2
$V_{DLR}(h)$	Double layer repulsion, J/m^2
$V_{BR}(h)$	Born repulsion, J/m^2
$V_{HR}(h)$	Hydrodynamic repulsion, J/m^2
$V_{IHL}(h)$	Interfacial hydrate layer, J/m^2
A	Hamaker constant, J
d	Characteristic dimension (core diameter), m
D	Solute diffusivity, m^2/sec
e	Electron charge, C
h	Separation distance, m
H	The ratio of separation distance to particle radius, m
k	Boltzmann's constant (1.38E-23 J/K)
K	Permeability, md (Darcy's Eq.)
L	Length of the cylindrical core, in (Darcy's Eq.)
n_b	Total ion density in the bulk
q	Flow rate, cm^3/min (Darcy's Eq.)
pH_o	Isoelectric point of the surface
r_p	Particle radius, m
t	Time, s
T	Absolute temperature, K
ΔP	Pressure differential, psia (Darcy's Eq.)

x	Length, m
z	Valence, dimensionless
δ	Collision diameter, m
ε	Electrical permittivity or dielectric constant of the medium, C^2/Nm^2
κ	Debye-Huckel reciprocal length, m^{-1}
λ	London wavelength, $\overset{0}{A}$
ρ	Density, kg/m^3
Ø	Porosity, vol %
μ	Fluid viscosity, cp
ς	Zeta potential, V
Φ_o	Surface potential, V

TABLE OF CONTENTS

Page

ABSTRACT iii

DEDICATION v

ACKNOWLEDGEMENTS vi

NOMENCLATURE vii

TABLE OF CONTENTS x

LIST OF FIGURES xiii

LIST OF TABLES xviii

1. INTRODUCTION: STATEMENT OF THE PROBLEM, OBJECTIVES OF RESEARCH AND METHODOLOGY 1

2. THE IMPORTANCE OF RESEARCH 3

    2.1 Introduction 3
    2.2 Damage mechanism of clay minerals 5

3. ORIGINS OF CLAY MINERALS IN SANDSTONE FORMATION 7

    3.1 Structure of the common clay minerals 11
        3.1.1 Kaolinite 13
        3.1.2 Illite 13
        3.1.3 Smectite 14
        3.1.4 Chlorite 15
        3.1.5 Mixed-layer clay minerals 16
        3.1.6 Palygorskite 17

4. CATION EXCHANGE OF CLAY MINERALS 18

    4.1 Free Energy Calculation 18
        4.1.1 Free energy for a dry interlayer 19
        4.1.2 Free energy for a wet interlayer 21
        4.1.3 Dependence of free energy on r_a and interlayer water content 22

Page

4.2 Rate of Reaction 25
4.3 Summary 28

5. STABILITY OF CLAY PARTICLES 30

5.1 Temperature Effect 31
5.1.1 Earlier investigation of the temperature effect 31
5.1.2 Introduction to the DLVO theory 32
5.1.3 Evaluation of forces between clay particles and rock surface 32
5.1.4 Calculation of forces 32
5.1.5 Results 40
5.2 Salinity Effect 41
5.3 Cation Fixation in Clays 42
5.3.1 Kaolin-NH_4Cl System 43
5.3.2 Zirconium Lactate Clay Stabilizer 45
5.4 Effect of pH on Kaolinite 47

6. COREFLOOD EXPERIMENTS 48

6.1 Coreflood Laboratory Procedure 48
6.2 Effect of Temperature on Permeability 52
6.2.1 Objective 53
6.2.2 Materials 53
6.2.3 Results 53
6.2.3.1 Fresh water injection 58
6.2.3.2 Flowback 59
6.2.3.3 Core effluent analysis 60
6.2.4 Summary 61
6.3 Effect of Temperature and Core Effluent Analysis 61
6.3.1 Objective 61
6.3.2 Materials 62
6.3.3 Results 62
6.3.3.1Core effluent analysis 65
6.3.4 Summary 69
6.4 Effect of Flowrate on Permeability 69
6.4.1 Objective 69
6.4.2 Materials 70

Page

6.4.3 Results 70
6.4.3.1 Core effluent analysis 71
6.4.4 Summary 74
6.5 Effect of pH on Clays Migration 74
6.5.1 Objective 74
6.5.2 Materials 75
6.5.3 Results 75
6.5.3.1 Effect of high-pH fluid 75
6.5.3.2 Effect of low-pH fluid 76
6.5.4 Summary 77
6.6 Effect of Salinity Variation on Clay Stabilization 78
6.6.1 Objective 78
6.6.2 Materials 78
6.6.3 Results 79
6.6.3.1 Core effluent analysis 80
6.6.4 Summary 82
6.7 Effect of Ammonium Chloride Salt on Fines Dispersion 83
6.7.1 Objective 83
6.7.2 Materials 83
6.7.3 Results 84
6.7.3.1 Core effluent analysis 88
6.7.4 Summary 90
6.8 Effect of Zirconium Lactate Clay Stabilizer on Clay Dispersion 90
6.8.1 Objective 90
6.8.2 Materials 91
6.8.3 Results 91
6.3.3.1Core effluent analysis 93
6.8.4 Summary 96

7. CONCLUSIONS 97

REFERENCES 98

VITA 103

LIST OF FIGURES

FIGURE		Page
1	Common mesogenic pathways for clay minerals in sandsones, where D is dickite, S is smectite, I is illite and C is chlorite.	8
2	The structures of the common clay minerals (a) kaolin, (b) illite, (c) chlorite and (d) dioctahedral smectite. The triangular motif represents tetrahedral layers. The solid grey bars represent octahedral layers.	12
3	Scan electron microscope (SEM) micrographs illustrating kaolinite	13
4	Scan electron microscope (SEM) micrographs illustrating illite	14
5	Scan electron microscope (SEM) micrographs illustrating smectite	15
6	Scan electron microscope (SEM) micrographs illustrating chlorite	16
7	Scan electron microscope (SEM) micrographs illustrating mixed chlorite-smectite mixture	16
8	Relationship between equivalent anionic radius (ra) and layer charge (for muscovite *ab*)	20
9	Change in exchange free energy ($\Delta G°ex$) with r_a for the reaction indicated where J^+ is an alkali cation. Calculations for smectite curves made for a 3 molal interlayer solution	22
10	Change in free enrgy ($\Delta G°ex$) with ra for the Ca-Na reaction indicated for several interlayer water contents	24
11	Rate of reaction of Na with standing tine.	26
12	Rate of reaction of Ca for standing time	27
13	The sphere-plate system for modeling fines stability	33
14	London Van der-Waals attraction potential increases and becomes nearly zero with a separation distance.	37

FIGURE Page

15 The Born Repulsion potential shows a rapid decrease with a proximal distance to the rock surface after which the force becomes null with any further distance 37

16 The double layer repulsion force between negatively charges clay particle and surface of the rocks weakens with separation distance 38

17 The double layer repulsion profiles at two elevated temperatures show a rapid decline at a small separation distance following a gradual decline for 200°F and increase for 300°F 39

18 Tree total summing forces show the initial decline at an increasing distance between negatively charged surfaces , after which only the total force at 300°F displays following increase (detachment occurs). 40

19 Evaluation of charge in kaolinite in water system model modified from Lawrence (1958) 44

20 One of the form polynucluear zirconium ions..... 46

21 Coreflood testing setup..... 50

22 SEM imaging tests results. Presence of kaolinite in Berea sandstone is determined..... 51

23 SEM imaging tests results. Presence of chlorite and mice in sandstone are determined..... 51

24 SEM imaging tests results. Presence of quartz and chlorite in sandstone are determined..... 52

25 Pressure profile for sandstone core showing injection of brine following fresh water injection at T= 74° 54

26 Pressure profile for Berea sandstone showing brine at T= 74°F injection, following brine at T=200° F, with final fresh water injection at T= 200°F .. 54

27 Pressure profile during flowback at T= 200°F for Berea sandstone core 55

28 Pressure profile for sandstone core at elevated temperature T=300°F, showing injection of brine following fresh water injection, and flowback at T= 300°F..... 55

FIGURE Page

29 Viscosity trends for 5 wt% NaCl aqueous solution obtained from measurements and using an existing correlation 57

30 Permeability analysis of three core samples at different temperatures 59

31 Pressure drop profile for Berea sandstone at room T = 74°F 62

32 Pressure drop profile for Berea sandstone core at T = 100°F 63

33 Pressure drop profile for Berea sandstone core at T = 200 °F 64

34 Permeability analysis at different temperatures 65

35 Sodium concentrations after coreflood for three cores for temperatures 74°F, 100°F, and 200°F respectively 66

36 Calcium concentrations after coreflood for three cores for temperatures 74°F, 100 °F, and 200°F respectively 66

37 Silicon concentrations after coreflood for three cores for temperatures 74°F, 100 °F, and 200°F respectively 67

38 Aluminum concentrations after coreflood for three cores for temperatures 74°F, 100 °F, and 200°F respectively 67

39 Iron concentrations after coreflood for three cores for the temperatures 74°F, 100 °F, and 200°F respectively 68

40 Sample after coreflood experiment with sediments on the bottom 68

41 Pressure profiles at three different flowrates of 5 cc/min, 2 cc/min, and 0.5 cc/min 71

42 Na concentration at different flowrates: 2 cc/min and 0.5 cc/min 71

43 Ca concentration at different flowrates: 2 cc/min and 0.5 cc/min 72

44 Mg concentration at different flowrates: 2 cc/min and 0.5 cc/min 72

45 Sample 10, sediments are accumulated at the bottom at flowrate of 2 cc/min 73

FIGURE Page

46 Sample 13, sediments are accumulated at the bottom at flowrate of 0.5 cc/min 73

47 Pressure profile at temperature T=200 °F, brine (5 wt% NaCl) following high pH fluid injection. Damage by 2 wt% NaOH is confirmed 76

48 Pressure profile at temperature T=200 °F, brine (5 wt% NaCl) following low pH fluid injection. Original permeability is preserved, no damage due to fresh water injection is confirmed 77

49 Pressure profile for coreflood for 15 wt% NaCl at high temperature 80

50 Na concentration for coreflood of 15 wt% NaCl at high temperature 81

51 Ca concentration for coreflood of 15 wt% NaCl at high temperature..... 81

52 Mg concentration for coreflood of 15 wt% NaCl at high temperature 82

53 Pressure profile for 5 wt% NH_4Cl salt at 300°F..... 85

54 Sediments accumulated in a few core effluent samples when fresh water was injected at high T at 5 cc/min..... 86

55 XRD analysis for the core effluent solutions containing sediments 87

56 Na concentration profile for core effluent..... 88

57 Ca concentration profile for core effluent 89

58 Mg concentration profile for core effluent..... 89

59 Pressure profile for 0.2 vol% Zr Lactate clay stabilizer at 300°F 92

60 Pressure profile for 2 wt% Zr Lactate clay stabilizer at 300°F 92

61 Zr concentration profile for Zirconium lactate clay stabilizer of 0.2 vol% concentration 94

62 Mg concentration profile for Zirconium lactate clay stabilizer of 0.2 vol% concentration 94

FIGURE Page

63 Mg concentration profile for Zirconium lactate clay stabilizer of 0.2 vol% concentration 95

64 Sediments after coreflood with 2 wt% Zirconium lactate clay stabilizer..... 96

LIST OF TABLES

TABLE		Page
1	Hydration free energies in Kcal/mole (calculated from Rossini et al. 1952) and ionic radii for alkali cation	19
2	Parameters for calculations of electrostatic forces)	35
3	Hydrated radii for different cations (Kieland 1937)	43
4	XRD analysis of the Berea sandstone rock sample	50
5	Calculated rock permeabilities	57
6	Fresh water volume injection	58
7	Pore volume of DI water injected before pressure buildup	64
8	Permeability variation in Berea sandstone cores with temperature	65
9	Pore volume of DI water injected before pressure buildup for different flowrates	70
10	Volume in cc of fresh water injected at 300°Fat 5 cc/min	79
11	Permeability analysis for different salinity brine injected	79
12	Volume in cc of fresh water injected at 300°F before damage for different salts	84
13	Permeability analysis for different salts injected	84

1. INTRODUCTION: STATEMENT OF THE PROBLEM, OBJECTIVES OF RESEARCH AND METHODOLOGY

Most sandstone formations contain a certain percentage of indigenous clays in their mineral composition which can cause a severe reduction in reservoir permeability, due to their tendency to migrate and, hence, plug interconnecting pore throats.

The main objective of the presented work is to determine the effect of different physical and chemical factors on the clay stability such as effect of temperature, amounts of salts, clay fixation, high/low-pH fluids, and effect of structural forces, flowrate and salt types.

The experimental setup which was used to conduct experiments includes: coreflood setup, Inductively Coupled Plasma (ICP), Scan Electron Microscope (SEM), and XRD (X-Ray Diffraction) machines. Multiple coreflood experiments were conducted to determine the damage in the sandstone formation under different conditions. The main material used was Berea sandstone rock which was dried and saturated over night for the further injection of various chemical solutions. The experiments were carried out at the temperature and pressure to simulate reservoir conditions.

Conclusive remarks and corresponding recommendations are presented at the end of this work. The work may be extended further by testing commercial chemical solutions and using various rock materials such as shale, tight sandstone, etc.

This thesis follows the style of *SPE Journal.*

This work can be useful for petroleum engineers as well as geologists and clay mineralogists.

2. THE IMPORTANCE OF RESEARCH

2.1 Introduction

There are many factors that are related to formation damage due to clay minerals. These factors include physico-chemical factors such as temperature, pH, water salinity flowrate, clay mineralogy, and others which affect stability and transport of clay particles in the sandstone formation.

The amount distribution pattern and morphology of clay minerals have significant effects on sandstone properties in terms of porosity, permeability, density, natural radioactivity, electrical conductivity, the water content of petroleum fields and reactivity to various enhanced oil recovery practices (Worden and Morad 2003).

Different clay-mineral cements can have different effects on permeability because they occupy different positions within the pore network. Clay minerals that are arranged tangentially to the grain surfaces have less of an effect on permeability than perpendicular clay minerals or clay minerals that sit within pores and pore throats. Thin clay layer on grain surfaces may have little effect on permeability unless they become interwoven at pore throats.

If thick coatings of illite or chlorite occur, permeability can again be seriously diminished, particularly in fine grained sandstones, even though porosity is relatively unaffected.

The possible active induction of quartz pressure dissolution and silica supplied by thin grain-coating illite serves to reduce both sandstone porosity and permeability by assisting compaction and cementation. Conversely, grain-rimming chlorite can inhibit quartz cementation and pressure dissolution. Thus, chlorite can be doubly beneficial to permeability by ameliorating pressure solution and preventing quartz surfaces (Worden and Morad 2003).

Clay mineral diagenesis is controlled by dissolution, transport and precipitation. In petroleum-bearing sandstones both precipitation and dissolution are controlled by the amount of mineral surface area exposed to water. Wettability is a key to understanding the effect of petroleum emplacement on clay diagenetic processes in sandstones. Water-wet systems will have unaffected rates of dissolution and precipitation, but transport will be slowed or stopped. Oil-wet systems will have totally impeded dissolution and precipitation, and diffusion and advection of species in water will be reduced to negligible rates. The Fe-rich chlorite may attract the polar compounds in the petroleum, encouraging oil-wetting and preventing access of water to grain surfaces, thus stopping aqueous geochemical processes such as quartz cementation. A contrast may be illite-cements sandstones because illite is water-wet and will not exclude water from grain surfaces, thus allowing aqueous diagenesis to potentially continue even in the presence of petroleum. The very low water saturation in gas reservoirs would hugely inhibit clay mineral reactions that require diffusion, and stop advective transport of material. The small amount of residual water probably would stop isocheimal clay transformations,

because even they involve aqueous dissolution and reprecipitation (Worden and Morad 2003).

2.2 Damage Mechanism of Clay Minerals

Most sandstone formations typically contain indigenous clays in their mineral composition. These clays can be present as part of the matrix, as coating on pore walls, or lying in the pores. Clay particles are often found at the junctions of sand grains, and in particular, are concentrated near shale lenses. Sandstone containing between 1.0% and 5.0% clay is considered to be 'clean' sand. Dirty sand would be one containing between 5.0% and 20% clay content (BJ 2003). Clay present in sandstones can cause a severe reduction in reservoir permeability due to their tendency to plug interconnecting pore throats. In conventional oil production, most of the clay related problems occur in the near well region, and are associated with well operations such as drilling, completion, workover, etc. Incompatible injection fluids often cause clay swelling or fines migration and this impairs the reservoir permeability (Zhou et al. 1996).

Clay particle migration is the most important mechanism of permeability reduction since sandstones containing very little or no swelling clays and a considerable amount of migratory or dispersible clays, such as kaolinite and illite, are water sensitive (Khilar and Fogler 1983).

From the chemical or physicochemical point of view, temperature is an important factor for rock-fluid interactions. Changes in temperature may induce inorganic and organic precipitation. In water-sensitive sandstone formations, the effect of temperature

is significant. Schembre et al. (2006) concluded that permeability reduction is observed with temperature increase and fines mobilization occurs repeatedly at a particular temperature that varies with solution pH and ionic strength. They experimentally found that fines released from the pore walls takes place under conditions of elevated temperature, high pH, and moderate aqueous-phase salinity. The greatest reduction in permeability occurs when the fines are produced in the effluent. Schembre et al. (2006) stated after performing experiments that the zeta potential becomes more negative as the pH and temperature increases. The fact that the zeta potentials are more negative, results in greater repulsive forces. The results show that the forces between the clay and the surface become repulsive at temperatures only slightly greater than room temperature. Studies also showed that the dispersion of clays is minimized at low pH and therefore, the damage during a water shock can be prevented with acidic solutions (Vaidya and Fogler 1992).

Khilar and Fogler (1983) studied the effects of temperature on permeability impairment in water-sensitive Berea sandstones, and found that permeability impairment becomes less severe as temperature decreases.

3. ORIGINS OF CLAY MINERALS IN SANDSTONE FORMATION

Diagenetic clay minerals occur in sandstones by direct precipitation from pore fluids (authigenesis), alteration of detrital silicates, mechanical clay infiltration and compaction of ductile argillaceous grains.

Eodiagenesis includes all processes that occur at or near the sediment surface, where the geochemistry of the interstitial waters is controlled by the depositional environment. Eodiagenesis also can be defined in terms of temperature, and depth, where the upper temperature limit is <70°C, typically equivalent to about 2 km burial.

Mesodiagenesis occurs during burial and includes all diagenetic processes following eodiagenesis and through to the earliest stages of low-grade metamorphism (Choquette and Pray 1970). In many cases, this includes sediments buried to depths with equivalent temperatures of about 200 to 250°C.

Telodiagenesis occurs in inverted basins that have experienced an influx of surface (usually meteoric) waters. Such water has the capacity to cause significant geochemical changes. Meteoric waters are commonly very dilute, oxidizing, saturated with CO_2 and thus, acidic. Telogenetic changes include the alteration of reduced iron-bearing cements (ankerite, siderite, and chlorite), and dissolution of calcite, dolomite, and sulphate cements). Most telogenetic processes occur within the first few meters of the surface Worden and Morad 2003).

There are eight main ways that clay minerals are incorporated into sandstones:

1. clay-rich rock fragments formed in the hinterland (extraclastic, allochthonous);

2. clay-rich clasts formed within the sedimentary basin (intraclastic, autochthonous);
3. flocculated mud particles and faecal pellets;
4. inherited clay rims on sands grains;
5. post-depositional incorporation of detrital mud into the sandstone by bioturbation and clay infiltration;
6. eogenetic reaction products in sandstone;
7. mesogenetic reactions in sandstones;
8. telogenetic reactions in sandstones.

Temperature and the integrated thermal history are master controls on the clay minerals in sandstones as shown in **Fig. 1**.

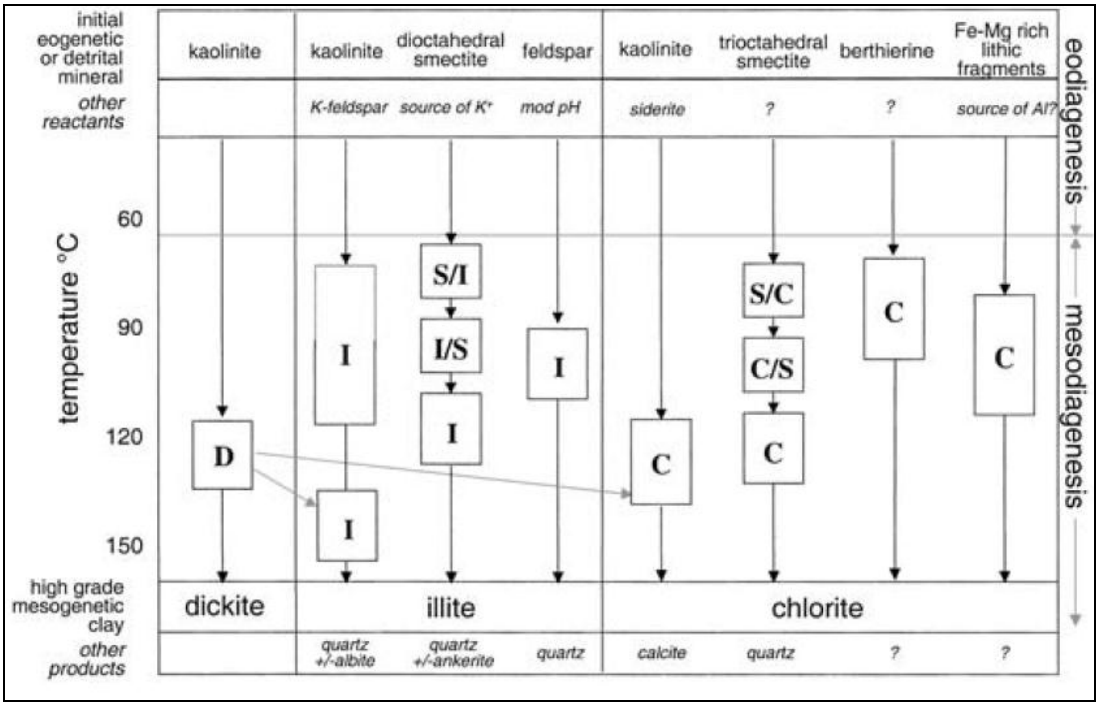

Fig. 1—Common mesogenic pathways for clay minerals in sandstones, where D is dickite, S is smectite, I is illite and C is chlorite (Worden and Morad 2003).

Upon increasing in burial depth and temperature, eogenetic kaolinite is transformed to dickite. This process is possibly aided by an increase in acidity of formation waters. With burial and heating, dioctahedral smectite transforms to illite. Diagenetic illites formed at moderate temperatures (<90 °C) in sandstones have at least a minor component of smectite within them. The transformation of kaolinite to illite is prevalent at temperatures greater than about 70 °C but becomes pervasive at temperatures greater than about 130°C.

Authigenic chlorite in sandstones may occur during mesodiagenesis as a result of the break-down of volcaniclastic grains and Fe-Mg-rich detrital minerals such as garnet, biotite or amphibole. This type of chlorite ultimately occurs as grain replacement. Chlorite occurs as coatings comprising small pseudo-hexagonal crystals, are arranged perpendicular to the sand grains. Transformation of precursor Fe-rich clay minerals to chlorite occurs at burial depths greater than about 2-3 km and temperatures 60-100°C. The precursors can be Fe-bearing berthierine, odinite, trioctahedral smectite and kaolinite (Ehrenberg 1993).

There are five dominant groups of clay minerals in sandstones: kaolin, illite, chlorite, smectite and mixed-layer varieties. Clay minerals are hydrous aluminosilicates that belong to the phyllosilicate group of minerals. They are composed of tetrahedral and octahedral sheets which are bound together in layers that extend for tens to thousands of nanometers. Sandstone geochemistry and clay diagenesis involve multiple components and not just alumina and silica. The oxides of iron, calcium, magnesium and potassium are also crucial, as well as CO_2. The presence of CO_2 can lead to enhanced formation

water acidity, which in turn, can lead to feldspar decay and clay mineral growth (Gaupp et al. 1993).

Under typical petroleum reservoir conditions, pH range 4 to 7, the surface of calcite has a positive surface charge and is preferentially oil-wet, owing to dipole attraction to negatively charged molecules in the petroleum. Conversely, quartz typically has a negative surface charge under these pH conditions because the change from negative to positive occurs at a pH of about 3. Positively charged transition metal ions from any source may become adsorbed onto negatively charged mineral surfaces, thus acting as a bridge between the mineral surface and negatively charged polar compounds (Worden and Morad 2003).

Even a thin coating of Fe-rich clay minerals on grain surfaces, representing a small fraction of the overall rock, may result in a rock being oil-wet. This may be one of the reasons that chlorite cemented sandstones can have high porosity and negligible quantities of quartz cement. The Fe-rich chlorite may attract the polar compounds in the petroleum, encouraging oil wetting and preventing access of water to grain surfaces, thus stopping aqueous geochemical processes such as quartz cementation. A contrast may be illite-cemented sandstones because illite is water-wet, and will not exclude water from grain surfaces, thus allowing aqueous diagenesis to potentially continue even in the presence of petroleum.

The repulsive power created by the negatively charged clay particles is greater than attractive Van der Waal's forces. Thus, colliding clay particles repel one another and tend not to coalesce in fresh water. However, in brackish water, cohesive Van der

Waal's forces become stronger than the cation-layer-induced repulsion, and cohesion or flocculation of clay particles can occur. The sequence in which clay minerals have a tendency to flocculate is kaolinite, illite, and finally smectite. Thus the order of deposition of clay aggregates will be kaolinite closest to the shore, followed by illite and then smectite furthest from the shore (Gibbs 1977).

On deposition, the primary sand comprises a mixture of minerals that were formed under a wide range of conditions (e.g., temperature, pressure, oxidation state, water composition). The main eogenetic clay minerals such as kaolinite and smectite are formed by precipitation from pore walls, replacement of framework sand grains, and replacement of precursor detrital or diagenetic clay minerals. On the other hand, illite and chlorite are depositional rather than eogenetic in origin.

The depositional environment is a master control on eodiagenesis because it controls the type and amount of water present in sediment, water influx versus evaporation rate, temperature, exposure to atmospheric oxygen plant-derived CO_2 and organic matter content.

3.1 Structure of the Common Clay Minerals

There are five dominant groups of clay minerals in sandstones: kaolin, illite, chlorite, smectite and mixed-layer varieties. A less common clay mineral in sandstones is palygorskite.

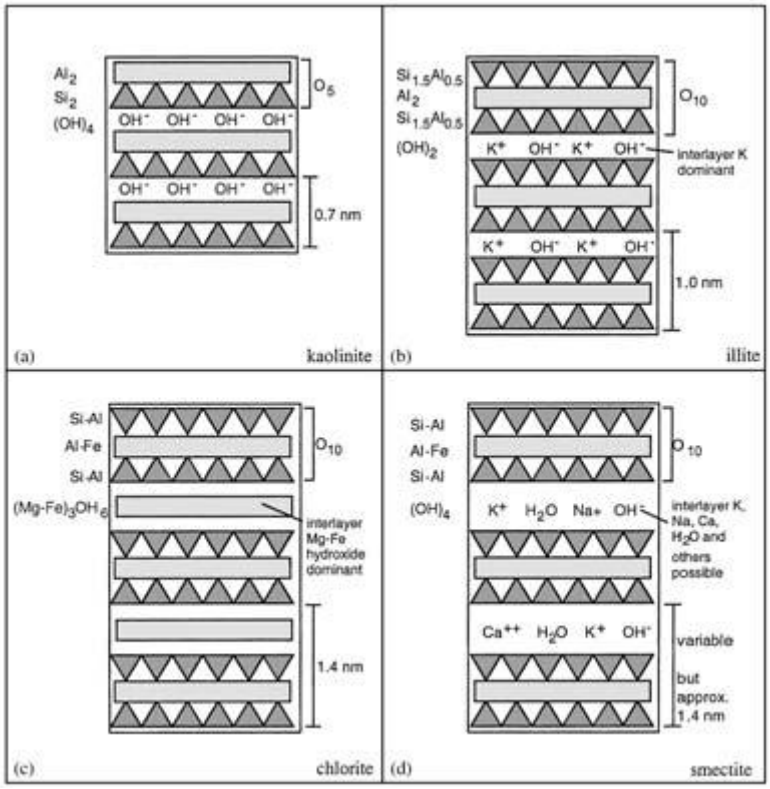

Fig. 2—The structures of the common clay minerals (a) kaolin, (b) illite (c) chlorite and (d) dioctahedral smectite. The triangular motif represents tetrahedral layers. The solid grey bars represent octahedral layers Worden and Morad 2003).

.

Clay minerals are hydrous aluminosilicates that belong to the phyllosilicate group of minerals (Deer et al. 1998). In addition to aluminium and silicon they also may contain other cations, including alkali, alkaline earth and transition metals. Clay minerals have a sheet-like structure in which the building blocks are either tetrahedra or octahedra linked to each other into planar layers by sharing oxygen ions between Si or Al ions of the adjacent tetrahedral or octahedra as shown in **Fig. 2** (Bailey 1980). The tetrahedral result from the close packing of four O ions, with the space between them occupied by a Si4+ ion or, to a lesser extent, an Al3+ ion. The octahedra result from the close packing of six

anions that are dominantly oxygen but also can include some hydroxyl (OH) ions. The Si and Al ions mainly occupy the space between the oxygen octahedra and tetrahedra but other cations, such as iron, calcium, magnesium and potassium, are required in the clay structure to ensure charge balance. Tetrahedral and octahedral sheets are bound to each other in layers that extend for tens to thousands of nanometers (nm).

3.1.1 Kaolinite

Kaolin series clay minerals as shown in **Fig. 3** are comprised of one tetrahedral layer linked to one octahedral layer with no interlayer cations and are termed 1: 1 layer structures connected by O–H–O bonds. The chemical formula of kaolin is $Al_2Si_2O_5(OH)_4$.

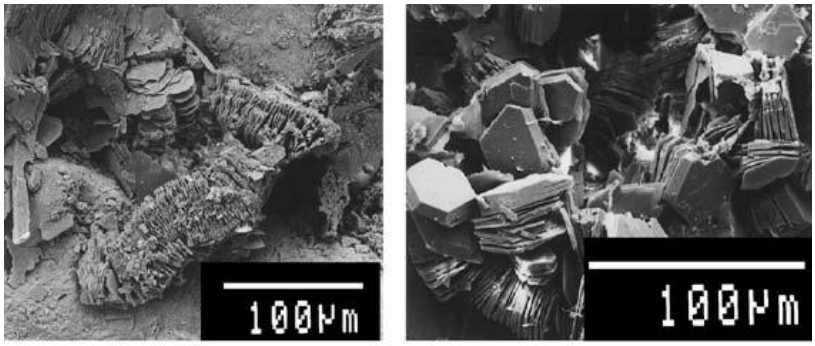

Fig. 3—Scan electron microscope (SEM) micrographs illustrating kaolinite Worden and Morad 2003).

.

3.1.2 Illite

Illite clays are K-rich dioctahedral clay minerals comprised of one octahedral layer sandwiched between two tetrahedral layers and so are termed 2 : 1 structures. O–K–O

bonds connect two opposing tetrahedral layers. The interlayer K+ is required for charge balance accompanying the partial substitution of Al3+ for Si4+ in the ehavior al and the substitution of divalent cations for Al3+ in the octahedral (Bailey 1984). The O–K–O bonding is strong and prevents swelling ehavior in illite and glauconite mica. Illite has octahedral sites dominated by Al, whereas glauconite has octahedral sites with abundant Fe3+. The general chemical formula for illite is $K_yAl_4(Si_{8-y},Aly)O_{20}(OH)_4$ (Velde 1985), where *y* is typically significantly less than 2. Illite can occur as flakes, filaments or hair-like crystals as shown in **Fig. 4**.

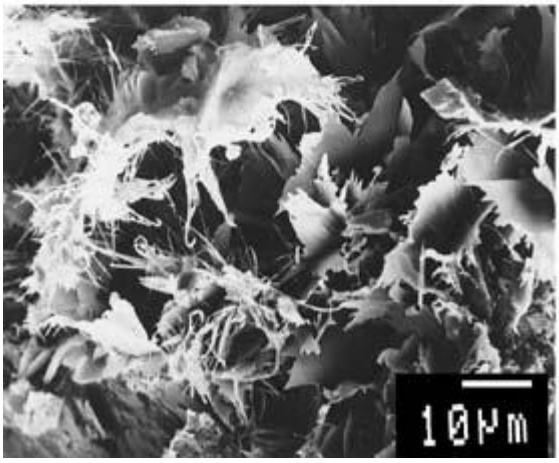

Fig. 4—Scan electron microscope (SEM) micrographs illustrating illite Worden and Morad 2003).

3.1.3 Smectite

Smectite is a group of 2 : 1 clay minerals with one octahedral layer sandwiched between two tetrahedral layers. Smectite has the general formula $(0.5Ca,Na)_{0.7}(Al,Mg,Fe)_4(Si,Al)_8O_{20}(OH)_4 \cdot nH2O$. Trioctahedral smectite has

octahedral sites dominated by divalent metals (Fe2+, Mg, Ca), whereas dioctahedral smectite has octahedral sites dominated by trivalent metals (Fe3+, Al). There is less binding of opposing tetrahedral layers by K+ than in illite, with interlayer water bound by weak Van der Waal's forces. Cations present between layers are exchangeable and reflect the chemistry of the aqueous medium with which the smectite was last in contact. Interlayer cations are variably hydrated, resulting in the swelling characteristic of smectitic clay minerals. Smectites are defined by their tendency to swell when exposed to organic solvents, which can be absorbed between interlayers. Smectite usually occurs as flakes curling up from an attachment zone on the detrital sand grain surface as shown in **Fig. 5** (Worden and Morad 2003).

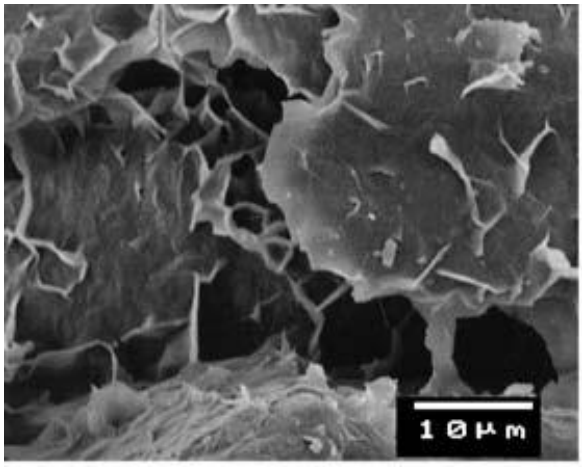

Fig. 5— Scan electron microscope (SEM) micrographs illustrating smectite Worden and Morad 2003).

3.1.4 Chlorite

Chlorite has a 2 : 1 : 1 structure comprised of a negatively charged 2 : 1 tetrahedral–octahedral–tetrahedral layered structure interlayered with an additional

octahedral layer that is positively charged and comprised of cations and hydroxyl ions (e.g. brucite layers; $Mg_3(OH)_6$). A general formula for chlorite is $(Mg,Al,Fe)_{12}[(Si,Al)_8O_{20}](OH)_{16}$. The chlorite clay mineral is illustrated in **Fig. 6**.

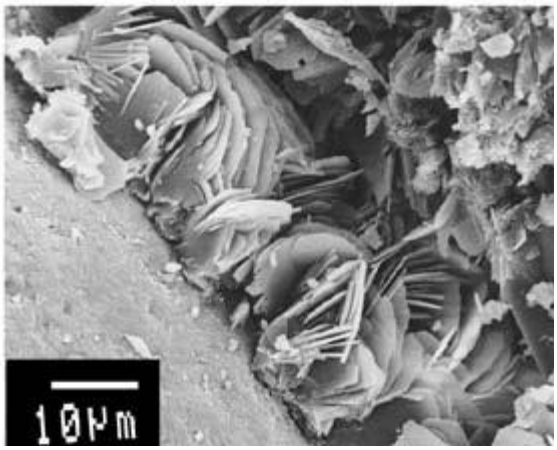

Fig. 6— Scan electron microscope (SEM) micrographs illustrating chlorite Worden and Morad 2003).

3.1.5 Mixed-layer clay minerals

Mixed-layer clay minerals as shown in **Fig. 7** result from the interstratification of different mineral layers in a single structure (Srodon 1999).

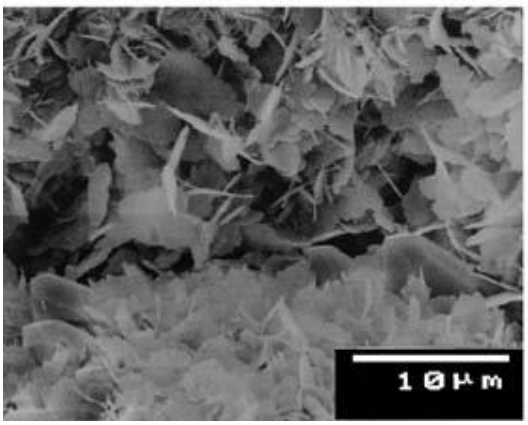

Fig. 7— Scan electron microscope (SEM) micrographs illustrating mixed chlorite-smectite mixture Worden and Morad 2003).

3.1.6 Palygorskite

Palygorskite is comprised of laterally continuous two-dimensional trioctahedral sheets (dominated by Mg with OH ions) but does not have continuous SiO4 tetrahedral sheets between the octahedral sheets.

4. CATION EXCHANGE OF CLAY MINERALS

4.1 Free Energy Calculation

Eberl (1980) in his paper proposes that cation selectivity is a function of layer charge. Also, water content has an effect in the difference in cation selectivity. Two variables must be considered when calculating exchange free energies for 2:1 clays. The first variable is anionic field strength, as expressed by equivalent anionic radius (r_a), and the second variable is interlayer water content, as expressed by interlayer molality. All exchange free energies are calculated relative to Cs^+ because Cs^+ is considered to be unhydrated both in solution and in the clay interlayer. Cation exchange between a Cs-saturated, 2:1 clay (CsX) and a hydrated alkali cation in dilute solution $J^+(aq)$ can be represented by:

$$CsX + J^+(aq) \Leftrightarrow Jx + Cs^+(aq) \quad \text{.....(1)}$$

The 2:1 clay in the above reaction can exist in two end-member states. It can be dry, a state in which interlayer cations are not hydrated and are fixed (illite-like or mica-like structure); or the clay can be water swollen, a state in which interlayer cations are hydrated and float between the 2:1 layers (smectite or vermiculites structure) (Eberl 1980).

4.1.1 Free energy for a dry interlayer

The free energy of exchange (ΔG°ex) for an illite-like structure in the above reaction is the energy required to remove Cs^+ in the clay to a hydrated state in solution, plus the energy required to dehydrate a cation from the solution and fix it to the clay interlayer, or:

$$\Delta G^{\circ} ex = (G^{\circ} Cs^{+}(aq) - \Delta G^{\circ} CsX) + (\Delta G^{\circ} JX - \Delta G^{\circ} J^{+}(aq)) \quad \ldots\ldots\ldots\ldots\ldots\ldots\ldots\ldots\ldots (2)$$

Various formulation of hydration free energy for alkali cations are given in **Table 1** (Eberl 1980).

Table 1—Hydration free energies in Kcal/mole (calculated from Rossini et al. 1952) and ionic radii for alkali cation.

J^+	ΔG°hyd J^+	ΔG°hyd J^+	ΔG°hyd J^+	J^+
	absolute hydration energy, Kcal/mole	referred to gaseous Cs^+, Kcal/mole	assumes ΔG°hyd Cs^+=0, Kcal/mole	Ionic radius (A)
H^+	-363.574	-260.095	-192.307	-0.4
LI^+	-225.196	-121.717	-54.307	0.78
N^{a+}	-201.295	-97.816	-30.406	0.98
K^+	-183.65	-80.171	-12.761	1.33
Rb^+	-178.583	-75.104	-7.694	1.48
Cs^+	-170.889	-67.14	0	1.69

The energy of interlayer surface fixation is a function of the radius and charge of the cation, and the anionic field strength (E) of the clay. E is a function of the clay's *ab* unit cell area and its layer charge and can be expressed most conveniently as an "equivalent anionic radius" (r_a). This value is the radius of a sphere of unit negative charge that has the same electrostatic energy of interaction for the interlayer cation as do

the basal oxygen planes which bound the interlayer cation. The equivalent anionic radius (in $\overset{0}{A}$) for the interlayer of a 2:1 clay can be calculated from:

$$r_a = (-A/8\pi C)^{1/2} \quad \text{.....(3)}$$

where C is the layer charge in equivalent per $O_{10}(OH)_2$ (or per half unit cell) and A is the *ab* area in $\overset{0}{A}^2$. This relationship does not take into account an effect for charge location, r_a has been calculated for a range of layer charges based in the muscovite *ab* are as in **Fig. 8**.

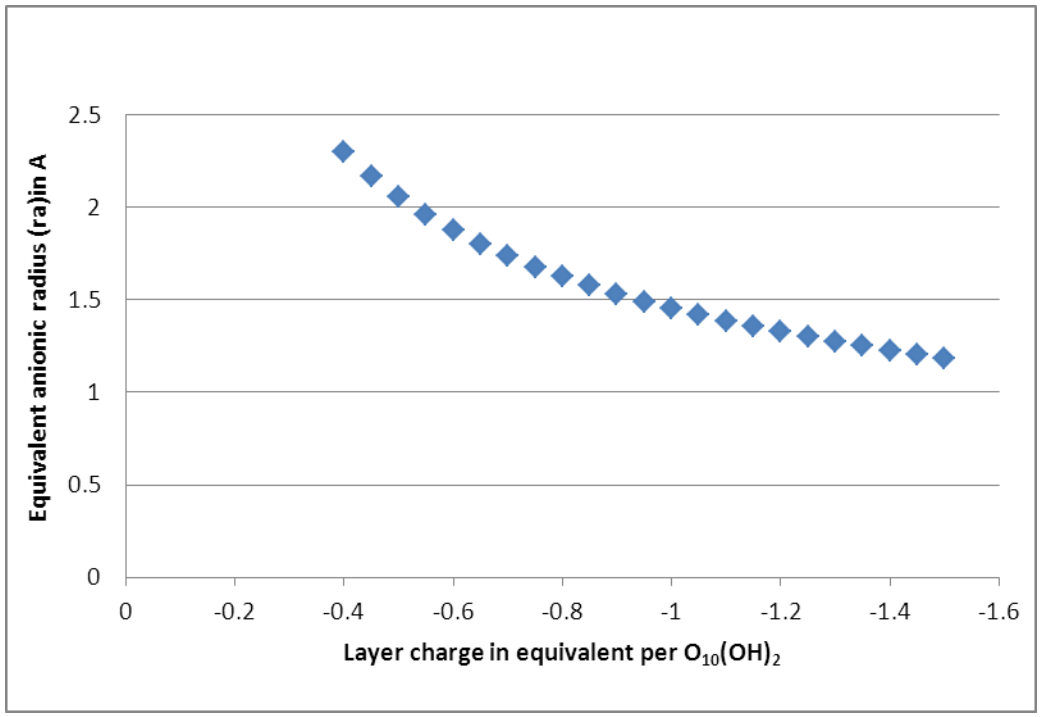

Fig. 8—Relationship between equivalent anionic radius (ra) and layer charge (for muscovite *ab*)

Once the r_a has been calculated for a particular clay, the potential energy (PE) expressed by the cation and the clay's interlayer surfaces can be treated as an attraction between two spheres using Coulomb's law:

$$PEJX = \Delta H^{\circ} JX = (332 q_1 q_2 / (r_a + r_c) \approx \Delta G^{\circ} JX \quad \text{.....(4)}$$

where ΔH°JX is the enthalpy of fixation in kcal/mole, q_1 and q_2 are the charge of the cation (+1) and the equivalent anion (-1), and r_c is the radius of J^+, the fixed alkali cation as in **Table 1** (Eberl 1980).

4.1.2 Free energy for a wet interlayer

The cation-clay-interlayer water system is treated as an alkali halide-inlayer water solution of a given molality where clay of a specific r_a is represented by a halide ion with the same anionic radius. The free energy ΔG°ex for alkali exchange can be calculated with a formula:

$$\Delta G^0 ex = 2RT(\Phi - \ln \gamma \pm m\pm)_{CsX} - 2RT(\Phi - \ln \gamma \pm m\pm)_{JX} \quad \text{.....(5)}$$

Where Φ, m±, and γ± are the osmotic coefficient, mean ionic molality and mean ionic activity coefficient for the subscripted species.

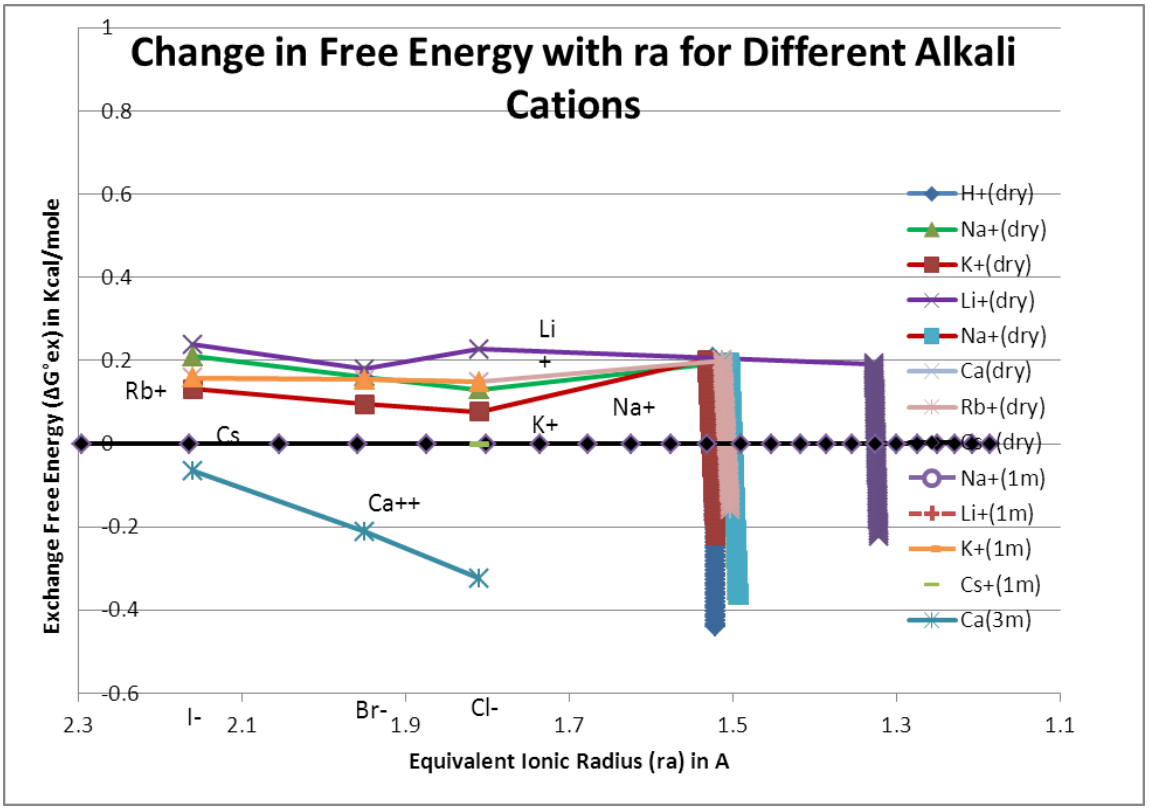

Fig. 9—Change in exchange free energy (ΔG°ex) with r_a for the reaction indicated, where J^+ is an alkali cation. Calculations for smectite curves made for a 3 molal interlayer solution.

The lowest curve is for the cation that is most preferred by the clay, and the separation between curves is a measure of how much is preferred (Eberl 1980).

4.1.3 Dependence of free energy on r_a and interlayer water content

In **Fig. 9**, curves to the right for dry clays are steep, whereas curves for water swollen clays for different molalities are more gently sloping to the left.

The number of interlayer water molecules per cation is 55.6/m. So, for the molality of 3, there will be 18 water molecules per interlayer cation. The lowest curve

for a given r_a indicates the cation most preferred by the clay, and the distance between curves is a measure of how much is preferred. To the left of the intersection point cation exchange with a water swollen clay such as smectite or vermiculite is preferred, while to the right the exchange with a dry layer is preferred. As the water content in the interlayer decreases (molality increases), the curves steepen and rotate clockwise to approach the "dry" curves, thereby revealing a greater change in selectivity with layer charge for the drier clays (Eberl 1980).

According to Eberl (1980) higher free energy implies a higher selectivity of the cations. If the reactions are compared at the different interlayer molarities, then the selectivity of sequence can be apparently changed. The physical meaning of the dry curves and their inflection points can be brought into focus if the fixation process is viewed as a two-step process. First, a cation is dehydrated by the negatively charged interlayer surfaces, and secondly, it then migrates into hexagonal holes in the surfaces. The inflection (the intersection) points in **Fig. 9** indicate the layer charge required for the first step of the fixation process, and thus represent energies which must be exceeded in order for the cations to be fixed in the holes. Cations will be held in the holes by energy greater than the potential energy between the cation and the clay's interlayer surface, because fixation in the holes allows the cation to approach more closely the seat of the negative charge.

Fig. 3 suggests that with increasing layer charge potassium is the first ion to dehydrate. With potassium dehydration (which occurs greatly between layer charge of -0.77 and -0.86), selectivity for K^+ increases rapidly. For the aforementioned range of

layer charges, potassium is thereby dehydrated, concentrated, and fixed in the smectite interlayer, forming illite, while Na^+ and interlayer water are expelled to the pore solution (Eberl 1980). The modification was made that a divalent cation was introduced in calculations for free energy. The results displayed in **Fig. 9** show that divalent cations such as Ca, have a higher affinity ability to clays than monovalent cations. Therefore, a solution with a presence of this cation can be considered as a potential clay stabilizing solution, if no adverse effects such as precipitation or scale take place in the formation.

Fig. 10 shows that as water content of the interlayer decreases, the curves steepen and rotate clockwise, thereby revealing a great change in selectivity with the layer for their drier clays.

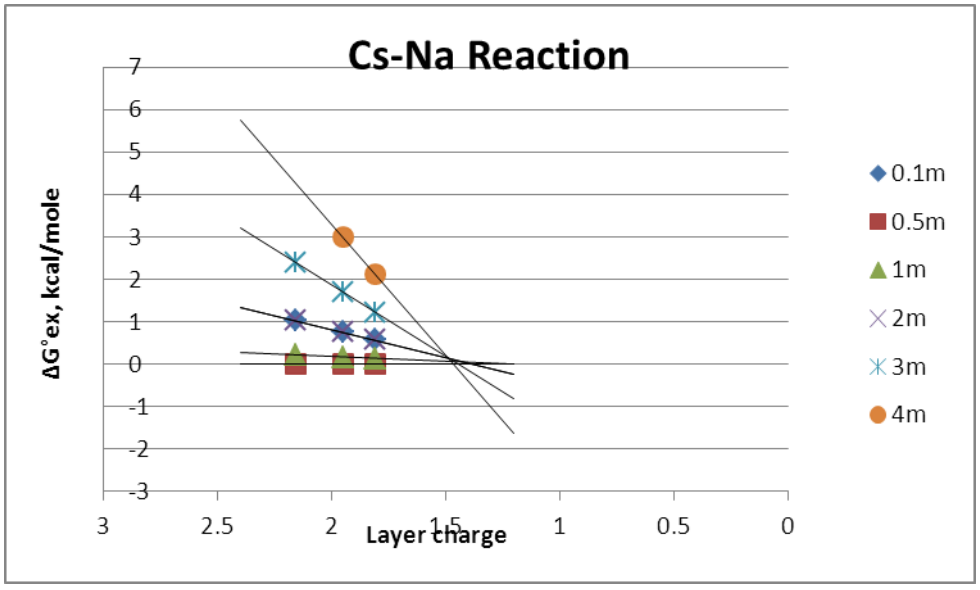

Fig. 10—Change in free enrgy (ΔG°ex) with ra for the Ca-Na reaction indicated for several interlayer water contents.

For any molarity, the relative selectivity sequence for a given r_a will not change, but only the magnitude of the selectivity. For example, montmorillonite with r_a of 2.16 $\overset{0}{A}$ (layer charge = -0.4 for a muscovite unit-cell area), the selectivity sequence is $Cs^+ > Rb^+ > K^+ > Na^+ > Li^+ > H^+$ no matter what the interlayer molality, provided the reactions are compared at the same interlayer molality If the reactions are different, the selectivity of the alkali cation sequence can be altered (Eberl 1980).

4.2 Rate of Reaction

The main objective of the experiment was to determine reaction rate qualitatively. The mixtures containing clays were tested at different time periods, and the cation concentrations were measured as an identification of stabilization of reaction of clay with solution.

Two types of clays- montmorillonite and kaolinite were used for the experiment below. The procedure for the sample preparation was the following: 10 grams of each clay (both clays were in powder form) were placed in a 50-mL tube, and 40 mL of liquid solution was added. For all experiments, below 5 wt% NaCl solution was used. After mixing, some samples were shaken for 1-2 min and then left for a few minutes for the supernatant fluid to separate, and for the clay particles to settle down. The filtered out supernatant was diluted, using the Atomic Adsorption equipment, and the concentration of sodium and calcium was determined.

The samples of clays mixed with 5 wt% NaCl solution as described above were tested at different times (seconds, hours and days). **Fig. 11** and **Fig. 12** show the Na and

Ca concentration over time for both montmorillonite and kaolinite. As can be observed from **Fig. 11**, for Na ions, the reaction time of about 150 hours was sufficient to establish equilibrium for montmorillonite in 5 wt% NaCl, while a more representative result is obtained for kaolinite. After 50 hours, Na concentration flattened out and stayed constant, showing that this is the time that is required for the complete reaction of kaolinite in 5 wt% NaCl solution to take place.

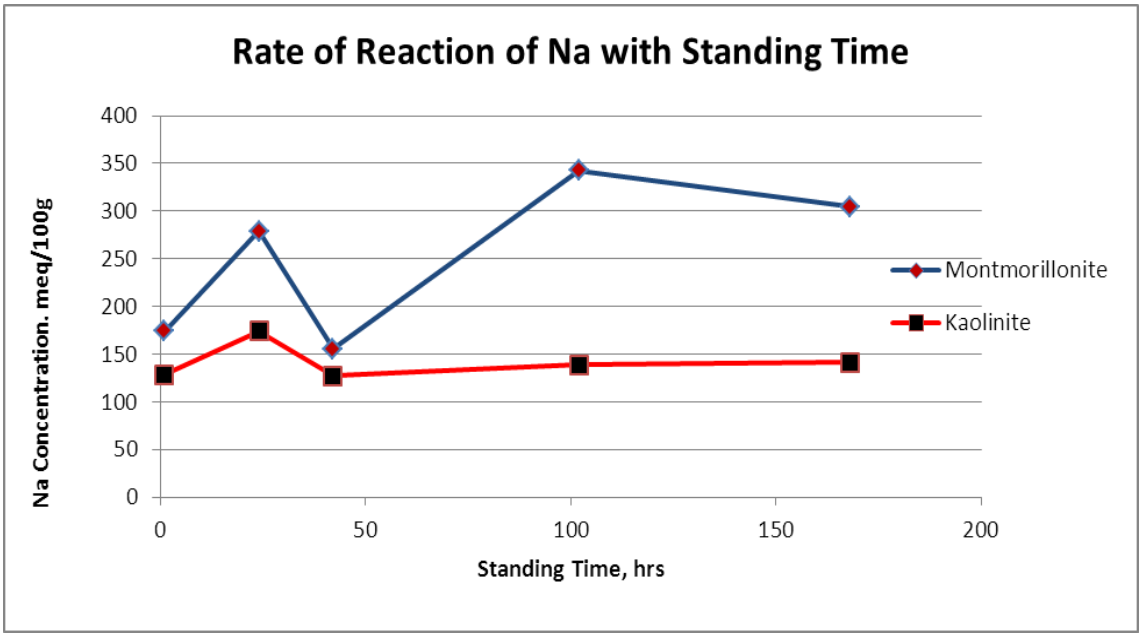

Fig. 11—Rate of reaction of Na with standing time.

Fig. 12 shows that for montmorillonite, reaction time is about 40 hours. After this time, the concentration values for Ca after 40 hours fall in one range of values- between 350 and 300 meq/100gram. For kaolinite, the equilibrium has been established already after a few minutes- time which took the clay particles to settle down and supernatant to

separate out. **Fig. 11** shows the accurate and consistent values of Na concentration for kaolinite clay reaction rate in 5 wt% NaCl.

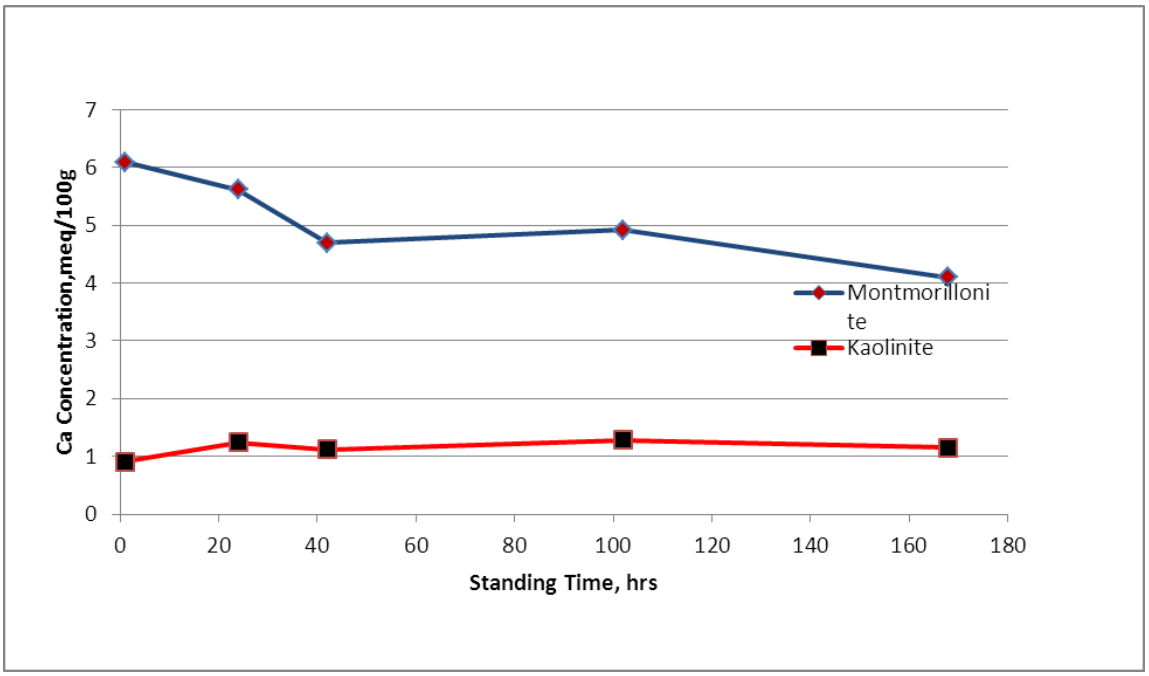

Fig. 12—Rate of reaction of Ca for standing time.

Therefore, combining the results of reaction time for both Na and Ca ion concentrations, it can be concluded that the reaction time for montmorillonite in 5 wt% NaCl is observed to be about 150 hours, whereas for kaolinite the reaction time is only 50 hours. Another outcome from conducted experiments is the average concentration of Na and Ca for both montmorillonite and kaolinite. For montmorillonite, the average of Na and Ca concentrations are 165 meq/100gram and 3.3 meq/100gram, respectively. For kaolinite, the average concentrations of Na and Ca are 140 meq/100gram and 1meq/100gram, respectively. For both clays, Na concentrations are much higher than Ca

concentrations because the original solution for mixing with clays used was 5 wt% NaCl.

The results show that montmorillonite is more reactive, and therefore it takes more time it takes for this type of clay to reach equilibrium, whereas kaolinite is much less reactive, and equilibrium is established faster. The reason for this observation may be in the structure, which is different for each clay.

Montmorillonite is 2:1 clay, with a silica-layer being sandwiched by two alumina- layers. It has different interlayer cations. In our experiments, we observed the presence of Ca in montmorillonite. This can lead to the conclusion that a type of montmorillonite has been used in Ca-montmorillonite which has Ca ions as interlayer cations which bond clay layers together. Kaolinite has a 1:1 alumina-silica structure, being bonded by hydrogen bonding, which is very strong, with no interlayer cations between layers.

For kaolinite, the exchange reaction takes place practically as soon as the contact is established. It can be implied that the exchangeable cations are held on the surface of the soil. Montmorillonite does not show stabilization in cation exchange, rather, it shows a decreasing Ca concentration with time, and Na concentration with time trends.

4.3 Summary

The exchange of free energies was estimated by treating the interlayer either as a concentrated alkali-halide solution or as an electrostatic attraction between two spheres.

Free energy calculation plots redeveloped and modified show that divalent cations are more effective for intruding clays due to high affinity to clays, and monovalent cations vary in their affinity to balance negative charge on clays. Rate of reaction for montmorillonite does not show stabilization after contact with Na and Ca cations, while kaolinite shows an early stabilization when reacting with the same cations. Therefore, the neutralization process becomes easier for kaolinite in a stable system, as opposed to montmorillonite.

5. STABILITY OF CLAY PARTICLES

5.1 Temperature effect

Based on these data it is possible to suggest that the increase of temperature should increase the stability of clay particles in suspensions. In sandstone, the temperature increase therefore, should stimulate clay particle dispersion from the mineral grains.

This conclusion is in an agreement with the experimental results obtained by Tchistiakov (2000). In spite of the fact that the effect of temperature on clay particles' stability and formation damage was intensively investigated in reservoir engineering, there is still no robust agreement between experimental results and the theory.

5.1.1 Earlier Investigation of the temperature effect

In many instances, field operations cause temperature changes in the formation. From a mechanical point of view, the change in temperature induces thermal expansion or contraction in the formation. The results of the effect of temperature on the rock permeability are conflicting in the literature.

From a chemical or physicochemical point of view, temperature is an important factor for rock-fluid interaction. Changes in temperature may induce inorganic and organic precipitation. In water-sensitive sandstone formations, the effect of temperature is significant (Liu et al. 1995). They concluded that permeability reduction is observed

with temperature increase and fines mobilization occurs repeatably at a particular temperature that varies with solution pH and ionic strength.

Schembre and Kovsek (2005) experimentally found that fines release from the pore walls takes place under conditions the elevated temperature, high pH, and moderate aqueous-phase salinity. The experiments were performed on Berea Sandstone rock at temperatures of 120 and 180°C at pH between 7 and 10 for moderate salinity (0.01M-0.05 M). Schembre and Kovsek (2005) concluded that permeability measurements showed reductions from 35% to 95%. Extreme, rapid reductions were attributed in part to the fact that cores were exposed to thermal shock. The permeability reduction might indicate the presence of the swelling clays or that of fine release occur, but they do not mobilize. The greatest reduction in permeability occurs when the fines are produced in the effluent (Schembre et al. 2006). In addition, Schembre et al. (2006) state that the mechanism of fines release provides a new mode of wettability alteration as a function of temperature.

Schembre et al. (2006) state after performing experiments that zeta potential becomes more negative as the pH and temperature increases. The fact that the zeta potentials are more negative results in greater repulsive forces. The results show that the forces between the clay and the surface become repulsive at temperatures only slightly greater than room temperature. Also, the quartz-illite system is more sensitive to changes in temperature, thus it is more prone to detachment than the quartz-kaolinite system (Schembre et al. 2006).

Zlotchevskaia R. I., Korolev V. A. (1988) performed the electro-osmosis measurements in Na-forms of kaolinite and montmorillonite which showed that the z-potential grows almost linearly when the temperature increases from 50°C to 70°C. The increase of the z-potential for kaolinite amounts to 40% and for montmorillonite reaches 55%.

Mungan (1995) experimentally showed that the brine (NaCl) damage does not depend on test temperature.

Khilar and Fogler (1983) studied the effects of temperature on permeability impairment in water-sensitive Berea sandstones, and found that permeability impairment becomes less severe as temperature decreases. Results also indicated that the particle capture coefficient is independent of temperature, whereas the release coefficient and temperature obey an Arriietihis-type relationship.

5.1.2 Introduction to the DLVO theory

The Derjaguin, Landau, Verwey, and Overbeek (DLVO) theory of colloidal stability is used in conjunction with laboratory, core-scale experiments to demonstrate that high temperature, alkaline pH, and low salinity are sufficient to induce fines mobilization (Schembre et al. 2005).

5.1.3 Evaluation of forces between clay particles and rock surface

In this thesis, the DLVO theory was applied to prove the effect of the observations of temperature effect on the permeability. The Excel file developed, and

graphical results are presented in **Figs. 14-18**. All calculations were done using the sphere-plate system presented in **Fig. 13** (Schembre and Kovscek 2004).

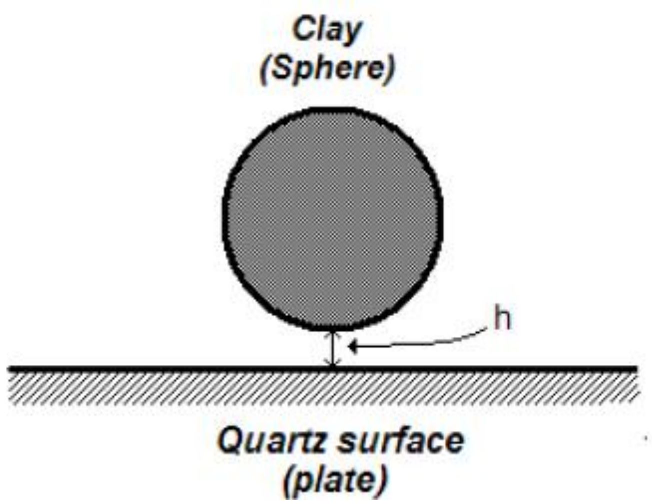

Fig. 13—The sphere-plate system for modeling fines stability (Schembre and Kovscek 2004).

Schembre and Kovscek (2004) in their paper state that stability or, on the contrary, detachment of the in-situ clay particles in a reservoir is determined by the balance between the forces affecting a clay particle in a reservoir. The interaction between a clay particle and a pore surface can be described by the following equation:

$$V_t(h) = V_{LVA}(h) + V_{DLR}(h) + V_{BR}(h) + V_{HR}(h) + V_{IHL}(h) \qquad (6)$$

Where V it total potential and subscripts represent: t-total; LVA, the London Van der Waals attraction; DLR, the double layer repulsion,; BR , the Born repulsion; HR, the hydrodynamic repulsion; and IHL, interfacial hydrate layer. The resulting potential of a clay particle is repulsive (unstable) if Vt is positive, and attractive (stable) if Vt is negative. London - Van der Waals attraction force has a negative sign, all other repulsion forces - a positive one (Tchistiakov 2000).

The Van der Waals dispersive forces are attractive. They play an important role with respect to intergranular and wetting behavior. The London Van der Waals potential for sphere-plate system is estimated numerically as (Hamaker 1937):

$$V_{LVA}(h) = -\frac{A}{6}\left[\frac{2(H+1)}{H(H+2)} + \ln\left(\frac{H}{H+2}\right)\right], \quad \text{.....(7)}$$

where H is the ratio of the distance of separation to particle radius (=h/r_p).

The Born repulsion, VBR (h), measures the short-range molecular interaction resulting from the overlap of electron clouds. It is suggested to follow the relationship (Kia 1987):

$$V_{BR} = \frac{A\delta^6}{7560}\left[\frac{8r_p + h}{(2r_p + h)^7} + \frac{6r_p - h}{h^7}\right] \quad \text{.....(8)}$$

The Double-Layer Repulsion forces can be computed using the formula (Schembre et al. 2006):

$$V_{DLR}(h) = \frac{\varepsilon r_p}{4}\left(\Phi_{01}{}^2 + \Phi_{02}{}^2\right)\left[\left(\frac{2\Phi_{01}\Phi_{02}}{\Phi_{01}{}^2 + \Phi_{02}{}^2}\right)\ln\left(\frac{1+\exp(-\kappa h)}{1-\exp(-\kappa h)}\right) - \ln(1-\exp(-2\kappa h))\right] \quad \text{.....(9)}$$

The potential of each surface, Φ_{0i}, is taken to be **ζi**, the electrical potential at the boundary between the Stern layer and the diffuse layer. In turn, the zeta potential is approximated by the Nernst equation (Schembre et al. 2006):

$$\varsigma_i = \Phi_{0i} = -2.3\left(\frac{kT}{e}\right)(pH - pH_{oi}) \quad \text{.....(10)}$$

The formula above was used to generate double-layer repulsion for T=74°F assuming a constant charge on the surface.

In a static fluid environment, fines are released from the solid when the interaction potential is zero (Schembre et al. 2006). The constants for the calculation of attractive and repulsive forces are displayed in **Table 2**.

Table 2—Parameters for calculations of electrostatic forces.

Parameter	Unit	Numerical Value
T	K	300
e	Coulomb	1.6E-19
n_b	mol/dm^{-3}	0.1
k-Boltzman	JK^{-1}	1.38066E-23
ε_d (water)[a]	dimensionless	81
ε_o (free space)	$Farad*m^{-1}$	8.85E-12
ε_p=4*pi*ε_d*ε_o	$Farad*m^{-1}$	9.0082E-09
z	dimensionless	1
κ (Debye-Huckel)	m^{-1}	1.17142E-05
M (5wt%NaCL)	M	0.1
pH	dimensionless	8
pH1_wall	dimensionless	7
pH2_particle	dimensionless	7.4
ς _clay[b]	V	-0.059540894
ς _rock	V	-0.035724536
δ	m	0.000000005
Φ_o1_wall[c]	V	-0.059540894
Φ_o2_particle	V	-0.035724536
T_o_1	K	366
T_o_2	K	422

a- Dielectric constant of water, varies with temperature (Clipper Controls):

Table 2 (Cont'd above)—Parameters for calculations of electrostatic forces.

Temperature,°C	Dielectric constant of water
0	88
20	80.1
40	73.3
60	66.7
80	60.7
90	57.9
100	55.3
200	34.5

b- Zeta potential values of both clay and rock were calculated using **Eq. 10**;
c- Surface potential values of the wall and the particle were obtained from **Eq. 10**.

The zeta potential, a function of temperature, is obtained by fitting values of zeta potential reported in the literature for different temperatures, materials and fluid conditions (Dai and Chung 1995; Pagneoux et al. 1998; Ramachandran and Somasundaran 1986; Revil et al. 1999; Somasundaran and Kulkarni 1973). The resulting correlation is:

$$\varsigma(T) = 0.01712((T - T_0) + 1) + \varsigma(T_0) \quad \text{.....(11)}$$

The total potential is equal to the summation of all three calculated thus allowing to determine the final behavior of the clay particle in relation with the rock surface.

$$V_t(h) = V_{LVA}(h) + V_{DLR}(h) + V_{BR}(h) \quad \text{.....(12)}$$

where Vtotal (h) - the resulting force of a clay particle – pore wall interaction (positive if repulsion dominates, and negative if attraction dominates).

5.1.4 Calculation of forces

All attractive and repulsive forces which exist in the matrix-clay model are calculated, and their profiles are presented in **Figs. 14-18**.

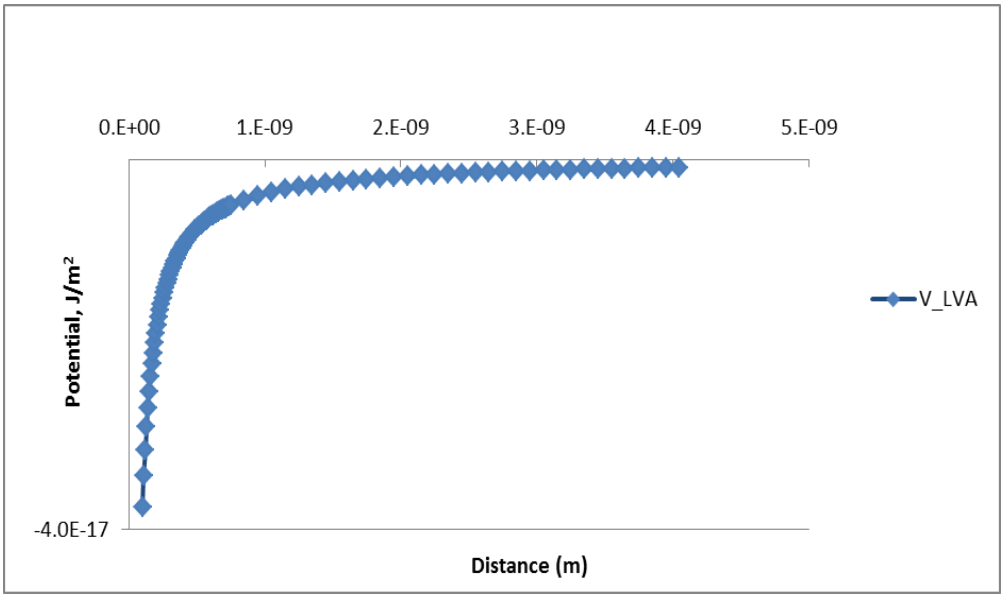

Fig. 14—London Van der Waals attraction potential increases and becomes nearly zero with a separation distance.

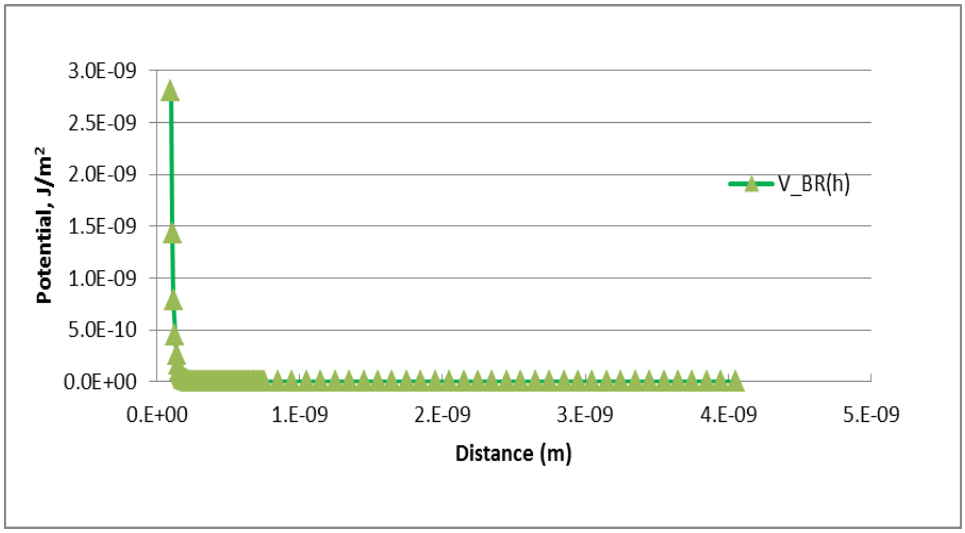

Fig. 15—The Born Repulsion potential shows a rapid decrease with a proximal distance to the rock surface after which the force becomes null with any further distance.

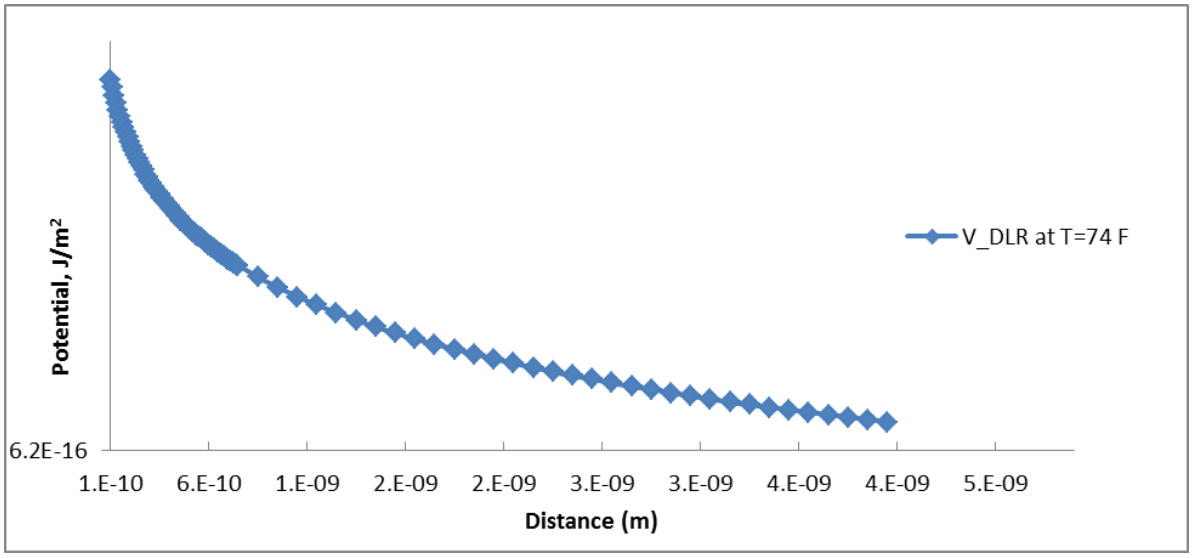

Fig. 16—The Double Layer Repulsion force between negatively charged clay particle and surface of the rocks weakens with a separation distance.

For the two elevated tested temperatures of 200°F and 300°F, the relationship of the zeta potential as a function of temperature was implemented and the DLR curves at different temperatures were generated.

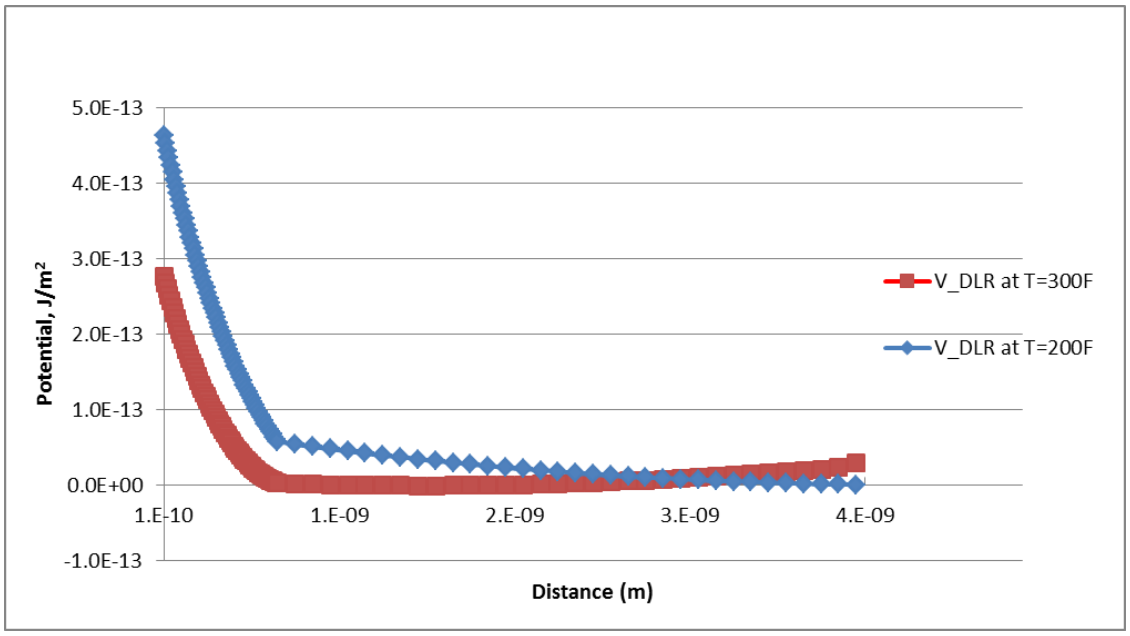

Fig. 17—The double layer repulsion profiles at two elevated temperatures show a rapid decline at a small separation distance following a gradual decline for 200°F and increase for 300°F.

As shown in **Fig. 17**, from the two curves of Double-Layer Repulsion (DLR) potentials at 200°F and 300°F, the following can be concluded:

The 200°F DLR trend shows a rapid decline of the repulsive force at the minimal distance range from the 1E-10m to 1E-9m, after which the repulsive double-layer force gradually decreases to nearly zero with increasing distance between the clay particle and the rock surface.

This shows that the negative repulsion between the clay particle and rock has no significant effect after the interval of the intensive repulsion force decline. The clay particle may be in a dispersed state if the bulk system is in the equilibrium. For the 300°F DLR trend there is a rapid decline at the same range as for the 200°F DLR curve at the beginning. Then the DLR at 300°F starts to increase from nearly 1E-9 m. The

increase in the repulsion DLR forces shows that the clay particle will detach after passing the turning point nearly 1E-9 m distance.

The fines migration becomes a real potential problem as the temperature is being increased.

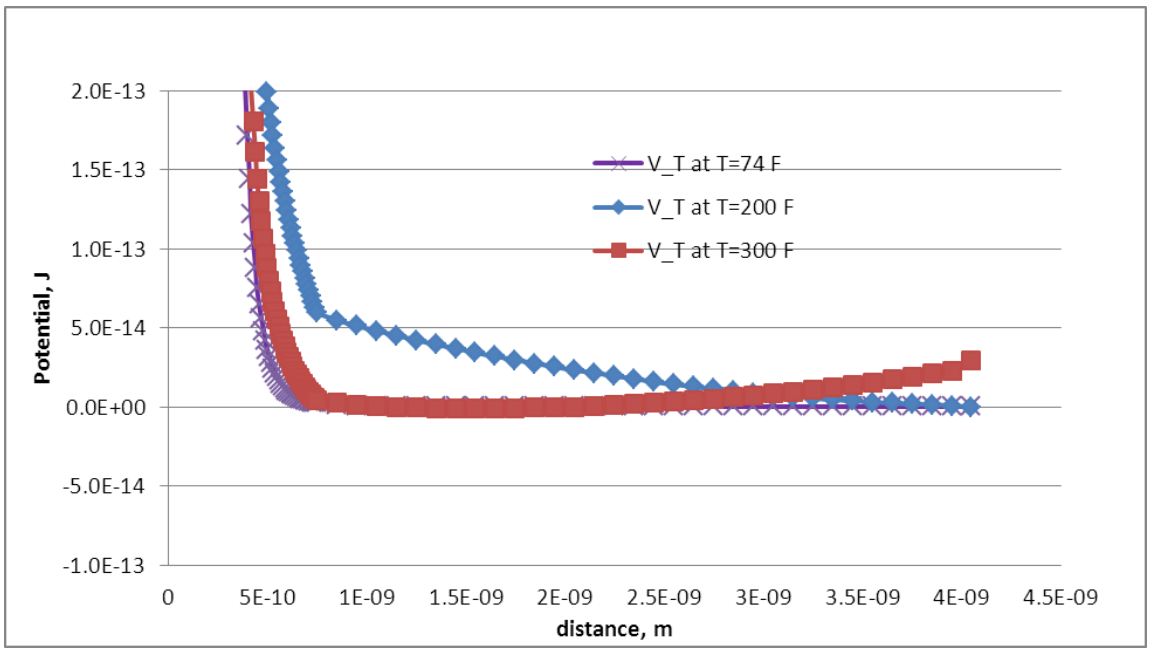

Fig. 18—Three total summing forces show the initial decline at an increasing distance between negatively charged surfaces , after which only the total force at 300°F displays following increase (detachment occurs).

5.1.5 Results

As shown in **Fig. 18**, the 200°F total potential shows a rapid decline to the nearly the same point as for 74°F profile. However, past that point the total potential starts to decline gradually and gets nearly zero. As for the total potential curve at 300°F, the trend displays the same rapid decrease behavior to the zero value, after which the potential has

a gradual increasing behavior, meaning that the repulsive force will dominate thus causing clay particles to disintegrate from the rock surface at an elevated 300°F temperature.

The results of the coreflood experiments show that increase in temperature accelerates the fines migration process, thus damaging rock permeability.

5.2 Salinity Effect

Generally, if other physico-chemical conditions (moisture, temperature, particle size, pH, surface potential) are constant, the increase of salt concentration causes reduction of the double ionic layer and a decrease of the zeta-potential (Gregory 1989). This is explained by the fact that if the salt concentration in the pore solution increases, some of the cations move from the diffuse layer to the adsorption layer and consequently, the zeta-potential decreases (Tschistiakov 2000).

For the Na-form of the minerals, a possible mechanism that would increase the zeta-potential may be the following. While only distilled water is present in a pore medium, some of the H+ diffuses to the exchange complex of clay minerals. The permeating of NaCl solution causes exchange of some H+ for Na+ which leads to increase of the clay zeta potential. Further increase of NaCl causes successive reduction of zeta-potential. A similar mechanism can be suggested for polyvalent form of clay

minerals (Tchistiakov 2000). Higher salinity brine induce flocculation that results in a dramatic clay particle agglomeration (Bishop 1997).

In this presented work, experiments with different (both high and low) concentrations of brine (salt water) were performed with analysis presented in the Experimental part.

5.3 Cation Fixation in Clays

Schembre and Kovsek (2005) showed that temperature increases fines release under conditions of alkaline pH and moderate salinity. The experiments were performed on Berea sandstone rock at temperatures of 120 and 180°C at pH between 7 and 10 for moderate salinity (0.01-0.05 M). Schembre and Kovsek (2005) concluded that permeability measurements showed reductions from 35% to 95%. Extreme, rapid reductions were attributed in part to the fact that cores were exposed to thermal shock.
In kaolinite crystal, there is a minimum of four possible types of crystal where one may expect adsorption of cations and anions. There are Al^{3+}, Si^{4+}, O^{2-} and $(OH)^{-}$. Consideration of the bond energies results in the following replacement series
$L^{+} < Na^{+} < NH_4^{+} < K^{+} < Mg^{++} < Ca^{++} < Al^{+++} < H_2O^{+}$ (Lawrence 1958). This series means that it is harder to replace a cation with a smaller hydrated radius than one with a larger hydrated radius.

The ionic radius of NH_4^{+} is between 0.136 nm (Aranda and Ruiz-Hitzky 1999) and 0.143 nm (Pironon et al. 2003). This radius is close to the radius of K^{+} and Rb^{+} ions (Shannon 1976). The hydrated radii values are summarized in **Table 3**.

Table 3—Hydrated radii for different cations (Kieland 1937).

Cations	Hydrated ionic radii, A
Na+	4-4.5
K+	3.0
NH_4+	2.5
Mg+	8.0
Ca++	6.0
Al+++	9.0

The addition of an acid salt causes the exchange reaction shown by **Eq. 13:**

$$ClayOH - H + NH_4Cl \Leftrightarrow clayOH - NH_4 + HCl \quad \text{.....(13)}$$

Cl acid is one of the reaction products, therefore it will cause the decrease in the pH value (Johnson and Norton 1941).

The addition of a neutral salt slightly changes the by-product as shown in **Eq. 14**:

$$Clay - OH - H + NaCl \Leftrightarrow clayOH - Na + HCl \quad \text{.....(14)}$$

The formation of the sodium-clay again has been brought about, but, as a by-product, an acid will be always the result.

5.3.1 Kaolin-NH_4Cl system

The ions present formed by the dissociation of NH_4Cl and the consequent hydrolysis result in OH^-, NH_4^+, Cl^-, and H_3O^+ ions. The large radius of the chloride ion (1.81 nm compared with 0.32 nm radius for OH^-) makes a large misfit within the kaolinite structure. The repulsion by the negative surface of clays and other anions results in no bonding of chloride ion in the system. The hydroxide OH^- ion will be adsorbed on the cation sites. The kaolin surface will adsorb OH^- and H_3O^+ ions which form the neutral water structure with no development of the charge. The NH_4^+ ion will

be present in far excess of the H_3O^+ ion and owing to the mass-action effect will satisfy the negative sites (Lawrence 1958).

Thermal energy always keeps the ions surrounding kaolinite in a state of motion and the ions having the lowest bond energy are broken away and replaced by similar or different cations, therefore the negative sites on the crystals are never satisfied. For a given saturation of electrolyte as the temperature increased, the charge on the particle should be increased

The number of negative sites on the crystal that are neutralized by the adsorption of cations at any given time will depend on temperature and on the mass-action effect. The original model of evaluation of charge in kaolinite in water system (Lawrence 1958). This model was modified to account for higher temperatures and for a presence of different electrolyte solution as shown in **Fig. 19.**

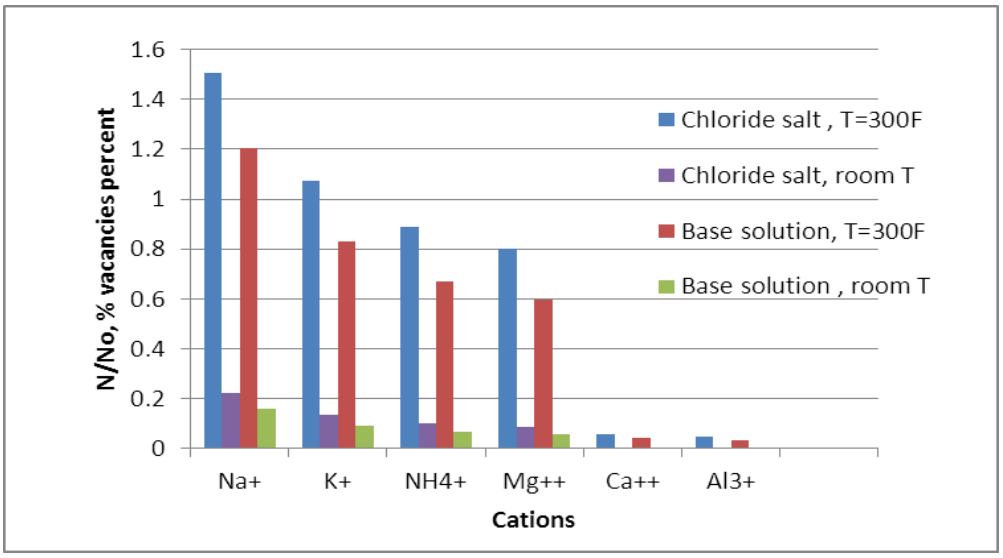

Fig. 19—Evaluation of charge in kaolinite in water system model modified from Lawrence (1958).

From the model presented several conclusions can be derived. First of all, higher temperature results in an increasing number of unsatisfied negative sites in kaolinite in water system. Another conclusion is that as the valence of the cation increases, the attraction forces between cation and anion sites will increase which is favorable for clays stabilization in place.

Complexes of tetravalent zirconium with organic acids, such as citric, tartaric, malic, and lactic acids, and a complex of aluminum and citric acid have been claimed to be active as dispersants (Fink 2003)

5.3.2 Zirconium lactate clay stabilizer

The greater the number of positive charges present in the atmosphere, the closer the platelets will be held together. In his discussion of the Schulze-Hardy rule, however, von Olphen states that when comparing different cations as clay stabilizing agents, the concentration becomes secondary in importance to the valence of the respective cations. The higher the valence of ions, the greater their flocculating power and hence, the lower their flocculating concentration. According to von Olphen, this difference of one positive charge per ion will result in a several-fold increase in flocculating ability.

Permeabillity damage caused by clays can be minimized by stabilizing clay particles to prevent dispersion.

The hydrolysable metal ion zirconium carries a charge of +4. According to the Schulze-Hardy rule, the additional charges per ion alone would make zirconium many times more effective as a clay stabilizer than the divalent cations. In aqueous solutions,

however, zirconium salts hydrolyze to form polynuclear ions that perform as ions of much higher charge, as shown in **Fig. 20** (Peters and Stout 1977).

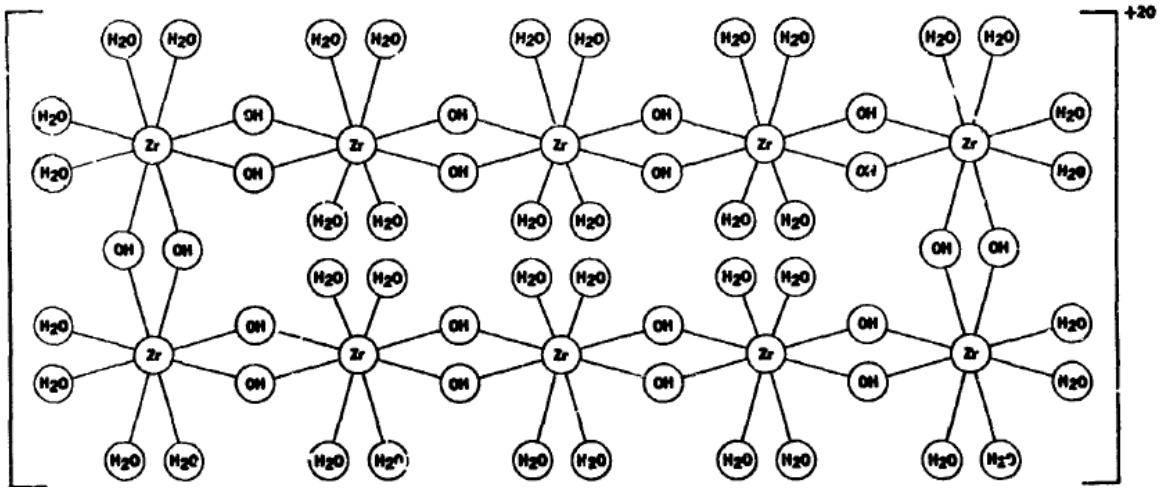

Fig. 20—One of the forms polynucluear zirconium ions.

The experimental work was done to test zirconium salts. Peters and Stout used a Berea sandstone core, and injected the following series of fluids: hexane and iso-propanol (to clean the core), 3% $CaCl_2$ followed by $ZrOCl_2$ solution, followed by distilled water and 3% NaCl brine. The permeability drop was minimized dramatically to only about 5%, while 95% permeability drop was observed when using brine solution after calcium chloride solution. It also was noted that the zirconium ion permanently replaced other cations and no further damage was caused, regardless of the type flowed through the core.

5.4 Effect of pH on Kaolinite

The zeta potential of the Na-kaolinite is sensitive to temperature changes in the system. The zeta potential becomes more positive at acidic pH and more negative at alkaline pH with increasing temperature (Ramachandran and Somasundaran 1986).

The kaolinite temperature response can be understood in terms of the processes taking place in the system and the different species active in a given pH range. For alkaline pH values, zeta potential is negative and tends to stabilize for larger pHs. This result can be understood in terms of the activity of Al^{3+}, which is very high in the acidic region and decreases rapidly with increasing pH, a change of 16 orders of magnitude for the studied pH range (from 2 to 9). In the alkaline region the major species are $H3SiO_4^-$ and $Al(OH)_4^-$ and their adsorption causes the mineral to be highly negatively charged, resulting in a negative zeta potential. For acidic pH values the mineral surface is in fact more positively charged at higher temperatures. This could be attributed to dissolution and readsorption of Al^{3+} and $Al(OH)^{2+}$ species, which have a high activity in this pH range. For pH values near the neutral range the releVant species are $Al(OH)_3$, H_4SiO_4, and $H3SiO_4^-$. The net negative potential on the surface is attributed to the adsorption of $H3SiO_4^-$, which is the only charged species that is active (Rodriguez and Araujo 2006).

6. COREFLOOD EXPEREIMENTS

Coreflood experiments were conducted in order to simulate reservoir conditions of the experiment. The presented laboratory experiments are performed on the Berea sandstone rock, and the maximum temperature of 300ºF is applied.

6.1 Coreflood Laboratory Procedure

A schematic diagram of the coreflood setup is presented in **Fig. 21** (El-Monier et al. 2010). The diagram includes a core holder. Also, three vertical vessels also called accumulators were connected in parallel to the holder and can be loaded with a maximum of 2 liters of the solution. In this experiment, only two of three vessels were used and filled with brine and fresh (DI) water. The experiment was performed at three different temperatures: 74°F, 200°F, and 300°F. The rock sample was Berea sandstone. Brine solution was prepared 5 wt% of NaCl and mixed for 20 min with a high speed magnetic stirrer. The core was first dried in the oven at 160°F for two hours, and then saturated with 5 wt% NaCl brine overnight. The pore volume of the core was calculated using taken dry and brine weight measurements. After that, the core was inserted inside the core holder, and a confining (overburden) pressure of 1500 psi was applied around the core to control the flow with a back pressure of 1000 psi. A brine, and later fresh water at an injection rate of 5 cc/min was maintained at all stages of the experiment. This rate was assumed to be very low so it would not induce any fines migration.

After the core sample was inserted in the core holder, the newly-prepared 5 wt% brine solution was injected until the pressure drop on the monitor was stabilized. After stabilization, the vessel with brine solution was closed, and simultaneously the vessel with fresh (DI) water was opened. The pressure drop was monitored by the program LabView at each stage, recorded, and used further to calculate rock permeability from the stage of stabilization.

If any other salt was tested, such as higher saline water, ammonium chloride, or zirconium lactate clay stabilizer, then after initial injection of 5 wt% NaCl solution, the testing solution was injected, and after this, fresh water would be finally injected to assess the effectiveness of the testing solution with respect to a damage that is fines migration which is caused by injection of fresh water.

XRD (X-Ray diffraction) analysis of the Berea sandstone sample is present in **Table 4**. The sandstone rock sample contains kaolinite clays in majority- 5 wt%, among other clay minerals present such as illite (1 wt%) and chlorite (2 wt%). The presence of aforementioned clays and their morphology is confirmed by elemental analysis and visual characterization with a Scan Electron microscope (SEM) instrument. Obtained results are presented in **Figs. 22-24**. The images were obtained using Berea sandstone. The sample was crushed and copated with carbon, after which the sample was analyzed using SEM under a high magnification, up to 10000X.

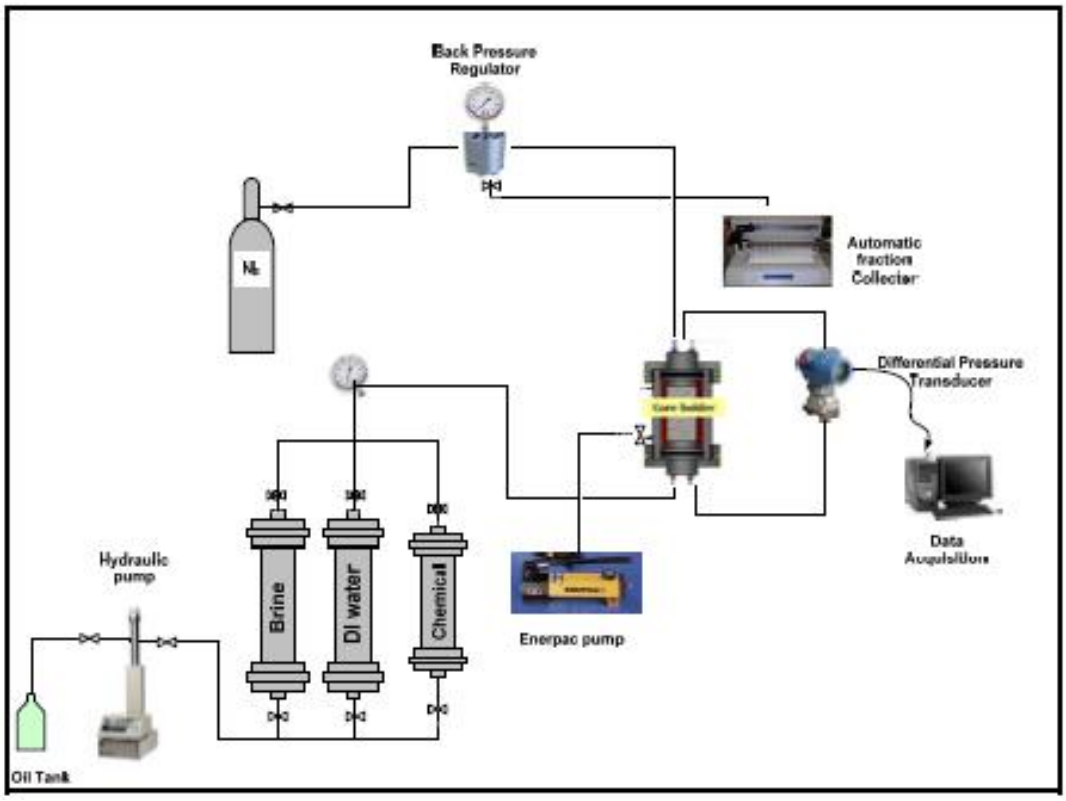

Fig. 21—Coreflood testing setup.

Table 4—XRD analyis of the Berea sandstone rock sample.

Mineral	Berea sandstone, wt%
Quartz	86
Dolomite	1
Calcite	2
Feldspar	3
Kaolinite	5
Illite	1
Chlorite	2
Plagioclase	--

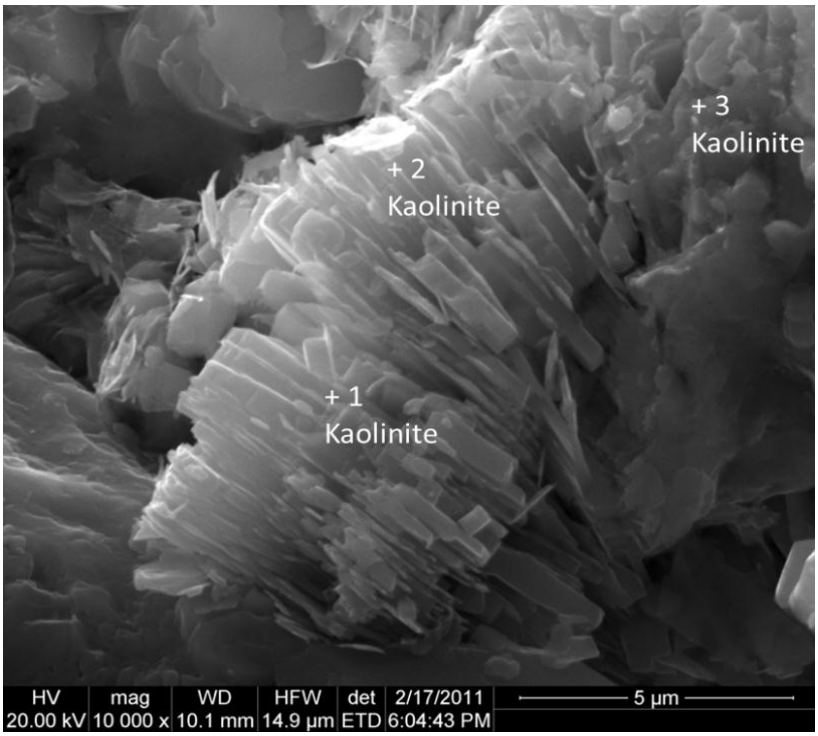

Fig. 22—SEM imaging tests results. Presence of kaolinite in Berea sandstone is determined.

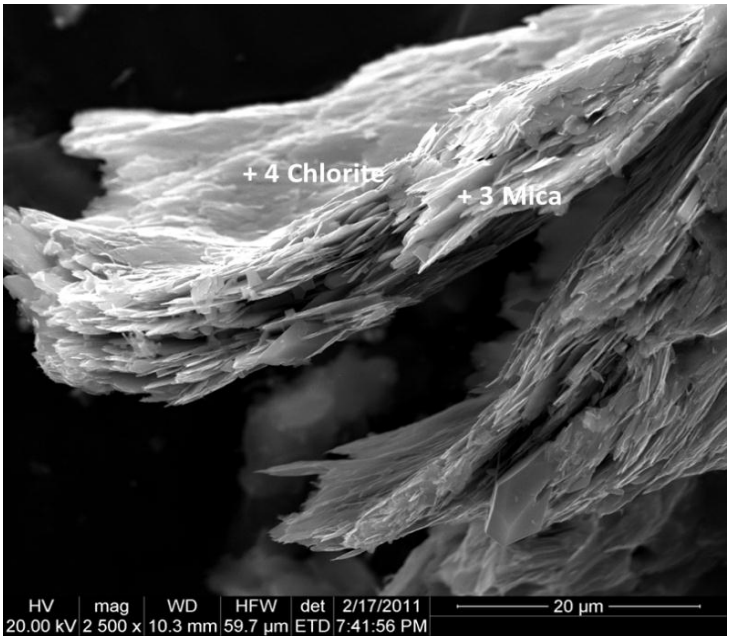

Fig. 23— SEM imaging tests results. Presence of chlorite and mica in sandstone are determined.

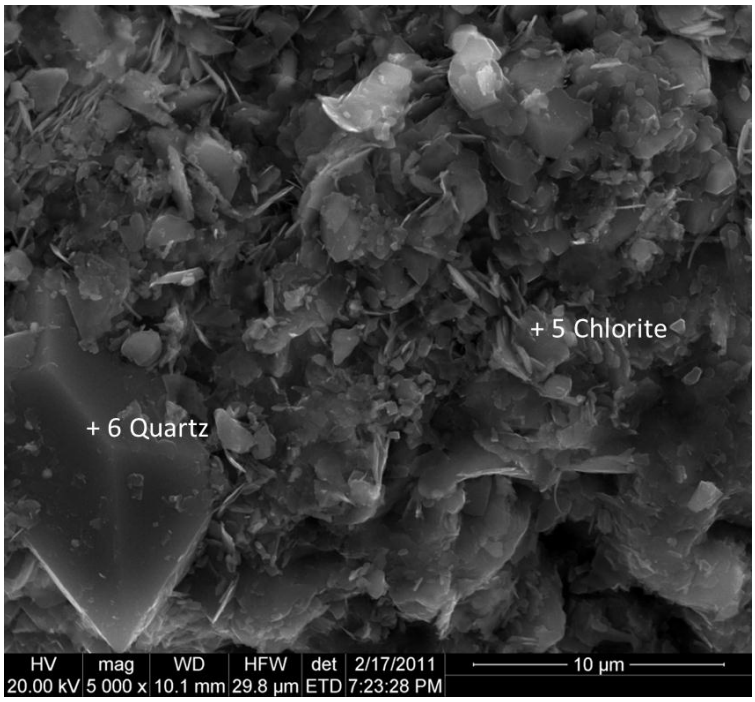

Fig. 24— SEM imaging tests results. Presence of quartz and chlorite in sandstone are determined.

The brine 5 wt% of NaCl was injected first, and the stabilization of the pressure drop was recorded. Darcy's Law in oilfield units system states that

$$K = 887.2\frac{q\mu L}{A\Delta p} \quad \text{.....(15)}$$

The Atomic Adsorption instrument was used to measure the concentration of the sodium in the samples collected after the three coreflood experiments.

6.2 Effect of Temperature on Permeability

The experiment conducted aimed to analyze another important parameter which is temperature. Temperature differs for different sandstone formations.

6.2.1 Objective

The main objective of the conducted coreflood experiments was to observe the effect of the saline and fresh water on the permeability of the rock at different temperatures such as 74°F, 200°F, and 300°F. The rock sample tested was Berea sandstone rock containing clay minerals present.

6.2.2 Materials

Berea sandstone cores of 6 in in length and 1.5 in. in diameter were first dyed in the oven at a temperature of 160°F, and then saturated in 5 wt% NaCl. Difference in measured weights allowed the determination of porosity of rock matrix. Working solution for coreflood was 5 wt% NaCl, and of saline solution 5wt% NaCl was measured to be 1.034 g/cc. Porosity was calculated and the porosity values are 10.9%, 11.1 %, and 11.3% for the cores, respectively.

6.2.3 Results

Figs. 25, 26, and 27 show a similar trend of the pressure profile. The initial injection of brine results in the pressure stabilization after time, from which further rock permeability can be determined. As the pressure in the system stabilizes, the following fresh water injection in the core takes place. The injection rate is maintained the same, 5 cc/min, however the pressure response becomes different. DI water injection causes a shock effect on the pressure profile with a rapid increase in pressure that represents significant damage for rock permeability.

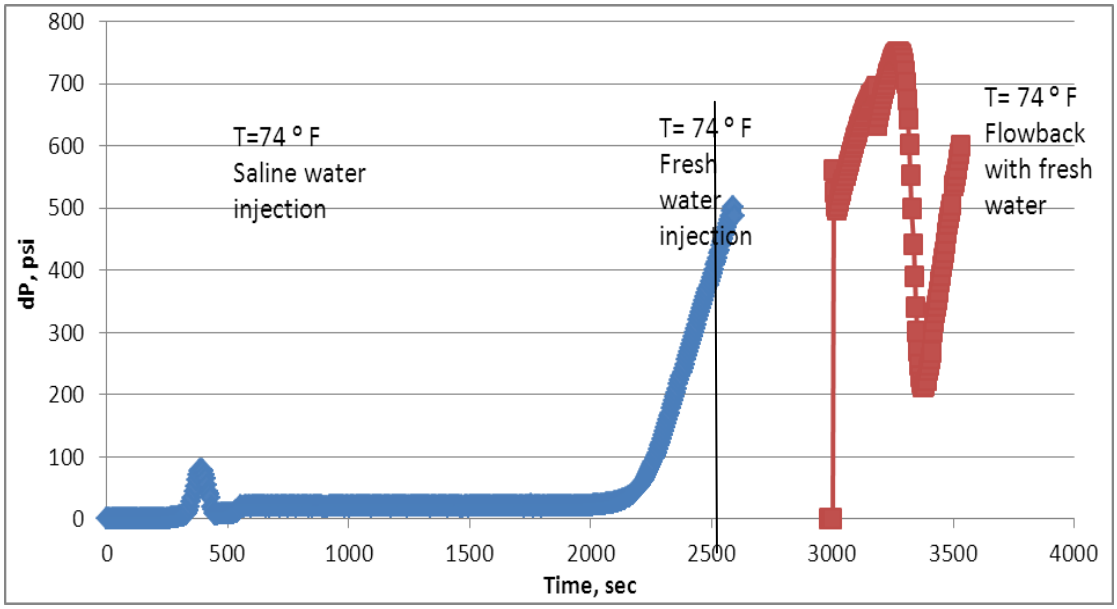

Fig. 25—Pressure profile for sandstone core showing injection of brine following fresh water injection at T= 74°F.

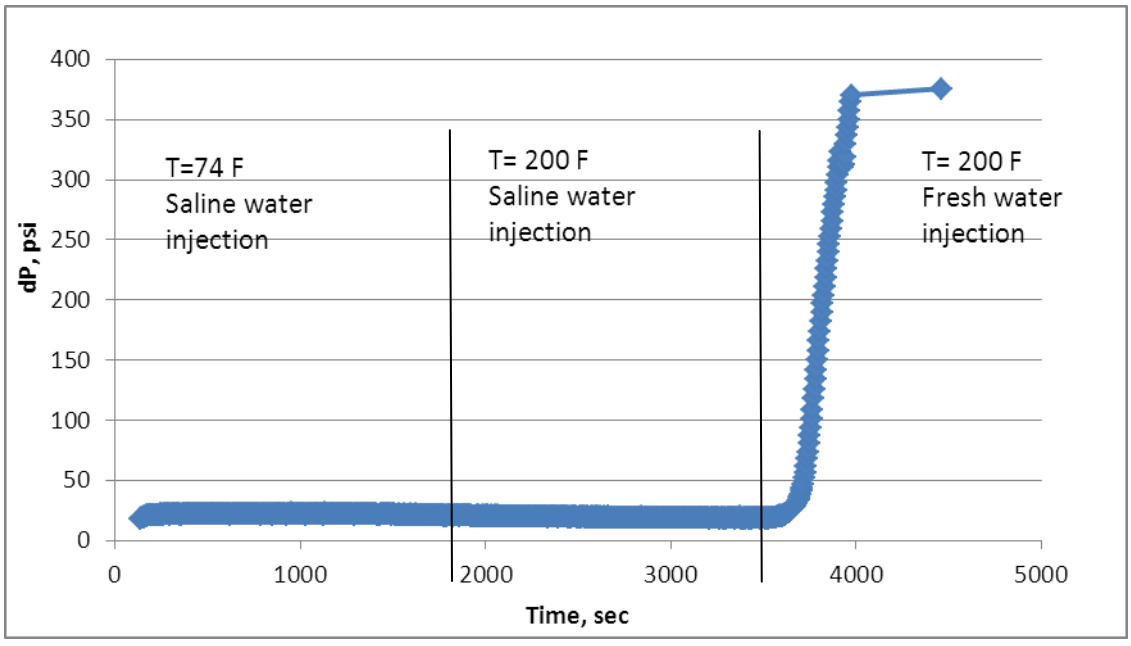

Fig. 26 —Pressure profile for Berea sandstone showing brine at T= 74°F injection, following brine at T=200°F, with final fresh water injection at T= 200°F.

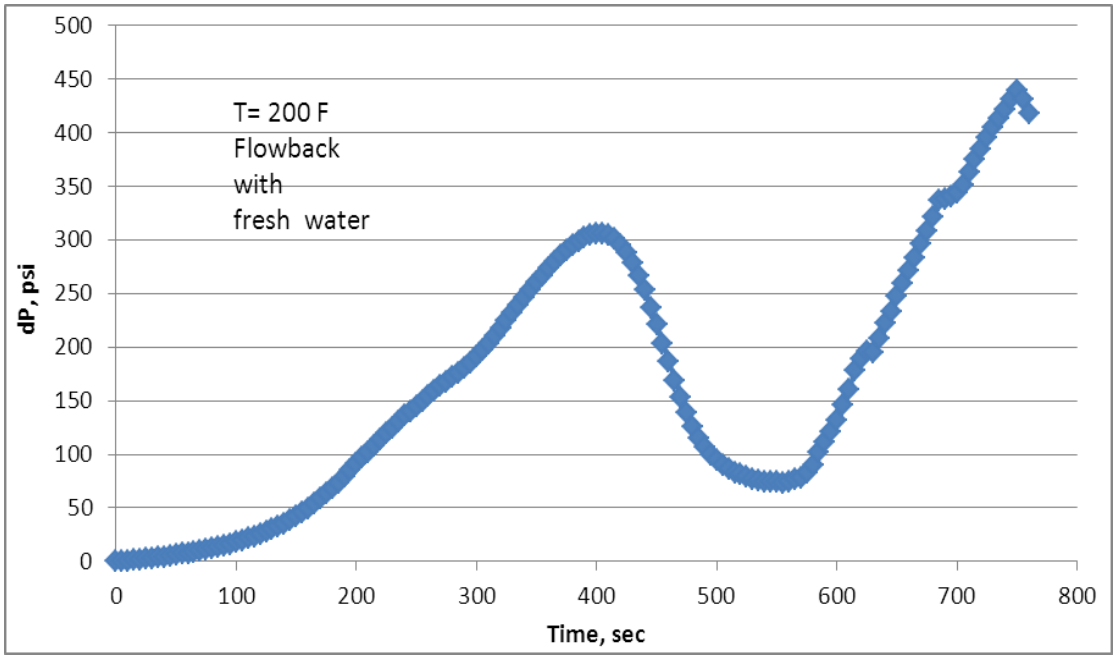

Fig. 27—Pressure profile during flowback at T= 200°F for Berea sandstone core.

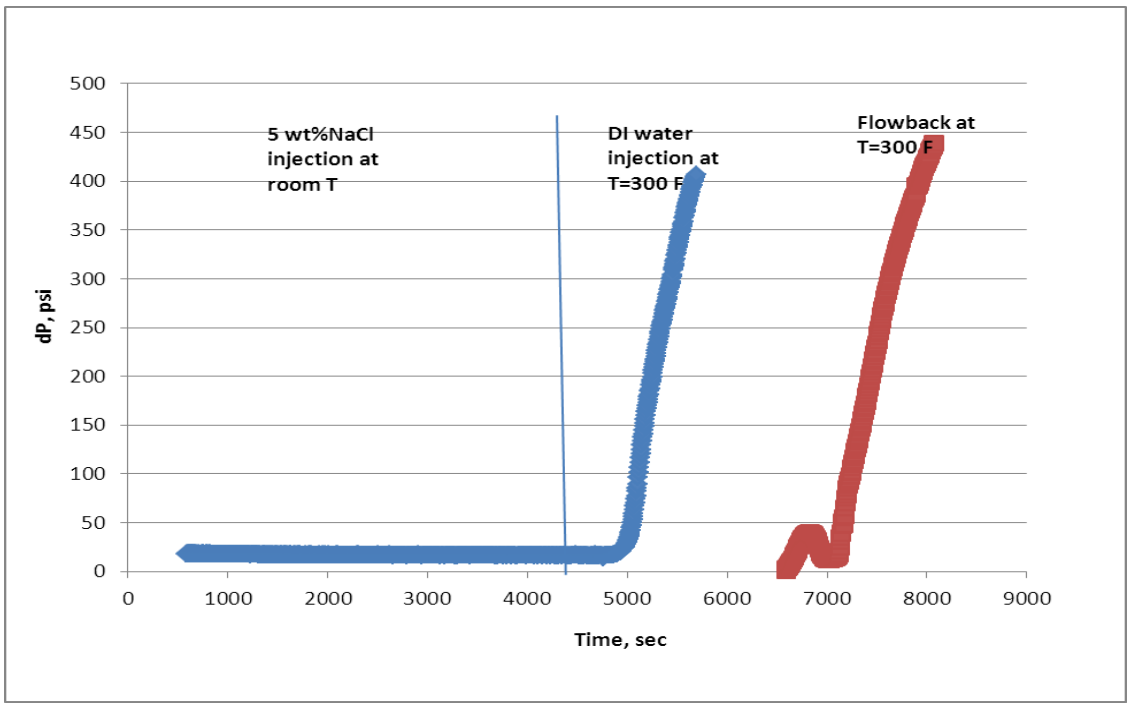

Fig. 28—Pressure profile for sandstone core at elevated temperature T=300°F, showing injection of brine following fresh water injection, and flowback at T=300°F.

Analyzing the pressure profiles obtained, saline water injection stabilizes pressure drop in the core, and does not change pressure drop significantly after the system is heated to a higher temperature. Positively charged sodium ions in brine solution tend to neutralize the negatively charged clay particles in the system. In other words, the presence of electrolytes in the system minimizes detachment of the clay particles from the rock, thus reducing clays' dispersion and increasing stability and preserving permeability. However, fresh water injection shows a different trend for pressure. The impairment of the permeability is displayed by a rapidly increasing pressure trend after injection of fresh water as shown in **Figs. 22, 23, and 24**. The possible explanation for this pressure profile behavior is that the sandstone rock mineral contains clays which get dispersed under water flooding conditions. In particular, kaolinite gets dispersed by discrete particles, and illite gets dispersed by pore bridging when the system in not in the equilibrium. The weak bond between the crystals permits water molecules to enter and expand the distance between the clay crystals. In general fresh water and sodium ions tend to swell expandable clays, but potassium and calcium ions tend to shrink them (Zhou et al. 1997).

The permeability of the rock can be estimated when injecting brine in the system, whereas a significant drop of the permeability of the sandstone rock takes place when injecting fresh (deionized) water. The fresh water injection profile shows a continuous decreasing trend for pressure in **Figs. 25-27**. Permeabilities were calculated at both room temperature and when the system was heated. **Table 5** displays the permeability values at various temperatures.

Table 5—Calculated rock permeabilities.

permeability at T=74°F	K, md	permeability after heating	K, md
core2, T=74°F	80.8	core 2, T=74°F	80.8
core3, T=74°F	68.9	core 3, T=200°F	24.2
core 4, T=74°F	73.2	core 4, T=300°F	10.3

Viscosity of 5 wt% NaCl aqueous solution profile is shown in **Fig. 29.** To generate this profile, the capillary viscometer was used to measure viscosity at different temperatures. Two trends- measured and from correlation- were plotted to get a correlation for viscosity as a function of temperature. The correlation was chosen such that viscosity y of water will be corrected with salinity which is 5 wt% of NaCl, temperature (200°F and 300°F), and –pressure (formation pressure) effects.

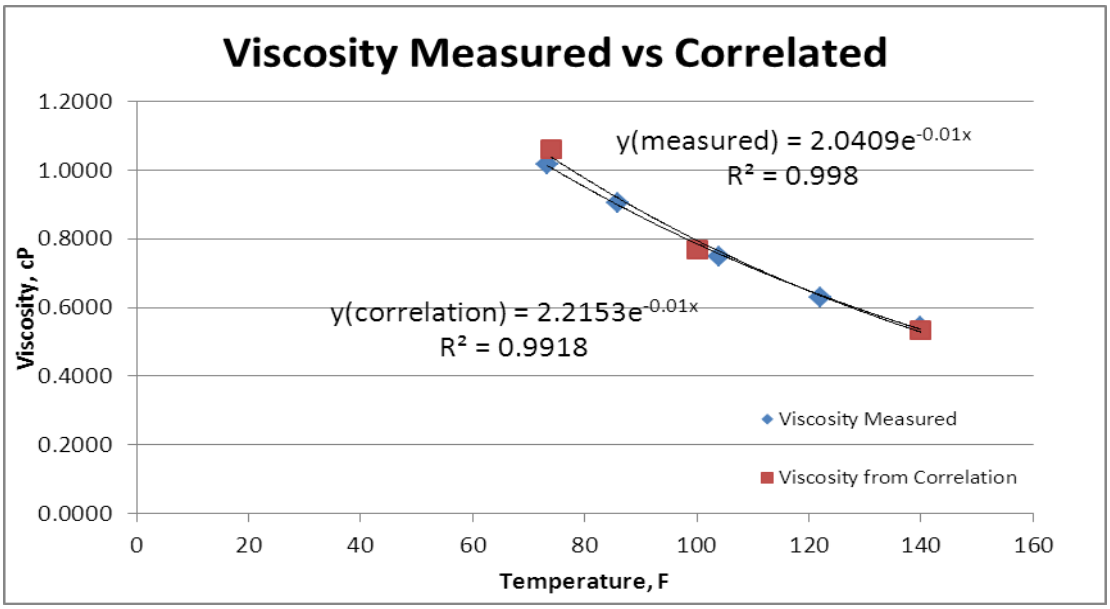

Fig. 29—Viscosity trends for 5 wt% NaCl aqueous solution obtained from measurements and using an existing correlation.

6.2.3.1 Fresh water injection

Table 6—Fresh water volume injection.

T ,F	V, fresh water injected, cc	PV inj
74	37.5	0.51
200	18.6	1.02
300	12.5	1.5

Figs. 25, 26 and 28 show the injection of fresh water after brine injection at different temperatures. The pressure profile shows a rapid pressure drop increase which shows that the damage takes place in the sandstone core, and no fluid can be produced. The numerical values for pore volume injected are presented in **Table 6**. From the results it can be concluded that permeability damage starts to take place earlier for the system at 300° F. This result supports the idea that fines migration causes permeability damage when clay particles start to move and plug pore throats in the rock.

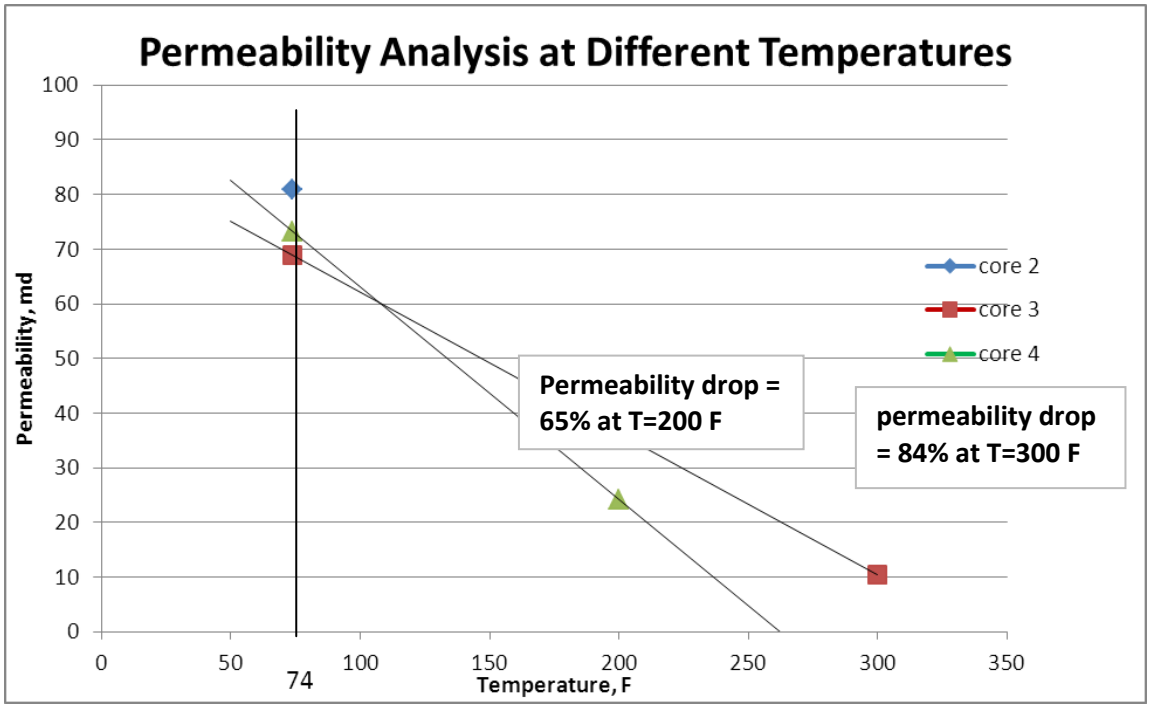

Fig. 30 —Permeability analysis of three core samples at different temperatures.

As shown in **Fig. 30**, injection of saline water at higher temperatures such as 200°F and 300°F causes a permeability drop for both cores. The analysis shows that a permeability drop measured at lower 200°F is less than permeability drop measured at 300°F. The decreasing trend of permeability with temperature can be explained by the increased rate of fines dispersion that block permeability.

6.2.3.2 Flowback

The flowback was done during the coreflood experiments in order to confirm the fact that clay particles induce fines migration in the rock and reduce the rock permeability. Three coreflood experiments were performed with a similar injection

scenario. First, the brine was injected at room temperature to determine the essential rock permeability. Next, the temperature was applied to the system, if needed, and brine was injected at a new temperature. After the new profile picture was recorded, the fresh water flooding was started. After a shock effect by fresh water injection took place, the direction of the fresh water injection was reversed. Once the flowback started, the permeability of the damaged core started to increase, then restore gradually.

The permeability with the reversal flow can be explained by assuming that clay particles come off the pore walls and migrate in the direction of flow until they are trapped by a pore throat. Obstruction of the sandstone pore throat in turn reduces the permeability of the core. When the flow of fresh water is reversed, the clay particles blocking the pores are dislodged and remain dispersed in a peptizing environment of fresh water. As a result, permeability temporarily increases. The particles then flow with the fluid until they reach another pore throat and block the constriction in the opposite direction, thereby reducing the permeability (Khilar and Fogler 1983).

6.2.3.3 Core effluent analysis

The core effluent test is conducted in order to verify the fines migration problem. Individual ion concentration can be measured. In our work, the concentration of sodium cations was measured. Collected effluent solutions were filtered and analyzed to verify the presence of clays migration.

Initial concentration of the brine solution (5 wt% NaCl) is 50,000 ppm. At 300°F, sodium concentration increases from about 15,500 ppm up to 25,000 ppm. This

significant increase shows that injection ions of sodium from injected brine were not effectively consumed by the clay particles for the stability, but rather these sodium ions will be present in the free solution. For other cases of 74°F and 200°F, the sodium concentration change happen at nearly 20,000 ppm and the increase is about 1000 ppm at both temperatures. These two trends may be explained so that injected brine was used up by the clay particles which are naturally negatively charged to neutralize the deficient charge on clays' surface.

6.2.4 Summary

The stability of the clay particles, in particular, the fines migration problem is affected by temperature change. Permeability retention of core changes with varying temperature. From experiments it is observed that with the increase of the temperature, permeability retention decreases, meaning that damage of the permeability due to fines migration occurs at a faster rate.

6.3 Effect of Temperature and Core Effluent Analysis

The analysis of the core effluent solution is presented, and the processes are explained accordingly.

6.3.1 Objective

The main objective for the experiment performed was to investigate the effect of temperature and core effluent analysis.

6.3.2 Materials

Three cores of Berea sandstone were saturated in 5 wt% NaCl overnight. The three coreflood experiments were run at room T (74°F), 100°F and 200°F. The values of permeabilities were measured, and the core effluent was collected.

6.3.3 Results

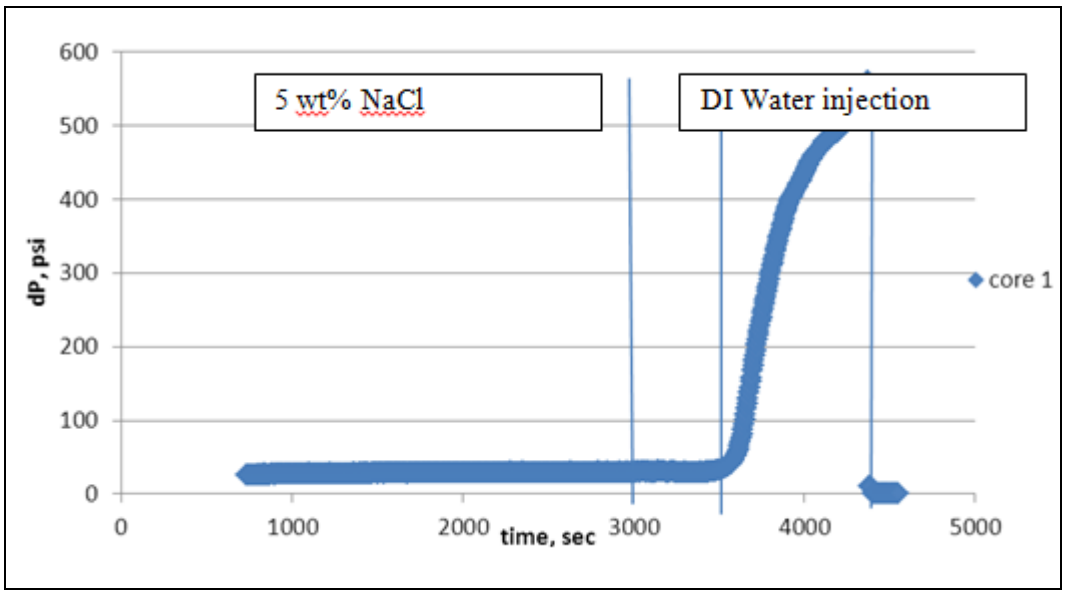

Fig. 31—Pressure drop profile for Berea sandstone at room T=74°F.

The **Figs. 31-33** show that pressure is stabilized when saline water is being injected. This implies the fact that clays do not block the pore throats in the saline environment. In this experiment as stated above, 5 wt% NaCl was used. The future research will include conducting coreflood experiments to investigate the effect of different salinity waters on permeability of sandstone.

DI water injection starts at time of 5940 sec at T=100°F as shown in **Fig. 26**. The amount of water having been consumed before the pressure drop increase occurs is shown in **Table 5.**

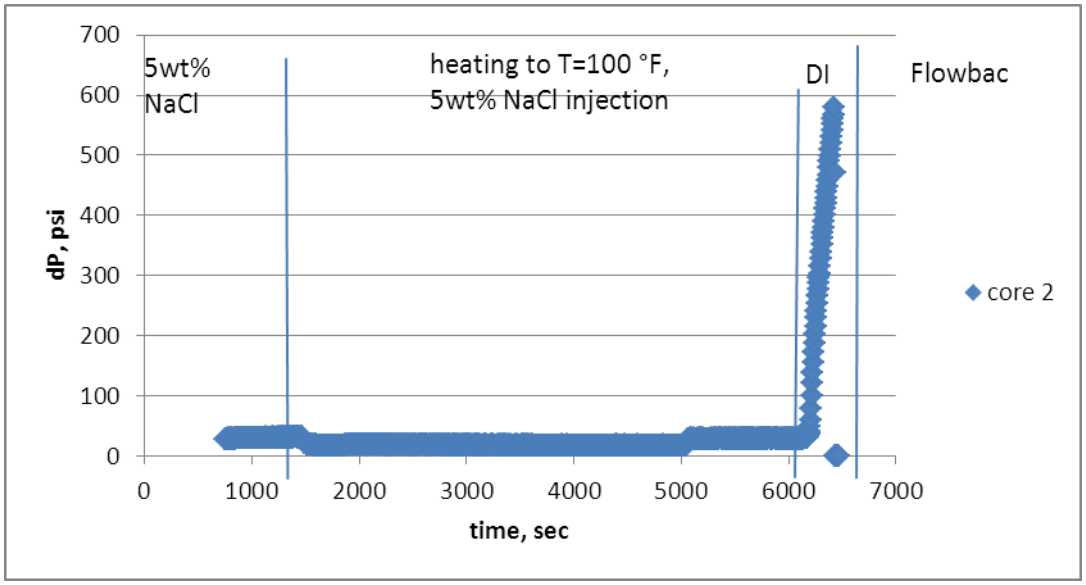

Fig. 32—Pressure drop profile for Berea sandstone core at T= 100°F.

DI water injection starts at time of 3030 sec at T=300°F as shown in **Fig. 24**. The amount of water having been consumed before the pressure drop increase occurs is shown in **Table 5.**

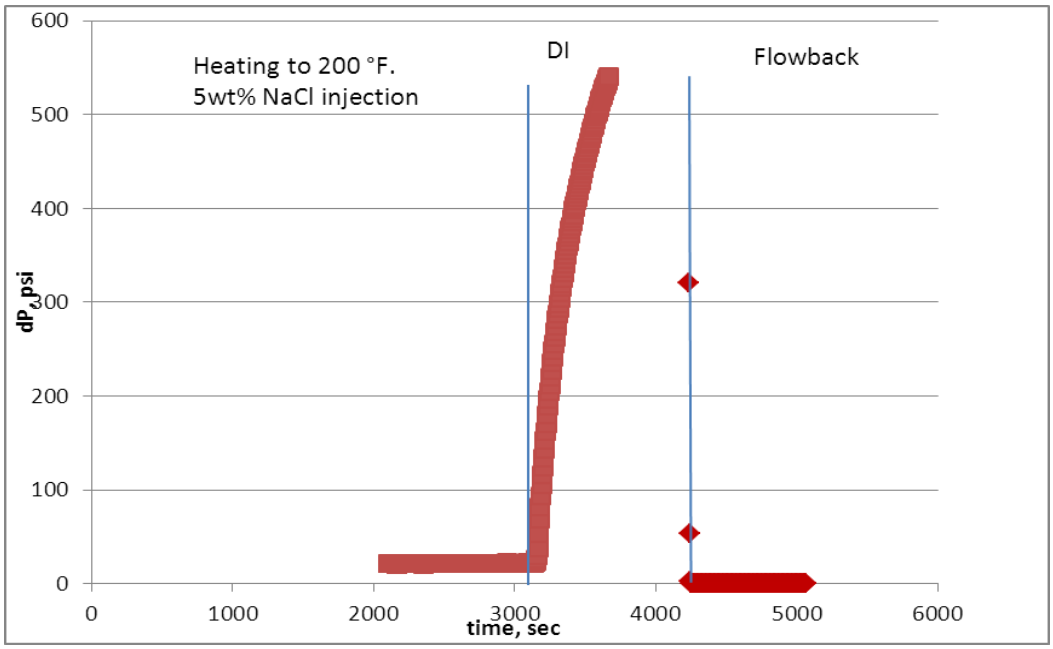

Fig. 33—Pressure drop profile for Berea sandstone core at T=200°F.

DI water injection starts at sec. The amount needed for pressure to buildup is shown in **Table 7**.

Table 7---Pore volume of DI water injected before pressure buildup.

	V of DI, cc	PV inj.
core 1, T=74°F	37.08	0.74
core 2, T=100°F	19.17	1.43
core 3, T= 200°F	17.9	1.51

From **Table 7**, can be concluded that pressure buildup which implies damage in the core as a result of gradual permeability drop occurs faster at higher temperature.

Permeability is calculated for each core for the three different experiments performed. The results of permeability at the three different temperatures are reported in **Table 8.**

Table 8—Permeability variation in Berea sandstone cores with temperature.

	Perm before, md		Perm after, md		% decrease
core 1	T= 74 °F	55.64	T=74 °F	55.64	0
core 2	T= 74 °F	57.08	T=100°F	45.18	20.85
core3	T= 74 °F	59.23	T=200°F	21.77	63.24

Fig. 34 shows that heating has a detrimental effect on permeability values. As the temperature increases, permeability goes down, and the degree of permeability drop is higher at higher temperature values.

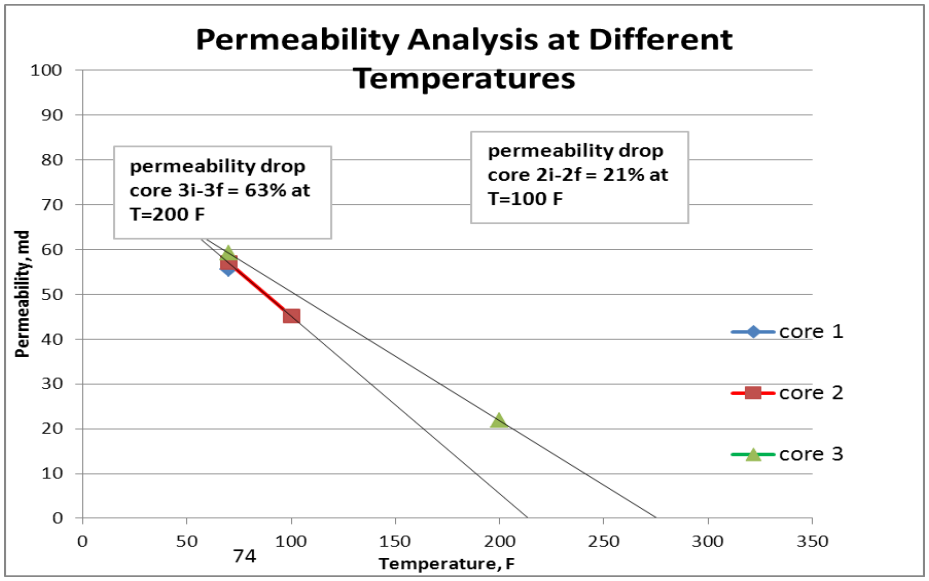

Fig. 34—Permeability analysis at different temperatures.

6.3.3.1 Core effluent analysis

Inductivity Coupled Plasma (ICP)- Optical Spectrometer Emission and Atomic Adsorption equipment were used to measure the concentration of the Na, Ca, Fe, Al, Si

elements. The core effluent was collected every 5 cc, and then the samples were diluted for Na and Ca. Al, Fe and SI were measured directly as shown in **Figs. 35-39**.

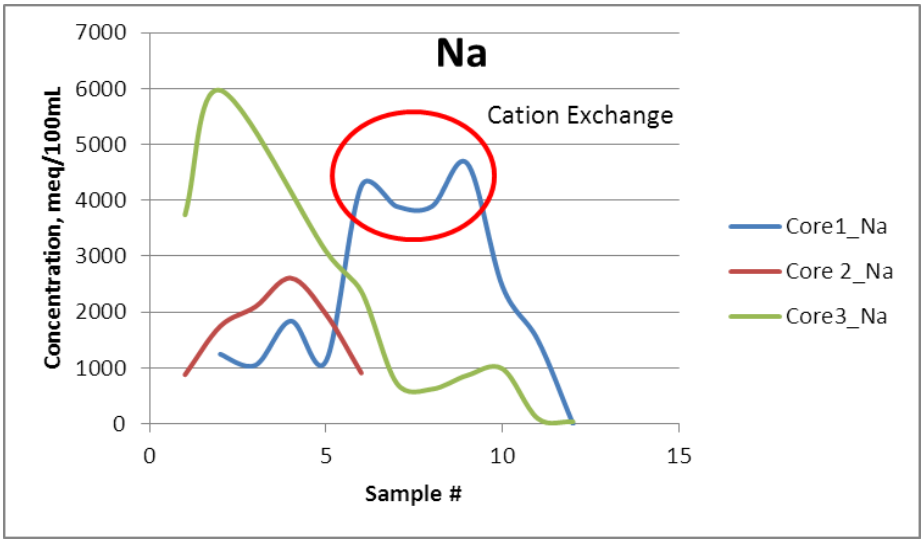

Fig. 35–Sodium concentrations after coreflood for three cores 1,2,3 for the temperatures 74°F, 100°F, and 200°F respectively.

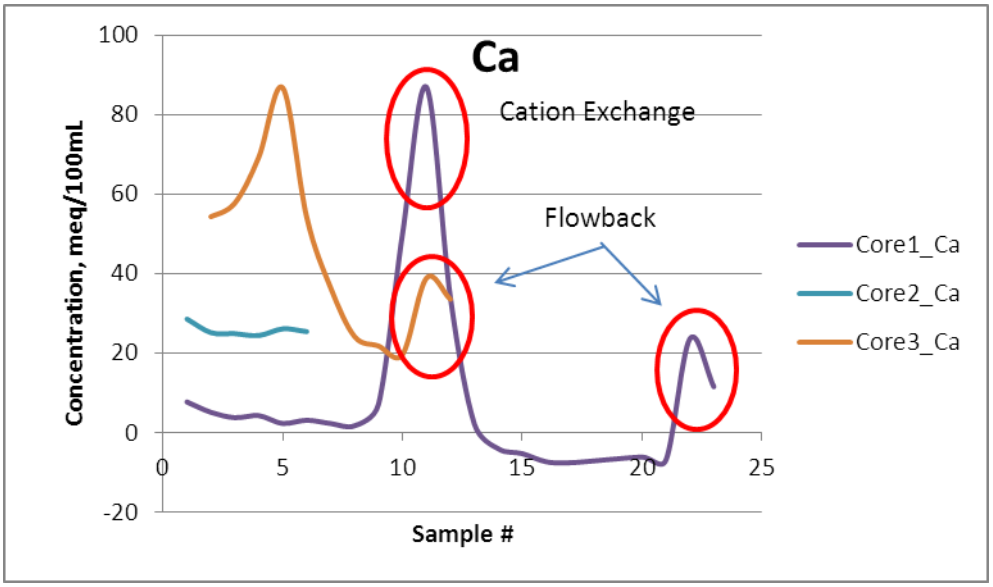

Fig. 36–Calcium concentrations after coreflood for three cores for temperatures 74°F, 100°F, and 200°F respectively.

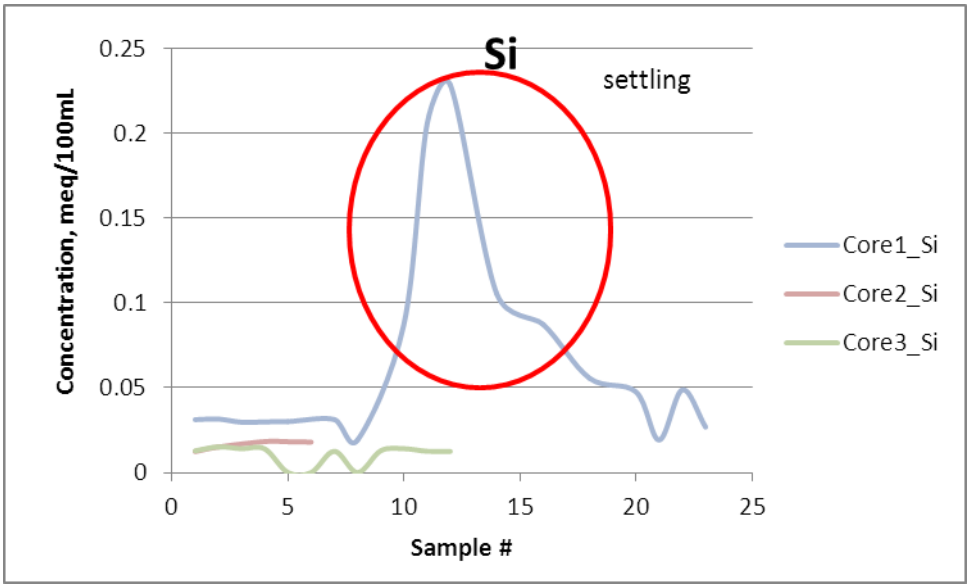

Fig. 37–Silicon concentrations after coreflood for three cores for temperatures 74°F, 100°F, and 200°F respectively.

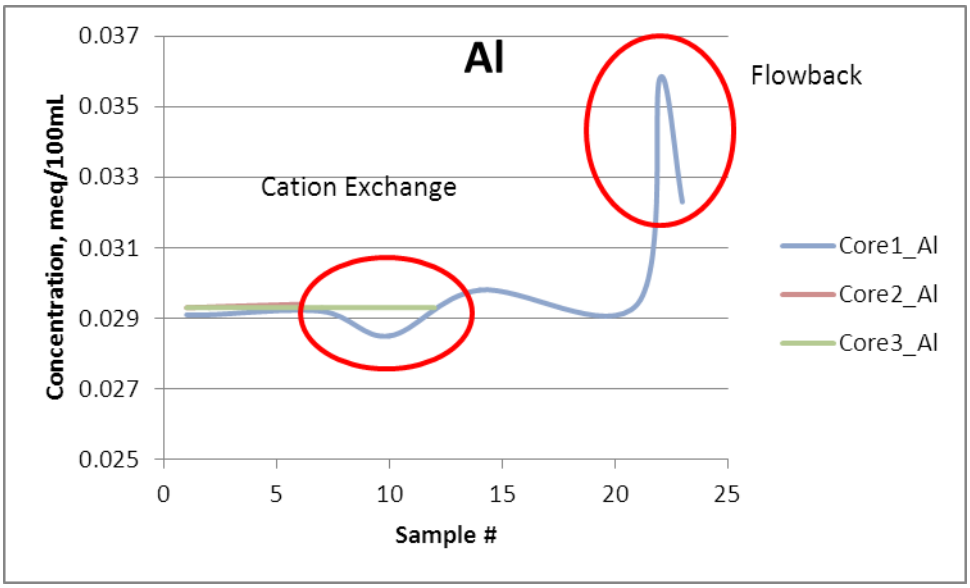

Fig. 38–Aluminum concentrations after coreflood for three cores for temperatures 74°F, 100°F, and 200°F respectively.

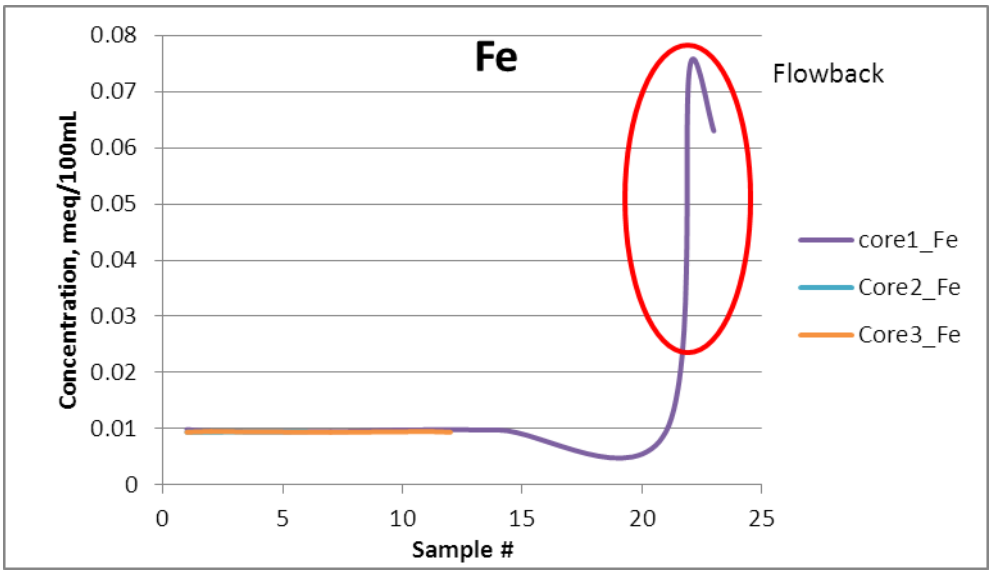

Fig. 39 –Iron concentrations after coreflood for three cores for temperatures 74°F, 100°F, and 200°F respectively.

From the core 1, samples from 11 to 19 all contained white settlement on the bottom of the tube as shown in **Fig. 40**.

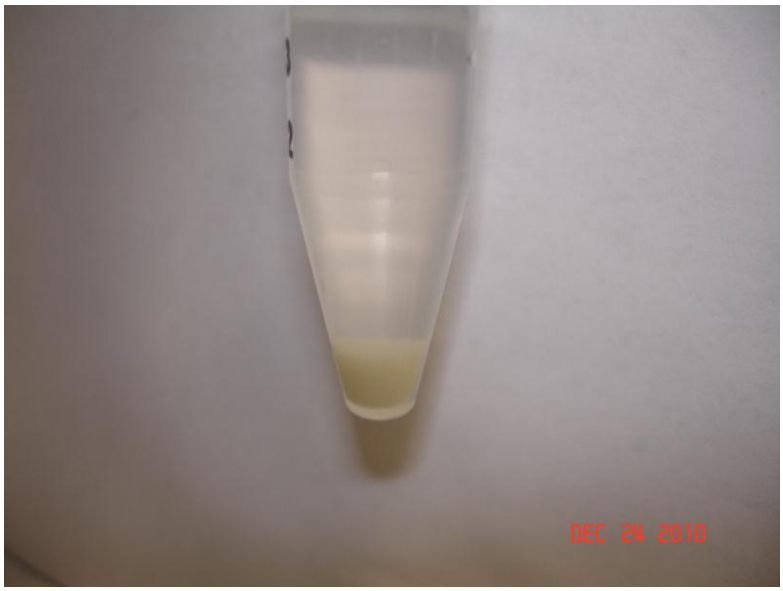

Fig. 40—Sample after coreflood experiment with sediments on the bottom.

6.3.4 Summary

Experimental results clearly show that increase in temperature deteriorates permeability due to the increased effect of clays' detachment from the matrix surface, and thus, increased rate of fines migration. When fines mobilize, they block small pores in the formation, and no flow area is available for the flow of hydrocarbon. Ultimately, the production of hydrocarbon ceases, and can reach zero in time. As a possible treatment, clay stabilizer solutions will have to be used to neutralize electronegativity of the clay particles to minimize their dispersion when a drilling/completion fluid will be introduced into the formation.

6.4 Effect of Flowrate on Permeability

The series of the experiment were conducted to instigate another parameter, flowrate, which has a potential to affect the behavior of clays in the sandstone formation.

6.4.1 Objective

A main objective of the conducted coreflood experiments was to determine the effect of flowrate on the permeability value at high temperature. The rock sample tested was Berea sandstone rock containing clay minerals. The core effluent samples were collected, and both AA and ICP measurements were done to determine Na^{++}, Ca^{++}, and Mg^{++} ion concentrations.

6.4.2 Materials

Density of saline solution 5wt% NaCl was measured to be 1.034 g/cc. Porosity was calculated and the porosity values were 10.9%, 11.1 %, and 11.3%

6.4.3 Results

Experimental results show that damage occurs earlier for a low rate of injection that is 0.5 cc/min, while pressure buildup is delayed for 2 cc/min. Values of volume for fresh water injection are tabulated in **Table 9**. Therefore, an optimum injection rate can be determined so that the damage will be postponed to a later time. Another observation done from the experiences was that after the increase in pressure drop, which was interpreted as damage due to fines migration, new permeability was established. The new permeability was significantly lower in comparison with initial one, with a loss in the range of 80-90%. However, the flow was established, and no total pore blockage effect was observed for the rates of 0.5 and 2 cc/min, as opposed to the flow rate of 5 cc/min. The graphical results are shown in **Fig. 41**.

Table 9—Pore volume of DI water injected before pressure buildup for different flow rates.

Core	V of DI before damage occurs, cc
Core 1, 74°F, 5 cc/min	12.9
Core 2, , 74°F, 2 cc/min	67.7
Core 3, , 74°F, 0.5 cc/min	10.8

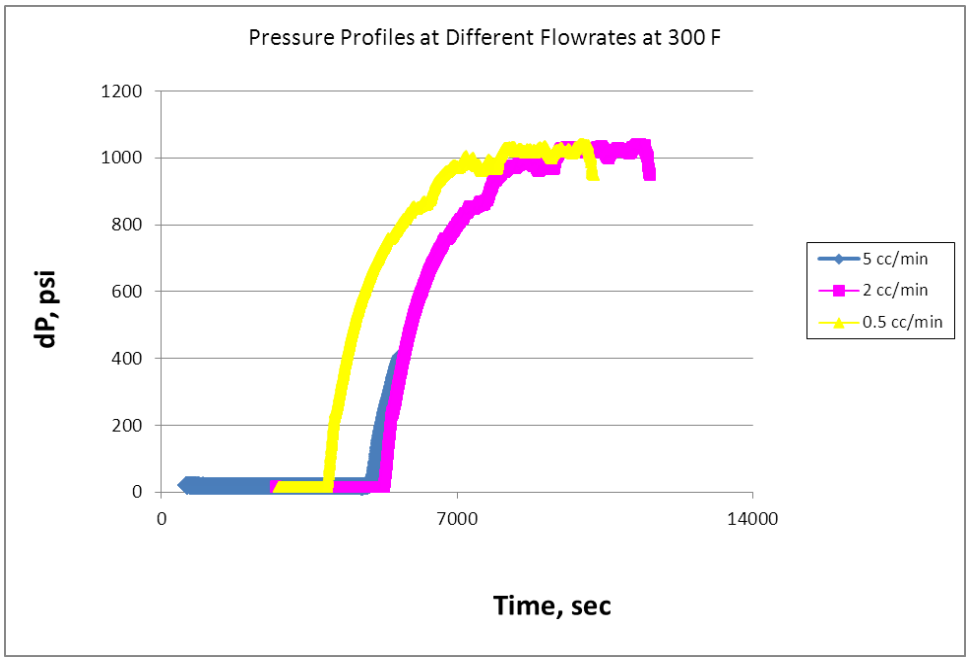

Fig. 41—Pressure profiles at three different flowrates of 5 cc/min, 2 cc/min, and 0.5 cc/min.

6.4.3.1 Core effluent analysis

Figs. 42-44 show that Na, Ca and Mg concentration is decreasing because clay minerals try to attract positive ions to stabilize themselves and neutralize their charge.

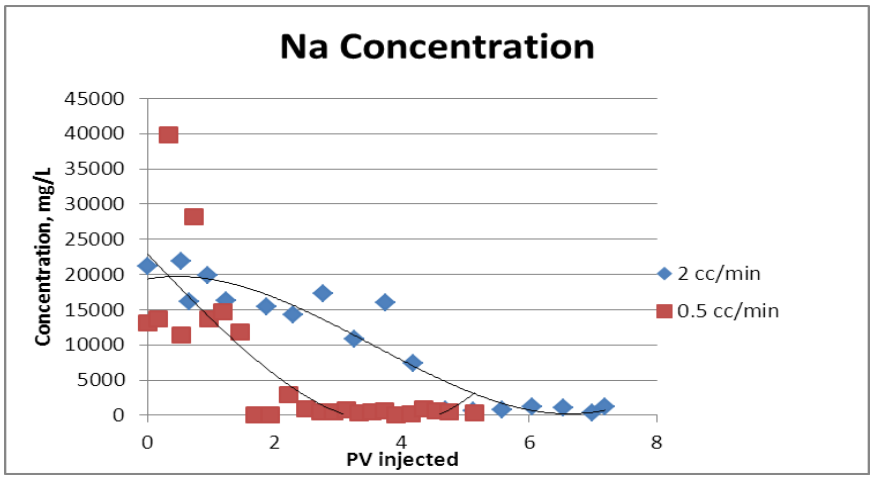

Fig. 42 –Na concentration at different flowrates: 2 cc/min and 0.5 cc/min.

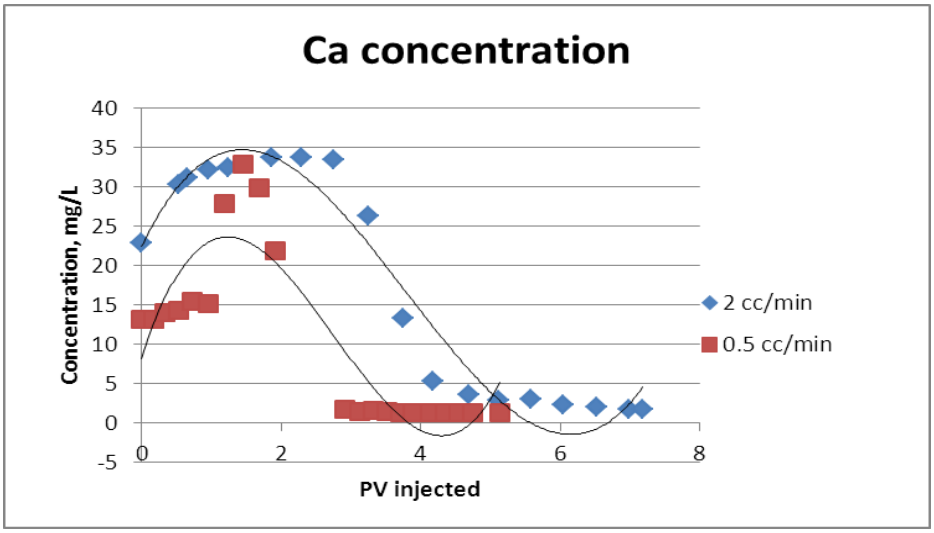

Fig. 43 –Ca concentration at different flowrates: 2 cc/min and 0.5 cc/min.

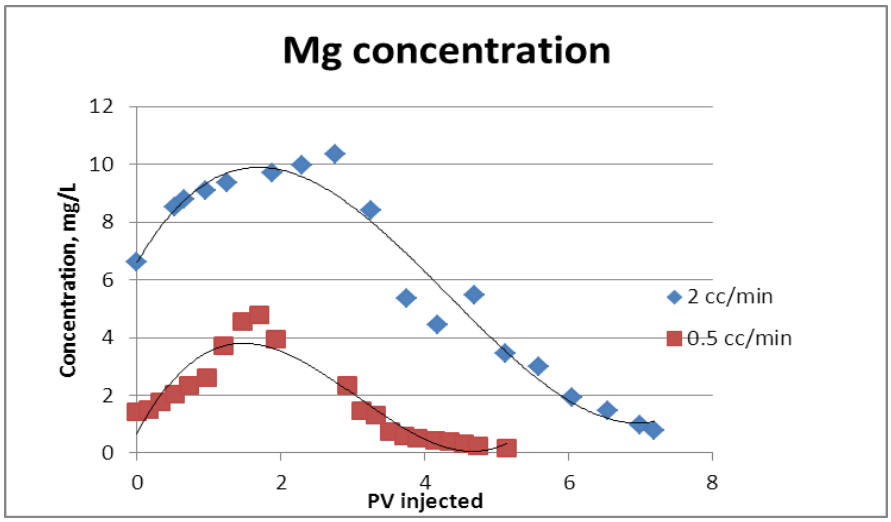

Fig. 44 –Mg concentration at different flowrates: 2 cc/min and 0.5 cc/min.

Figs. 45 and 46 show two different samples collected after coreflooding at the flow rates of 2 cc/min and 0.5 cc/min, respectively.

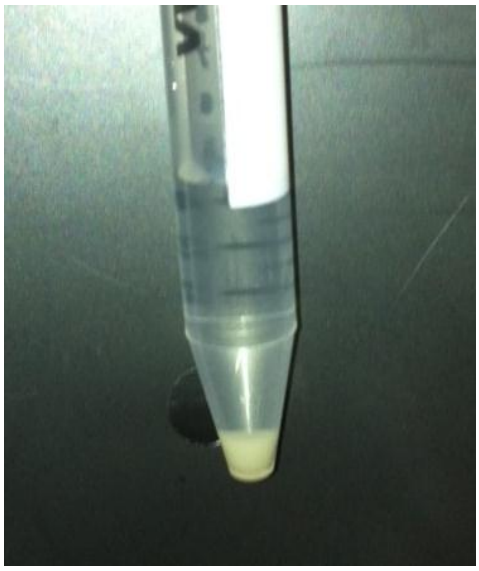

Fig. 45—Sample 10, sediments are accumulated at the bottom at a flowrate of 2 cc/min.

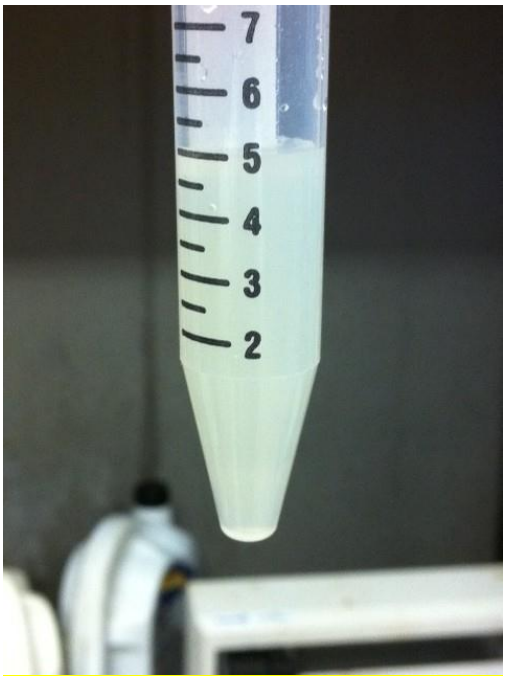

Fig. 46—Sample 13, sediments are accumulated at the bottom at a flowrate of 0.5 cc/min.

X-Ray Diffraction experiment was carried out to determine the elemental composition of the sediment which accumulated during the flowback, as shown in **Figs. 44 and 46**. The test results showed that particles coming out are mostly kaolinite clays, and few amounts of chlorite and mica were identified. The smectite presence is very unlikely.

6.4.4 Summary

The flow rate affects the permeability impairment. From the coreflood experiment, it can be concluded that the flow rate of 0.5 cc/min will cause a faster permeability decline than the flow rates of 2 cc/min and 5 cc/min. The pressure profiles at both 2 cc/min and 5 cc/min show very similar trends, and overlap each other, implying that a permeability decline at high flow rate occurs at a similar time.

6.5 Effect of pH on Clays Migration

The series of the experiment were conducted to instigate another parameter, pH, has a potential to affect the behavior of clays in the sandstone formation.

6.5.1 Objective

The main objective of the conducted coreflood experiments was to observe the effect of both high and low-pH fluids on clays dispersion and, thus, on the permeability of the rock at a temperature of 200°F.

6.5.2 Materials

The experiment was performed at a temperature of 200°F using two of fluids of both low and high pH values. The rock sample was Berea sandstone. Brine solution was used to prepare low-pH fluid of hydrochloric HCl acid with corrosion inhibitor present. High-pH fluid was prepared using sodium hydroxide NaOH base. The pore volume of the core was calculated using taken dry and brine weight measurements.

6.5.3 Results

6.5.3.1 Effect of high-pH fluid

2 wt% NaOH fluid was tested to determine the effect of high pH environment on clay stabilization. The pH of the 2 wt% NaOH fluid prepared in brine was measured to be 13.3 at T=74°F. **Fig. 47** shows that 2 wt% NaOH solution did cause damage at T= 200°F. The same experiment was performed at different temperatures, such as at T= 74°F and T=300°F, and the same damaging effect was observed.

In sandstone reservoirs with acid fluid in the porous medium the internal clays should be more stable relative to alkaline conditions, if the pore walls (e.g. quartz) remain being negatively charged. Changing the porous solution acidity (pH) from acid to alkaline may cause the clay release and the pore throat plugging. Moreover, extreme pH conditions (both alkaline and acid) can cause the clay disintegration or their transformation to another mineralogical form and consequent permeability reduction (Tchistiakov 2000).

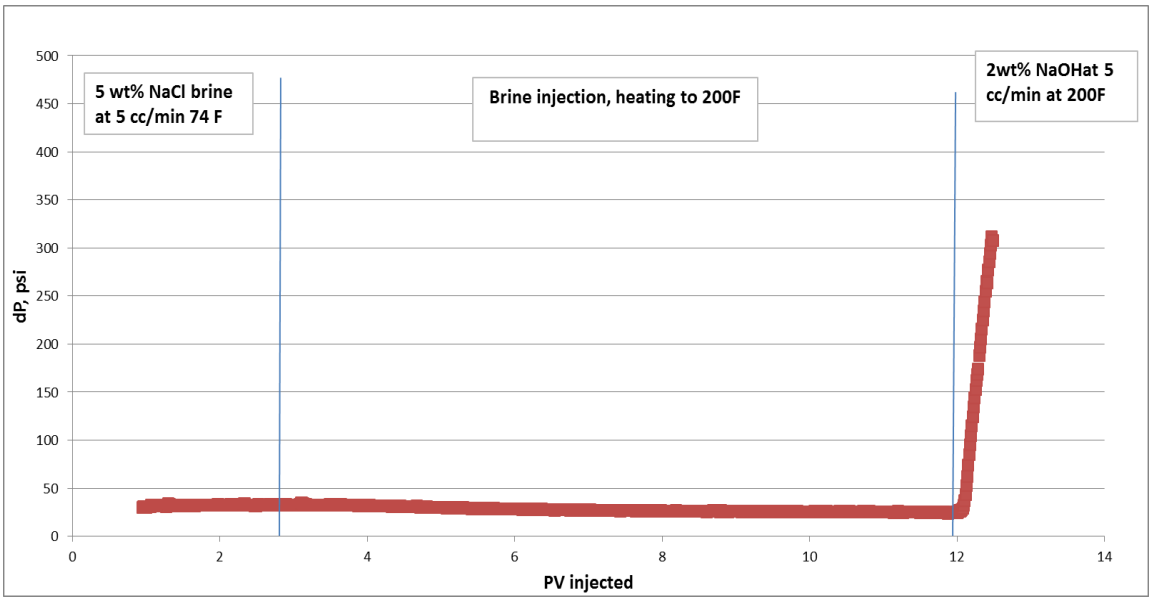

Fig. 47—Pressure profile at temperature T=200°F, brine (5 wt% NaCl) following high pH fluid injection. Damage by 2 wt% NaOH is confirmed.

6.5.3.2 Effect of low-pH fluid

15 wt% HCl with 0.8 wt% corrosion inhibitor was tested at a temperature of 200 °F, and measured pH value for a low pH fluid was 0-1. **Fig. 48** shows the coreflood experiment result. The original permeability was preserved after injection of the fluid at high temperature. Therefore, hydrochloric acid can be considered to work as a clay stabilizing agent. Berea sandstone does not contain a large amount of chlorite clay as it was determined after XRD analysis. However, it is important to be cautious about a potential problem of iron precipitation from the chlorite clay present in the formation. Solubility analyses indicated that chlorite clay is more susceptible to acid attack than illite, and kaolinite and feldspar minerals. Destruction of the crystalline structure of chlorite by strong acid resulted in the formation of an amorphous silica residue (Simon and Anderson 1990). Hartman et al. (2003) showed a damaging effect of 10 wt% HCl at

lower temperatures (T= 330°F and 174°F) in non acid sensitive and acid sensitive formations, respectively. The authors recommended to use 10 wt% of acetic acid, without damaging the formation at a higher temperature, than 10 wt% HCl.

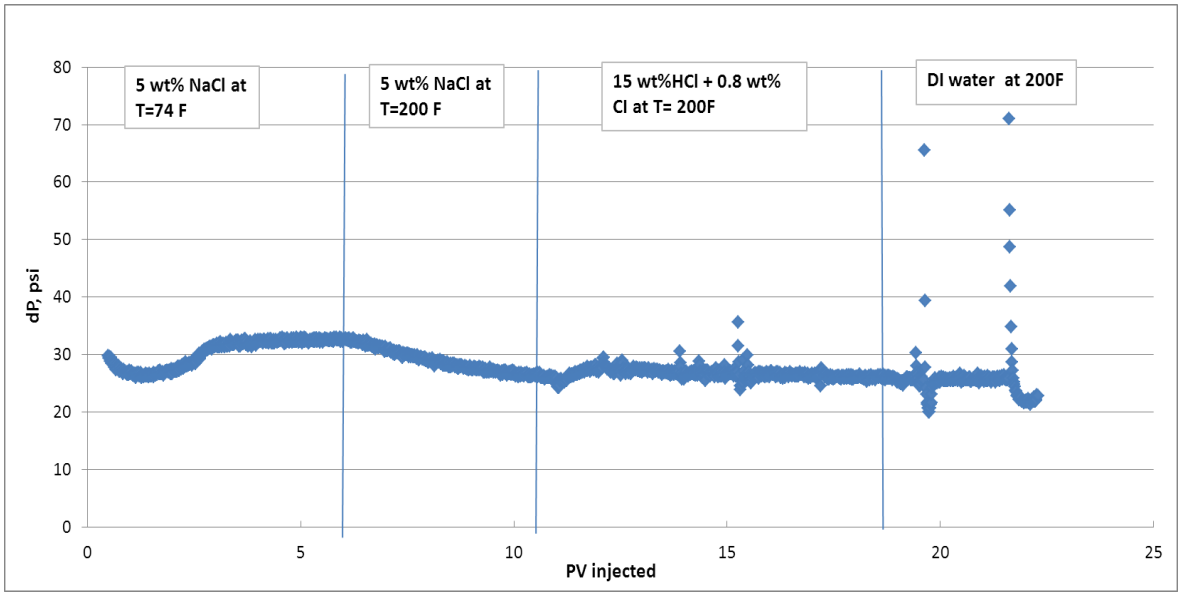

Fig. 48— Pressure profile at temperature T=200°F, brine (5 wt% NaCl) following low pH fluid injection. Original permeability is preserved; no damage due to fresh water injection is confirmed.

6.5.4 Summary

High –pH fluid shows permeability damage due to migration of the clays. This result is important when designing the drilling mud. In fact, commonly used for drilling water-based mud is a mixture of various chemicals which is to be tested on the pH. This final formulation should be in the range of the specific non-damaging pH.

According to the experiments result, acidic fluid shows no difference in permeability. A non-damaging effect was confirmed by injection of fresh water at 200°F.

Therefore, this result may be beneficial when designing the drilling fluid entering formation to prevent clay disintegration and migration and consequent pore blockage in Sandstone formations.

6.6 Effect of Salinity Variation on Clay Stabilization

The series of the experiment were conducted to instigate another parameter – salinity- which has a potential to affect the behavior of clays in the sandstone formation.

6.6.1 Objective

The main objective of the conducted coreflood experiments was to observe the effect of the different saline following fresh water on fines dispersion and, thus, on permeability of the rock at both low and high temperatures such as 74°F and 300°F accordingly.

6.6.2 Materials

The experiment was performed at two different temperatures: the room temperature of 74°F and an elevated temperature of 300°F. The rock sample was Berea sandstone. Brine solution was prepared of two different brine solutions with concentrations of 5 wt% of NaCl and 15 wt% of NaCl. The brines were mixed for 30 min with a high speed magnetic stirrer. The core was first dried in the oven at 160°F for two hours, and then saturated with 5 wt% NaCl brine overnight. The pore volume of the core was calculated using taken dry and brine weight measurements.

6.6.3 Results

The two coreflood experiments were conducted to determine the effect of brine concentration on clay stability. The results are shown in **Tables 10 and 11** show that the higher salinity has a better effect on permeability, and also a higher concentration of salt delays the damage occurring due to blockage of the pore throats by migrated fines in the sandstone rock. **Fig. 49** shows a test with 15 wt% NaCl solution performed.

Table 10—Volume in cc of fresh water injected at 300°F at 5 cc/min.

	V of DI,cc	Initially Injected Fluid
T= 300°F	12.9	5 wt% NaCl
T= 300°F	38.7	15 wt% NaCl

Table 11—Permeability analysis for different salinity brine injected.

		Before	Perm, md	After	Perm, md	% decrease
heating	15 wt%t NaCl	T=74°F	40.9	T=300°F	15.6	61.9
heating	5 wt% NaCl	T=74°F	56.8	T=300°F	8.5	85.0

The coreflood final result is shown in **Fig. 49**. It is observed that when flushing the core with fresh water after 15 wt% NaCl solution, some clay particles were not stable and released from the sandstone (quartz grain) surface. The injection of fresh water resulted in a rapid increase of the pressure drop, indicating that the blockage in the core occurred and no permeability will be preserved.

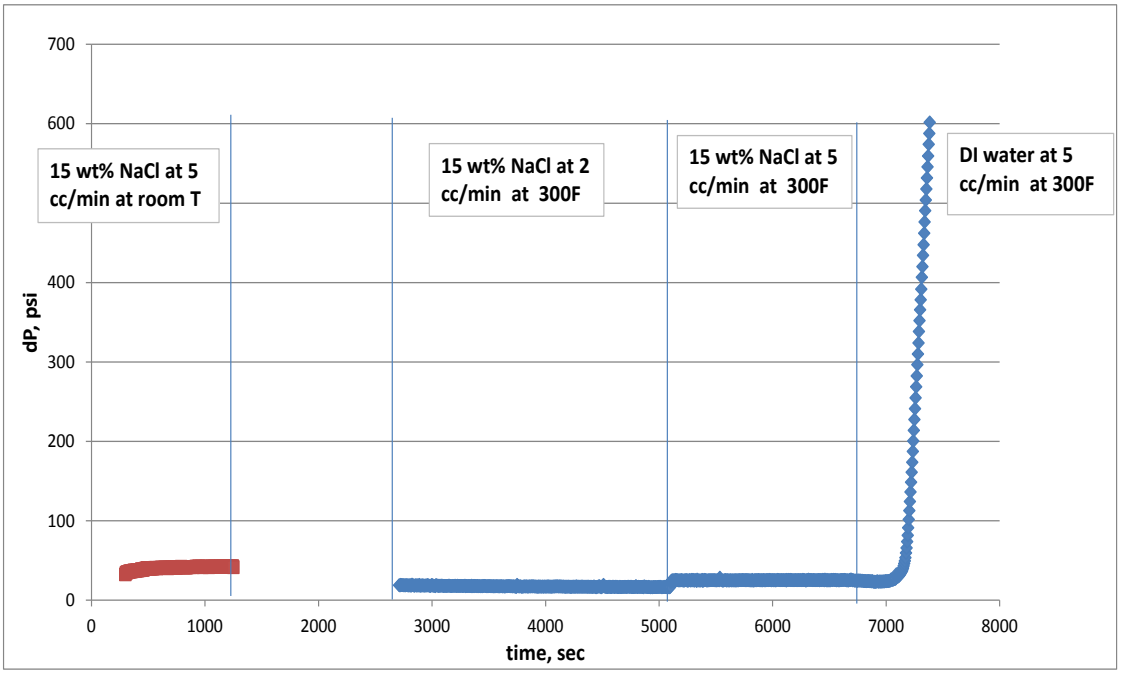

Fig. 49—Pressure profile for coreflood for 15 wt% NaCl at high temperature.

6.6.3.1 Core effluent analysis

The Inductively Coupled Plasma (ICP) was used to measure the concentration of the outcoming effluent solution from coreflooding. **Figs. 50-52** show that Na, Ca, and Mg are being consumed by the negatively charged clay particles, and a jump in Na concentration can be due to cation exchange reactions when lower valency cations are being displaced by higher valency cations in order to neutralize a negative particle. Two concentrations of sodium chloride solution representing both a high and a low concentration, are tested at 5 cc/min injection flow rate at a temperature 300°F. No sediments were coming out of the core due to blockage which occurred when fresh water was injected at high temperature.

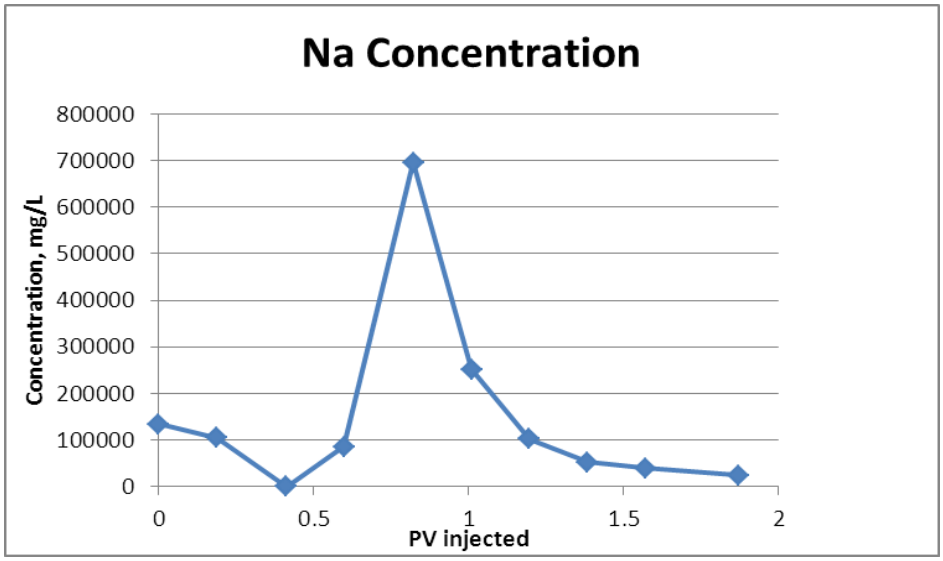

Fig. 50—Na concentration for coreflood of 15 wt% NaCl at high temperature.

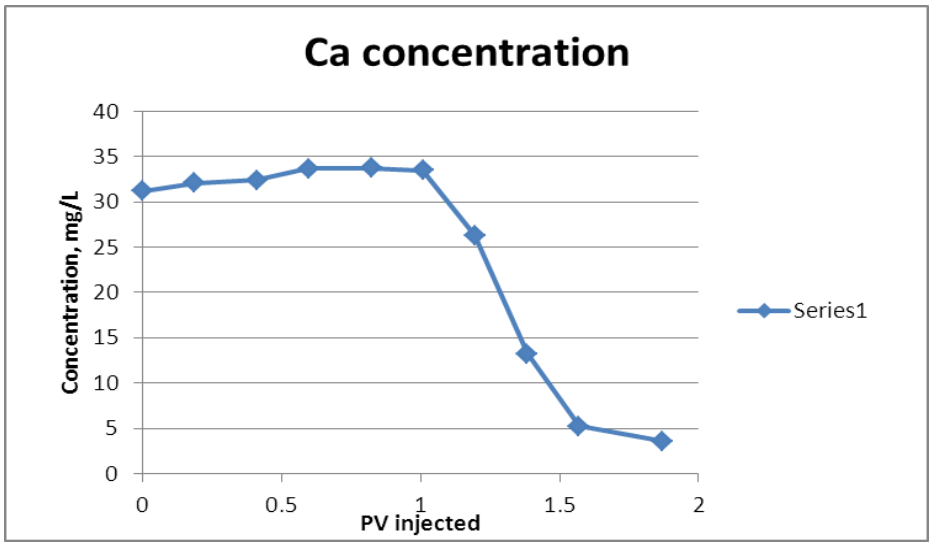

Fig. 51—Ca concentration for coreflood of 15 wt% NaCl at high temperature.

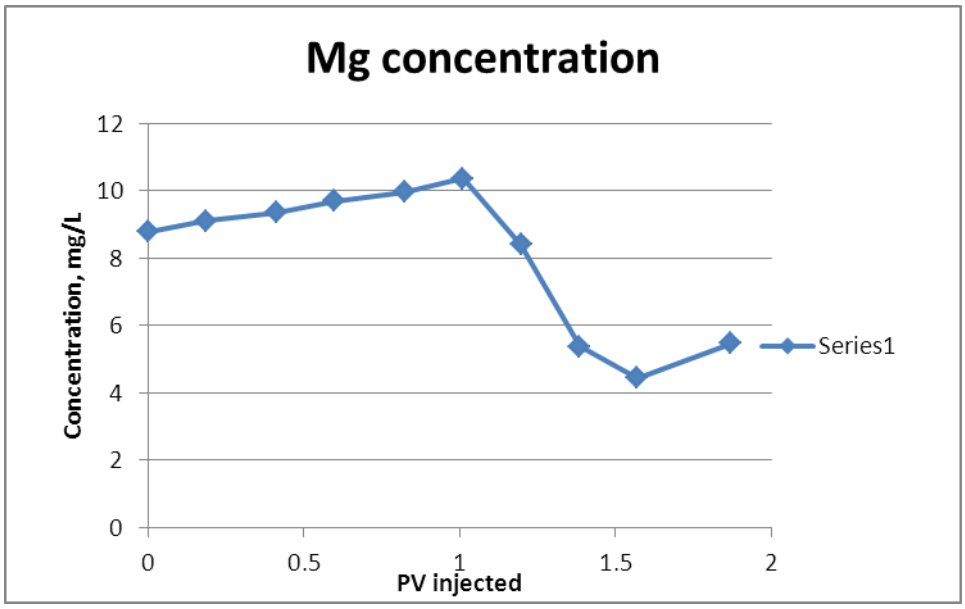

Fig. 52—Mg concentration for coreflood of 15 wt% NaCl at high temperature.

6.6.4 Summary

The results show that permeability loss is decreased for a higher concentration salt a high temperature. Also, 15 wt% of NaCl showed delayed formation damage caused by a blockage effect due to dispersed clay particles. The negative charge on the clays was not fully screened by the cations in a higher concentration solution of sodium chloride. Therefore, the repulsive forces between negatively charged particles will cause the clay dispersion and detachment from the rock surface.

The higher salinity of sodium chloride is recommended for the clay migration minimization problem. Another recommendation is using more effective clay stabilizing agents with a presence of multivalent cations, or monovalent cation having higher bond energy that sodium ions.

6.7 Effect of Ammonium Chloride Salt on Fines Dispersion

Ammonium chloride salt solution testing and effect of this salt on fines migration will be described in this section.

6.7.1 Objective

The main objective of the conducted coreflood experiments was to test the effectiveness of ammonium chloride salt on clay stabilization and, thus, on the permeability of the rock at low and high temperatures of 74°F and 300°F, respectively.

6.7.2 Materials

The rock sample tested was Berea sandstone rock containing clay minerals present. Porosity of the Berea sandstone rock was calculated to be 16.6%. Density of ammonium chloride was measured at room temperature (74°F) and was measured to be 1.0126 g/cc. After the core sample was inserted in the core holder, 5 wt% ammonium chloride solution was injected at high temperature (300°F) until the pressure drop on the monitor was stabilized. After stabilization, the vessel with ammonium chloride solution was closed, and simultaneously the vessel with fresh (DI) water was opened. The pressure drop was monitored by the program LabView at each stage, recorded, and used further to calculate rock permeability from the stage of stabilization.

6.7.3 Results

Earlier coreflood experiments were conducted to determine the effect of different salinities (5 wt% NaCl and 15 wt% NaCl) on clay stabilization. For this experiment, two coreflood experiments were conducted earlier to determine the effect of ammonium chloride on clay stability. The results as shown in **Tables 12 and 13** show the combined results for different salinity solutions and ammonium chloride salt. It can be concluded that ammonium chloride is more effective for clay stabilization since injection of fresh water does not block flow area and no blockage takes place. Moreover, the percentage of decrease of the permeability when using ammonium chloride is minimum in comparison with higher salt concentration solutions.

Table 12—Volume in cc of fresh water injected at 300°Fbefore damage for different salts.

	V of DI,cc	Salt tested
T= 300 F	12.9	5 wt% NaCl
T= 300 F	38.7	15 wt% NaCl
T= 300 F	no blockage	5 wt% NH4Cl

Table 13—Permeability analysis for different salts injected.

Salt tested	Before	Perm, md	After	Perm, md	% decrease
5 wt %NH_4Cl	T=74 °F	69.7	T=300°F	47.7	31.5
15%t NaCl	T=74 °F	40.9	T=300°F	15.6	61.9
5%t NaCl	T=74 °F	56.8	T=300°F	8.5	85.0

The coreflood final result for ammonium chloride salt is shown in **Fig. 53**. It is observed that when flushing the core with fresh water after 5 wt% NH_4Cl solution, some

clay particles were not stable and released from the sandstone (quartz grain) surface. The injection fresh water resulted in a pressure drop following pressure stabilization with no blockage of the pore space. The pressure stabilization resulted in a preservation of rock permeability.

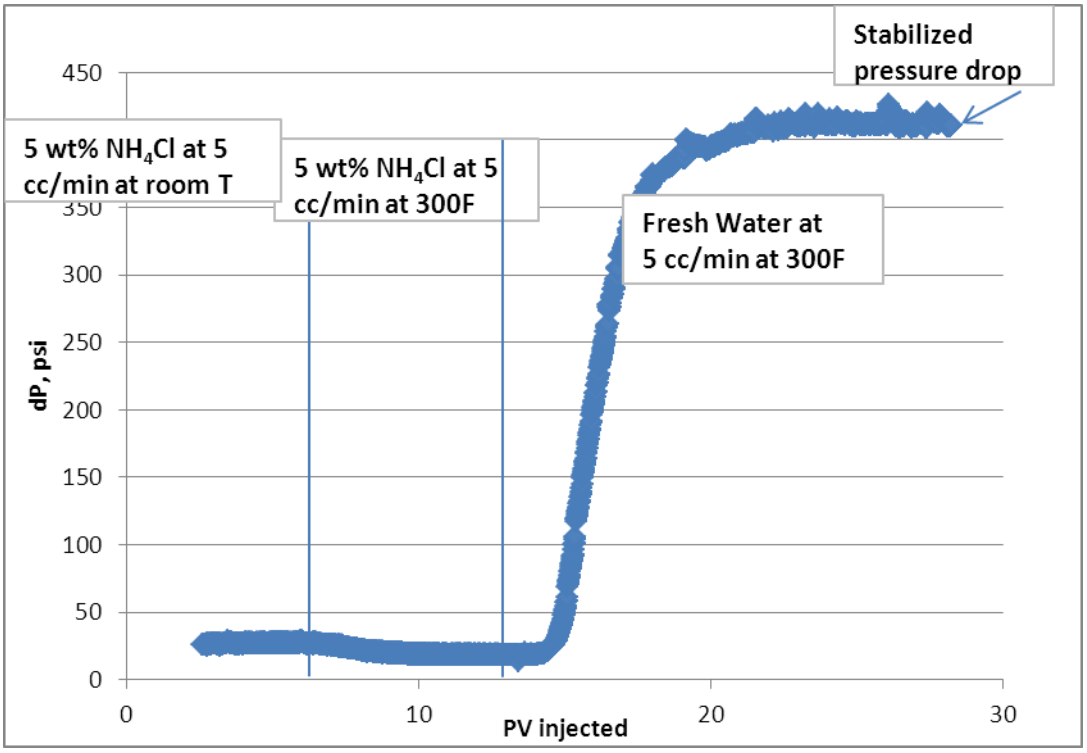

Fig. 53 —Pressure profile for 5 wt% NH_4Cl salt at 300°F.

When brine injection at high temperature was switched to the fresh water, the core effluent samples were collected and analyzed using the ICP. For the effluent solutions containing the flowback sediments as shown in **Fig. 54**, the additional analysis of the XRD test was conducted to determine the nature of the yellowish sediments after the injection of ammonium chloride salt.

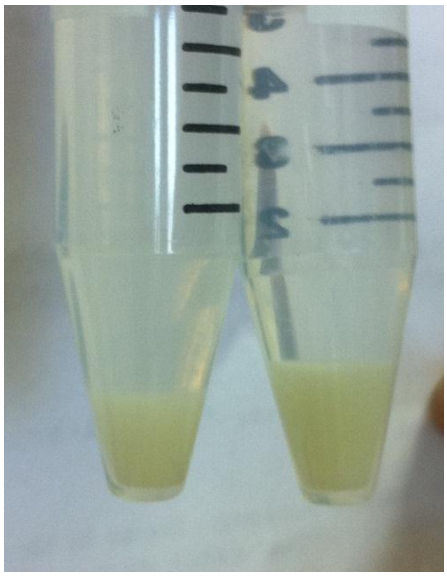

Fig. 54 —Sediments accumulated in a few core effluent samples when fresh water was injected at high T at 5 cc/min.

The analysis from using the X-Ray Diffraction is presented in **Fig. 55**. The results show that the sediments are the clays of different types. Kaolinite, chlorite, and mica (illite) clays were identified by the peaks. The presence of montmorillonite is very unlikely. The flowback of sediments when injecting DI water can result in pore throat blockage, as in the case of NaCl of low and high concentrations. However, when ammonium chloride solution was tested, no blockage occurred, thus resulting in preservation of permeability for the fresh water flow.

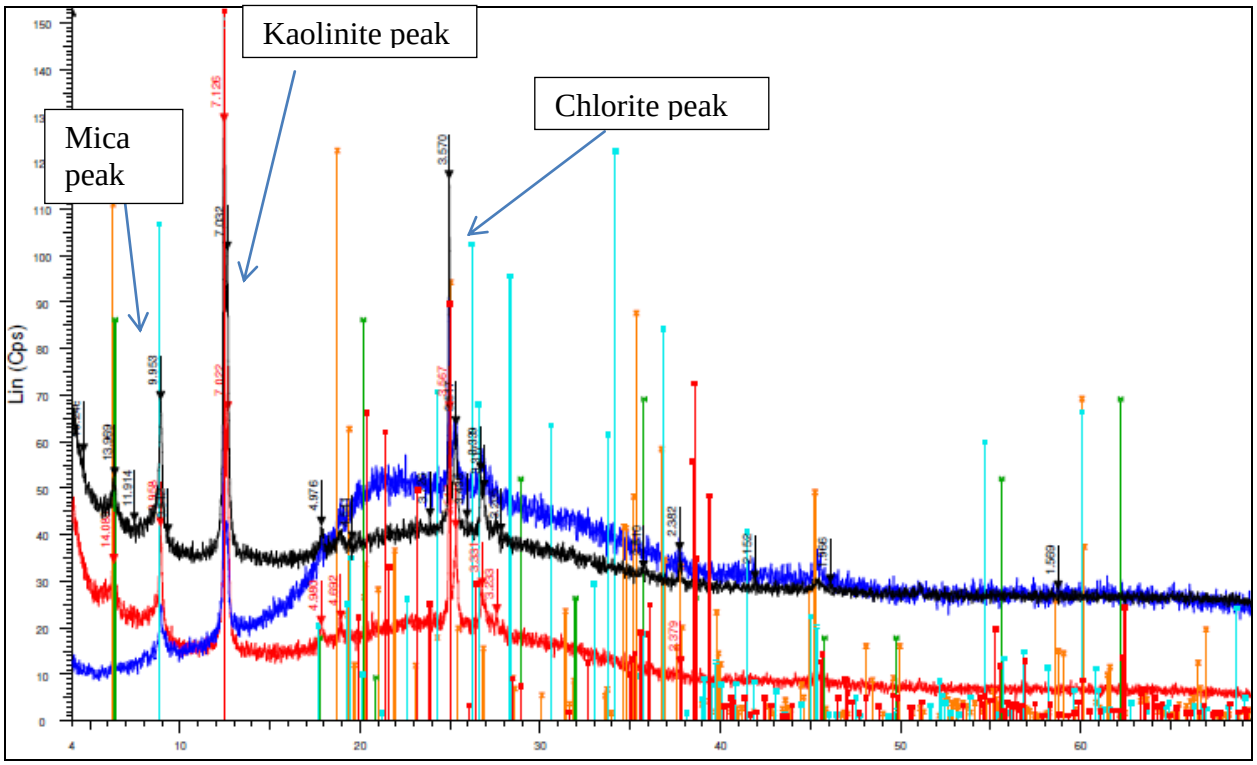

Fig. 55—XRD analysis for the core effluent solutions containing sediments.

The results from **Fig. 55** confirm the experimental outcome presented in **Tables 11 and 12**. 5wt% of NH_4Cl solution is more effective than both 5wt% NaCl and 15wt% NaCl solutions. The smaller size of the ammonium chloride ions in their hydrated forms results in a better screening effect of this salt in comparison with sodium chloride salts, which have a larger hydration radius. The negatively charged sites on the kaolinite if covered with the ammonium chloride ions will have a higher bond energy which will result in a more effective fixation than hydrated sodium ions.

6.7.3.1 Core effluent analysis

The Inductively Coupled Plasma was used to measure the concentration of Na, Ca and Mg ions in the core effluent samples. The Na profile for flowback is shown in **Fig. 56**. The amount of fresh water injected was about 12 PV. The analysis shows that after a flash of ammonium chloride solution, the sodium start to be exchanged with ammonium ions which are more tightly bound. As more fresh water is injected, no sodium occurs up to 6 PV of fresh water, and from 6 to 10 PV the release of Na+ ions is observed due to their hydration and loss of binding strength. **Figs. 57 and 58** show that Ca and Mg divalent cations were consumed by the negatively charged clay particles in order to stabilize in the porous media.

As the pressure stabilizes when 5 wt% of NH_4Cl is injected, ammonium ions will try to replace all sodium ions to screen the negative charges on the clay edges for dispersed clays, therefore the sodium ions will be detached and flushed out with fresh water flooding.

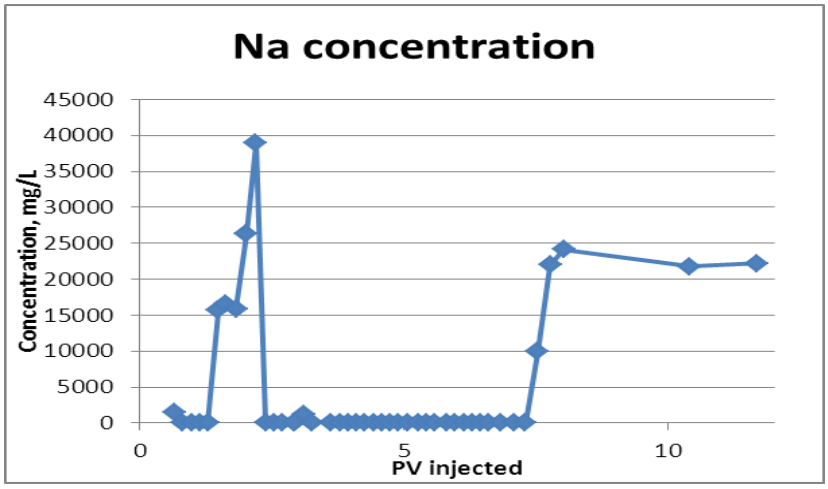

Fig. 56—Na concentration profile for core effluent.

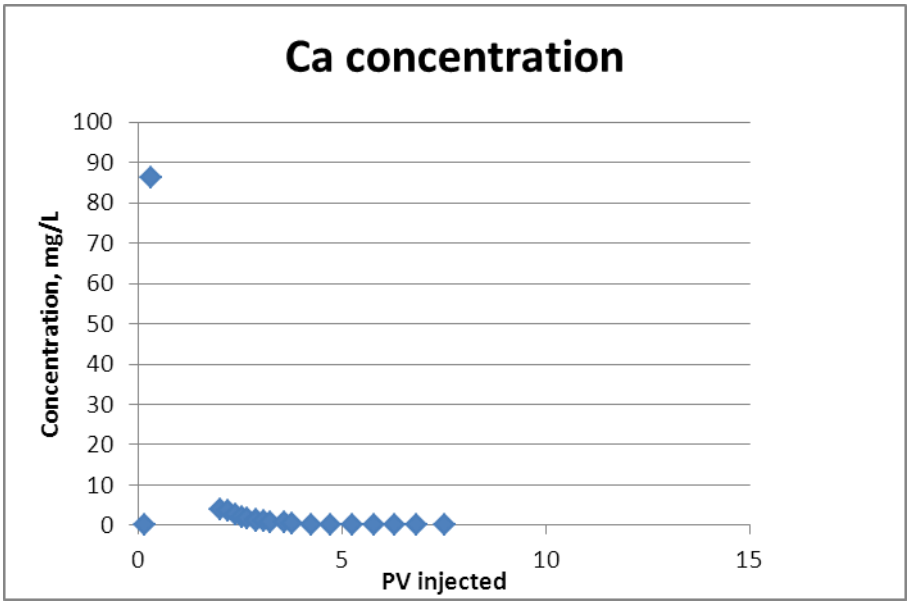

Fig. 57—Ca concentration profile for core effluent.

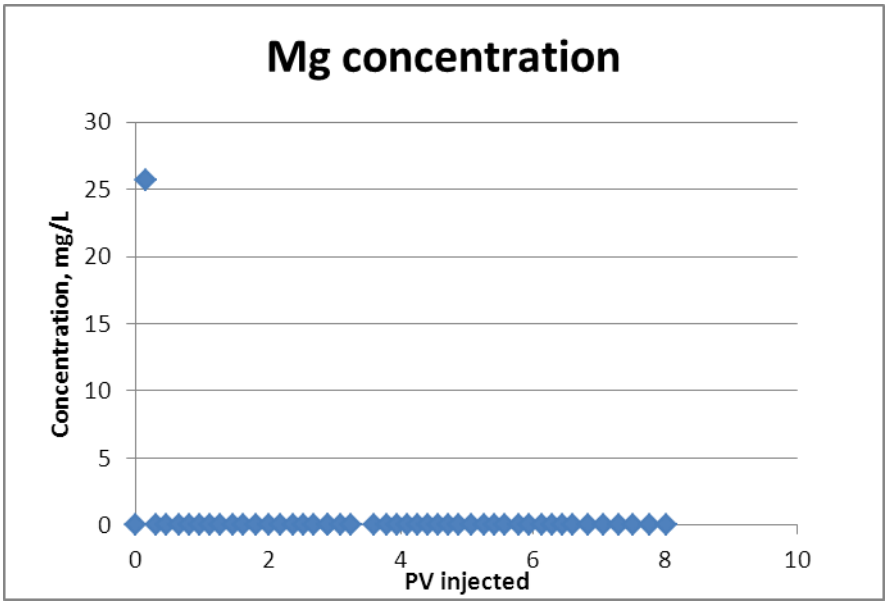

Fig. 58—Mg concentration profile for core effluent.

6.7.4 Summary

Ammonium chloride salts shows a good screening, thus a good stabilizing effect on the migrated fines in the sandstone rock. The concentration of the tested acid salt (5 wt%) showed a better clay migration inhibition effect than earlier tested brines of 5 wt% NaCl and 15 wt% NaCl. From the experiment conducted, the permeability was preserved after flooding of ammonium chloride salt with fresh water at high temperature. The salt is environmentally friendly and will not cause a scale problem if the sandstone formation is subjected to further acidizing, as ammonium salt is compatible with mud acid.

6.8 Effect of Zirconium Lactate Clay Stabilizer on Clay Dispersion

Testing of zirconium lactate clay stabilizer chemical and its effect on clay dispersion will be presented in this section.

6.8.1 Objective

The main objective for a set of experiments with zirconium lactate clay stabilizer was to determine the effectiveness and required concentration of the proposed clay stabilizer.

6.8.2 Materials

Two different concentrations of zirconium lactate clay stabilizer solution were tested: 0.2 vol % and 2 wt%. For a better clay stabilizing effect, the solutions were prepared in saline water. The working solution to determine initial permeability in the core was 5 wt% NaCl. The core used was form a Berea sandstone formation. Density of Zr lactate containing solution was measured at room temperature (74°F) to be 1.005 g/cc. Density of 2 wt% Zr lactate solution in brine was measured at room temperature (74°F) to be 1.0336 g/cc.

5 wt% of NaCl solution was injected initially, and then once pressure drop stabilization was reached, the solution was switched to a testing solution that is Zirconium lactate clay stabilizer. After testing the solution, the final injection fluid was fresh water to assess the damage in the core and thus, estimate the effectiveness of the clay stabilizer. Porosity of the Berea sandstone rock was calculated to be about 17%.

6.8.3 Results

Two pressure profiles are shown in **Figs. 59**-**60** for 0.2 vol% of Zirconium lactate clay stabilizer and 2 wt% Zirconium lactate clay stabilizer, respectively. Both profiles show an increase in pressure drop indicating that solutions are not effective for clay stabilization purposes.

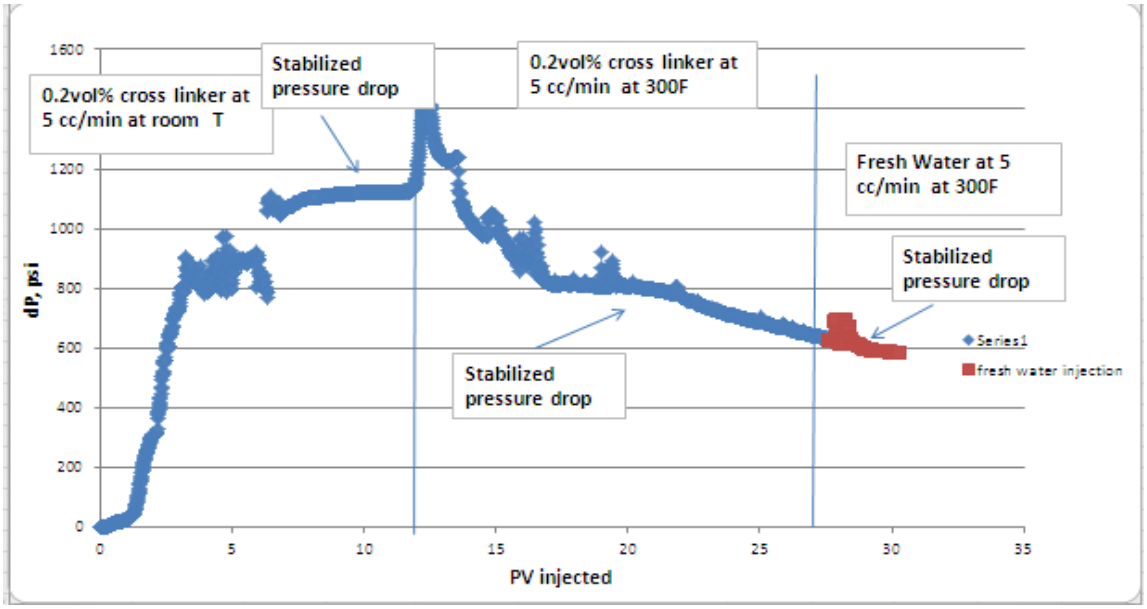

Fig. 59 —Pressure profile for 0.2 vol% Zr Lactate clay stabilizer at 300°F.

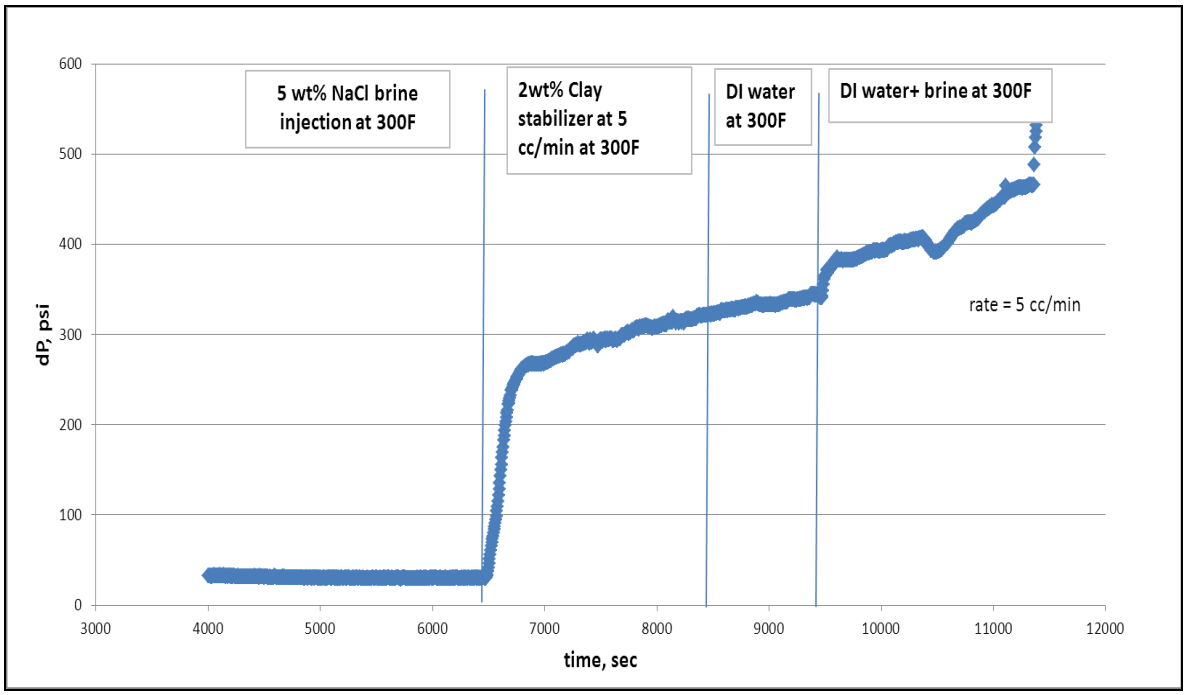

Fig. 60 —Pressure profile for 2 wt% Zr Lactate clay stabilizer at 300°F.

A potential way to increase the effectiveness of the Zirconium lactate clay stabilizer solution would be to increase the concentration of clay stabilizer. However, due to the high cost of this chemical and a large amount needed, this increase will not be financially favorable for any petroleum operations. Therefore, other clay stabilizer solutions are needed to be tested for minimizing clay dispersion in the sandstone formations.

6.8.3.1 Core effluent analysis

An inductively coupled plasma instrument was used to measure concentration of Zr, Ca, and Mg cations. Obtained results are summarized in **Figs. 61-63**. It can be concluded that Zr concentration is nearly zero, implying that all Zirconium cations in the clay stabilizer solution were consumed by negatively charged clay particles. Ca and Mg concentraton fall in the range of 12 and 37 mg/L, respectively. The concentration for the former cation is still in the low range, therefore because the damage does take place in the core, it can be implied that the charge on the clays has not been stabilized with 0.2 vol% of Zirconium lactate solution, and the concentration had to be increased.

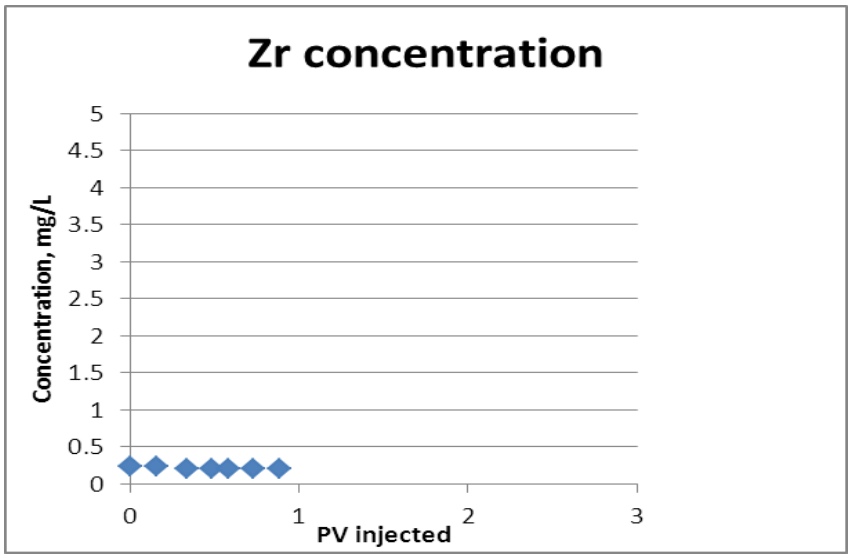

Fig. 61—Zr concentration profile for Zirconium lactate clay stabilizer of 0.2 vol% concentration.

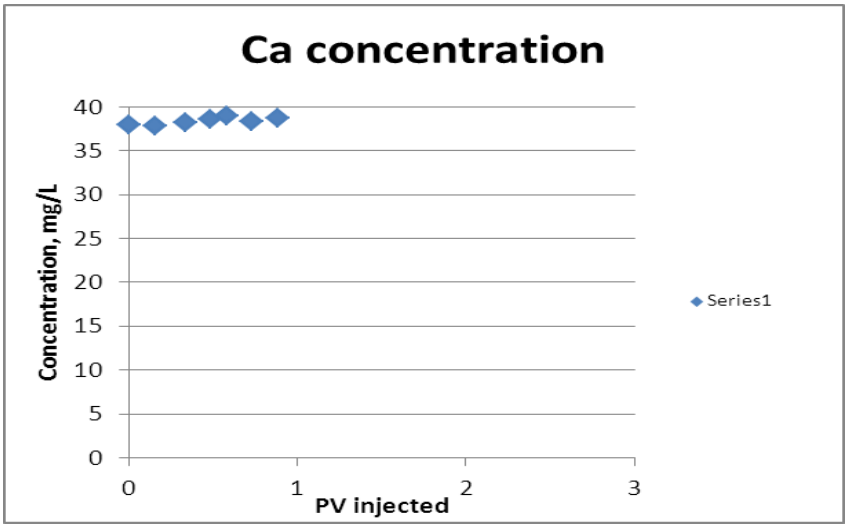

Fig. 62—Ca concentration profile for Zirconium lactate clay stabilizer of 0.2 vol% concentration.

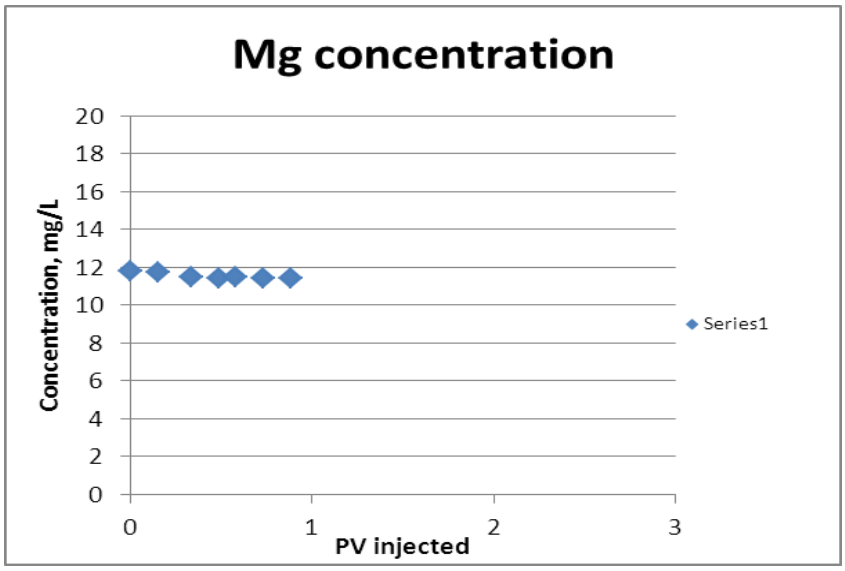

Fig. 63—Mg concentration profile for Zirconium lactate clay stabilizer of 0.2 vol% concentration.

The concentration of clay stabilizer was increased to 2 wt% of Zirconium lactate clay stabilizer. From **Fig. 64**, a damaging effect was noted, meaning that the clay stabilizer was not performing an effective clay fixation. Core effluent samples contained sediments of a reddish color which was due to high concentrations of an iron solution. This phenomenon took place because lactic acid is known to be used in the GLDA chemical solutions which are used as chelating agents for scale treatment.

Fig. 64—Sediments after coreflood with 2 wt% Zirconium lactate clay stabilizer.

6.8.4 Summary

The results show that concentration of 0.2 vol% of the solution containing zirconium solution was not sufficient to shield the negative charge on the clays. The concentration of the solution had to be increased for the next experiment. The ICP test showed that all zirconium was consumed for neutralizing the clays.

Upon the increase of the clay stabilizer concentration, 2 wt% of Zirconium lactate clay stabilizer was used. However, it did not show favorable results for clay stabilization purposes as well. Conducted coreflood experiment showed no preservation and no improvement of permeability. The core effluent shows iron coming out of the core. This takes place because lactic acid itself acts like a chelating agent for metal ions.

7. CONCLUSIONS

This thesis summarizes both theoretical and experimental work main objective of which was to determine physical and chemical factors which will affect clay stability in sandstone formations. The theoretical work done is represented by creation and modification of the models on clay fixation, and an energy-based model, as well as application of force balance (DLVO theory) calculation. The experimental work is solely based on conducting multiple coreflood experiments. The novelty of the research is that all the experiments were conducted at high temperature, which has a significant effect on fines immigration in the formation.

1. A severe damage to permeability is observed when injecting fresh water in the system, and no stabilized pressure drop value can be obtained.
2. Among the Lon der Waals attraction force, the double layer repulsion repulsive force, and the Born repulsion, the temperature change has the most significant effect on the double layer repulsion force.
3. One of the factors that affects stability of the clay particle is temperature. The results of the coreflood experiments show that increase in temperature accelerates the fines migration process, thus damaging rock permeability.
4. Among tested salts, ammonium chloride of concentration 15 wt% is considered to be a good clay stabilizer when working at high temperatures.

REFERENCES

Aranda, P. and Ruiz-Hitzky, E., 1999. Poly(ethylene oxide)/NH4+-smectite nanocomposites. *Applied Clay Science* **15**: 119–135.

Bailey, S.W. 1980. Structures of layer silicates. *Crystal Structures of Clay Minerals and their X-ray Identification* (Ed. by G.W. Brindley and G. Brown), Mineralogical Society of London, London.

Bailey, S.W. (Ed.). 1984. Micas. Reviews in Mineralogy, Mineralogical Society of America, Washington, DC, **13**:584.

Choquette, P.W. & Pray, L. 1970. Geologic nomenclature and classification of porosity in sedimentary carbonates. *AAPG Bull.*, **54**, 207–250.

Dai, Q. and Chung, K.H. 1995. Bitumen–sand interaction in oil in sand processing. *Fuel* **74** (12): 1858–1864.

Deer, W.A., Howie, R.A. & Zussman, J. 1998. *An Introduction the Rock-forming Minerals*. Longman, London.

Dielectric Constants of Materials. Clipper Controls, www.clippercontrols.com. 2011.

Eberl, D.D. 1980. Alkali cation selectivity and fixation by clay minerals. *Clays and Clay Minerals* **28** (3): 161-172

Ehrenberg, S.N. 1993. Preservation of anomalously high porosity in deeply buried sandstones by grain-coating chlorite: examples from the Norwegian continental shelf. *AAPG Bull.*, **77**: 1260–1286.

El-Monier, I.A. and Nasr El-Din, H.A. 2010. A New Environmentally Friendly Clay Stabilizer. Paper SPE 13606 presented at the SPE Production and Operations Conference and Exhibition held in Tunis, Tunisia, 8–10 June.

Fink, J.K. Oil field chemicals. 2003. Elsevier Science.

Formation Damage Manual. 2003. BJ Services. EDC, Tomball, Texas.

Gaupp, R., Matter, A., Platt, J., Ramseyer, K. & Walzebuck, J. 1993. Diagenesis and fluid evolution of deeply buried Permian (Rotliegende) gas reservoirs, northwest Germany. *AAPG Bull.* **77**: 1111–1128.

Gibbs, R.J. 1977. Amazon River sediment transport in the Atlantic Ocean. *Geology*, **4**: 45–58.

Hamaker, H. C. 1937. The London-Van der Waals attraction between spherical particles. *Physics* **4**: 1058.

Hartman, R.L., Lecerf, B., Frenier, W. et al. 2003. Acid Sensitive Aluminosilicates: Dissolution Kinetics and Fluid Selection for Matrix Stimulation Treatments. Paper SPE 82267 presented at the SPE European Formation Damage Conference, The Hague, Netherlands.

Khilar, K.C. and Fogler, H.S. 1983. Water sensitivity of sandstones. *SPE Journal* **23**(1): 55-64.

Kia, S. F. 1987. Effect of Salt Composition on Clay Release in Berea Sandstone. Paper SPE 16524 presented at the Proceedings of the SPE International Symposium on Oilfield Chemistry. San Antonio, Texas, February 4-6.

Lawrence, W.G. 1958. Theory of ion exchange and development of charge in kaolinite-water systems. *Journal of the American Ceramic Society* **41** (4): 136-140.

Liu, Z., Svensson, UJ., Dreybrodt, W., Daoxian, Y. and Buhmann, D. 1995. Hydrodynamic control of inorganic calcite precipitation in Huanglong Ravine, China: field measurements and theoretical prediction of deposition rate. *Geochimica et Cosmochimica Acta*, **59**, 3087–97.

Mungan, N. 1965. Permeability reduction through changes in ph and salinity. *SPE Journal of Petroleum Technology* **17**(12): 1449-1453.

Pagneoux, C., Serantoni, M., Laucournet, R., Chartier, T., Baumard, J.F. 1998. Influence of the temperature on the stability on aqueous alumina suspension. *J. Am. Ceram. Soc*: 1935 – 1948.

Pironon, J., Pelletier, M., de Donato, P., Mosser-Ruck, R., 2003. Characterization of smectite and illite by FTIR spectroscopy of interlayer NH_4^+ cations. *Clay Minerals* **38**: 201–211.

Ramachandran, R., Somasundaran, P. 1986. Effect of temperature on the interfacial properties of silicates. *Colloids Surf.* **21**: 355–369.

Revil, A., Pezard, P.A., Glover, P.W.J. 1999. Streaming potential in porous media 1. Theory of the zeta potential. *J. Geophys. Res*. **104** (B9): 20,021–20,031.

Rodríguez, K. and Araujo, M. 2006. Temperature and pressure effects on zeta potential values of reservoir minerals. *Journal of Colloid and Interface Science* **300** (2): 788-794.

Rossini, F.D., Wagman, D.D. , EVans, W.H., Levine, S., and Jaffe, I. 1952.*Selected values of chemical thermodynamic properties*, NBS Circ. 500, Pt. I.

Schembre, J.M., Tang, G.-Q. and Kovscek, A.R., 2006. Interrelationship of Temperature and Wettability on the Relative Permeability of Heavy Oil in Diatomaceous Rocks. *SPE Reservoir Evaluation & Engineering*, **9**(3): 239-250.

Schembre, J.M. and Kovscek, A.R. 2005. Mechanism of Formation Damage at Elevated Temperature. *Journal of Energy Resources Technology* **127** (3): 171-180.

Schembre, J.M. and Kovscek, A.R. 2004. Thermally Induced Fines Mobilization: Its Relationship to Wettability and Formation Damage. Paper SPE 86937 presented at the SPE International Thermal Operations and Heavy Oil Symposium and Western Regional Meeting, Bakersfield, California.

Shannon, R.D., 1976. Revised effective ionic radii and systematic studies of interatomic distances in halides and chalcogenides. *Acta Crystallographica* Section A **32**: 751–767.

Simon, D.E. and Anderson, M.S. 1990. Stability of Clay Minerals in Acid. Paper SPE 19422 presented at the SPE Formation Damage Control Symposium, Lafayette, Louisiana.

Somasundaran, K., R.D. 1973. A new streaming potential apparatus and study of temperature effects using it. *Journal of Colloid Interface Sci.* **45** (3): 591.

Srodón, J. 1999. Use of clay minerals in constructing geological processes: recent advances and some perspectives. *Clays and Clay Minerals* **34**: 27–37.

Tchistiakov, A.A. 2000. Colloid Chemistry of in-Situ Clay-Induced Formation Damage. Paper SPE 58747 presented at the SPE International Symposium on Formation Damage Control, Lafayette, Louisiana.

Vaidya, R.N. and Fogler, H.S. 1992. Fines Migration and Formation Damage: Influence of pH and Ion Exchange. *SPE Prod. Eng*. **7**(4): 325-330.

Velde, B. 1985. Clay Minerals: A physico-chemical explanation of their occurrence. *Developments in Sedimentology* **40**: 427.

Worden R.H. and Morad S. ed. 2003. Clay mineral cements in sandstones. Oxford: Blackwell Publishing.

Zhou Z., Cameron, S., Kadatz, B. et al. 1997. Clay Swelling Diagrams: Their Applications in Formation Damage Control. *SPE Journal* **2** (2): 99-106.

Zhou Z., Gunter, W.D., Kadatz, B. et al., 1996. Effect of Clay Swelling on Reservoir Quality. *Journal of Canadian Petroleum Technology,* **35** (7).

VITA

Name:	Darya Alexandrovna Musharova
Address:	Richardson Department of Petroleum Engineering Texas A&M University 3116 TAMU- office 603 College Station, TX 77843
Email Address:	darya.musharova@pe.tamu.edu
Education:	BS, Texas A&M University, Petroleum Engineering, 2010 MS, Texas A&M University, Petroleum Engineering, 2012